

Utilization of a Microbubble Dispersion to Increase Oxygen Transfer in Pilot-Scale Baker' s Yeast Fermentation Unit

Pramuk Parakulsuksatid

Thesis submitted to the Faculty of the
Virginia Polytechnic Institute and State University
in partial fulfillment of the requirement for the degree of

Master of Science
in
Biological Systems Engineering

Foster A. Agblevor, Chairman

John S. Cundiff

Allan A. Yousten

William H. Velander

April 18, 2000

Blacksburg, Virginia

Keyword: microbubble dispersion, oxygen transfer, pilot-scale, baker' s yeast fermentation

Utilization of a Microbubble Dispersion to Increase Oxygen Transfer in Pilot-Scale Baker' s Yeast Fermentation Unit

Pramuk Parakulsuksatid

(ABSTRACT)

In the large-scale production of *Saccharomyces cerevisiae* (baker' s yeast), oxygen transfer, which is one of the major limiting factors, is improved by using high agitation rates. However, high agitation rates subject the microorganisms to high shear stress and caused high power consumption. A microbubble dispersion (MBD) method was investigated to improve oxygen transfer at low agitation rates and thus reduce power consumption and shear stress on the microorganisms. The experiments were conducted at the 1-liter level and subsequently scaled-up to 50-liters using a constant volumetric oxygen transfer coefficient (k_La) method for scaling. In comparison to a conventional air-sparged fermentation, the MBD method considerably improved the cell mass yield, growth rate and power consumption in the 50-liter fermentor. Cell mass production in the MBD system at agitation rate of 150 rpm was about the same as those obtained for a conventional air-sparged system agitated at 500 rpm. Power consumption in the conventional air-sparged system was three-fold that required for the same biomass yield in the MBD system. However, at the 1-liter scale, the MBD system did not show any significant advantage over the air-sparged system because of the high power consumption.

ACKNOWLEDGMENTS

I wish to express my sincere gratitude and respect to my advisor Dr. Foster A. Agblevor for his ideas, patience, and advice throughout my Master's program. I am thankful for his willingness to take the time to make suggestions and help me achieve my goals. His support, guidance, and encouragement were most appreciated.

Thanks are also expressed to the members of my committee, Dr. John S. Cundiff, Dr. Allan A. Yousten, and Dr. William H. Velander. I would like to thank all of the graduate students and technicians that assisted in this research. In particular, I am grateful to Patcharee Hensirisak and Richard Affleck for their assistance with the laboratory work and analysis.

Finally, I would especially like to thank my parents for their love, support, and encouragement that they have given me throughout my academic career.

TABLE OF CONTENTS

	<u>Page</u>
ACKNOWLEDGMENTS	iii
TABLE OF CONTENTS.....	iv
LIST OF ILLUSTRATIONS.....	vii
LIST OF TABLES.....	viii
INTRODUCTION	1
LITERATURE REVIEW	4
2.1 BAKER’ S YEAST	4
2.2 CHARACTERISTICS OF BAKER’ S YEAST FERMENTATION	7
2.3 OXYGEN TRANSFER IN FERMENTOR	8
2.3.1 <i>Oxygen transfer</i>	9
2.3.2 <i>Factors in oxygen transfer</i>	12
2.4 MEASUREMENT OF OXYGEN TRANSFER	18
2.4.1 <i>Yield coefficient method</i>	21
2.4.2 <i>Dynamic method</i>	23
2.4.3 <i>Sodium sulfite oxidation method</i>	25
2.4.4 <i>Direct measurement method</i>	26
2.5 MICROBUBBLE DISPERSION UNIT.....	28
2.5.1 <i>Characteristics of Colloidal Gas Aphrons</i>	28
2.5.2 <i>Microbubble dispersion in fermentation</i>	33
2.6 SCALE-UP IN FERMENTATION	33
2.6.1 <i>Scale-up consideration</i>	35
2.6.2 <i>Scale-up method for fermentor</i>	36
MATERIALS AND METHODS.....	41
3.1 LABORATORY-SCALE FERMENTOR.....	41
3.2 PILOT-SCALE FERMENTOR	41
3.3 ORGANISM AND MEDIUM	42
3.4 FERMENTATION	43
3.4.1 <i>Preliminary experiments</i>	43
3.4.2 <i>1-liter fermentation with ordinary sparger air</i>	43
3.4.3 <i>1-liter fermentation with natural surfactant-stabilized microbubble</i>	45
3.4.4 <i>50-liter fermentation with ordinary sparger air</i>	47
3.4.5 <i>50-liter fermentation with natural surfactant-stabilized microbubble</i>	50
3.5 ASSAYS.....	50
3.5.1 <i>Dry cell mass concentration</i>	50
3.5.2 <i>Glucose concentration</i>	52
3.5.3 <i>The major metabolic parameter calculation</i>	52
3.5.4 <i>Determination of the k_La values</i>	53
RESULTS AND DISSCUSSION.....	55
4.1 SMALL SCALE FERMENTATION.....	55
4.1.1 <i>Air sparging system</i>	55
4.1.2 <i>MBD sparging system</i>	59
4.1.3 <i>Comparison between air sparging system and MBD sparging system</i>	59
4.2 LARGE SCALE CELL CULTIVATION	65
4.2.1 <i>Air sparging system</i>	65

4.2.2 MBD sparging system.....	68
4.2.3 Comparison between air sparging system and MBD sparging system.....	71
4.3 EFFECT OF MBD ON THE OXYGEN TRANSFER OF THE FERMENTATION.....	74
4.3.1 1-liter fermentation.....	74
4.3.2 50-liter fermentation.....	78
4.4 POWER CONSUMPTION.....	80
4.4.1 1-liter fermentation.....	80
4.4.2 50-liter fermentation.....	80
4.5 EFFECT OF SCALE-UP ON OXYGEN TRANSFER.....	82
4.5.1 Air sparging system.....	83
4.5.2 MBD sparging system.....	83
CONCLUSIONS AND RECOMMENDATIONS.....	89
REFERENCES.....	91
APPENDIX.....	97
VITA.....	100

LIST OF ILLUSTRATIONS

	<u>Page</u>
Figure 2.1 Schematic diagram of oxygen transport from a gas bubble to inside a cell (Baily, 1986).....	10
Figure 2.2 Different patterns of gas bubble dispersion in a stirred-tank reactor (Doran, 1995).....	15
Figure 2.3 Oxygen transfer coefficient versus gassed power per unit volume at different superficial velocity (Cooper et al, 1944)	20
Figure 2.4 Relationship between substrate yields and oxygen yields on different substrate (Mateles, 1971)	22
Figure 2.5 Relationship between dissolved oxygen concentration and time in dynamic gassing out method (Stanbury et al, 1995)	24
Figure 2.6 Colloidal gas aphon and sparged air bubble structures (Kaster, 1988).	29
Figure 2.7 The microfoam generator (Sebba, 1971).	31
Figure 2.8 The spinning disk CGA generator (Sebba, 1985).	32
Figure 2.9 The microbubble dispersion generator (Kaster, 1988).	34
Figure 2.10 The standard geometry of mixing tank (Tatterson, 1991).	37
Figure 3.1 1-liter fermentation with microbubble dispersion unit	46
Figure 3.2 50-liter fermentation with microbubble dispersion unit	49
Figure 3.3 The brass hose barb connected to the air connection.....	51
Figure 4.1 1-liter fermentation with air sparging at 144 rpm.	56
Figure 4.2 1-liter fermentation with air sparging at 476 rpm.	57
Figure 4.3 1-liter fermentation with MBD sparging at 144 rpm.	60
Figure 4.4 1-liter fermentation with MBD sparging at 476 rpm.	61
Figure 4.5 Comparison of yeast growth profiles in 1-liter cell cultivation.	63
Figure 4.6 Comparison of oxygen profiles in 1-liter cell cultivation.	64
Figure 4.7 50-liter fermentation with air sparging at 150 rpm.	66
Figure 4.8 50-liter fermentation with air sparging at 500 rpm.	67
Figure 4.9 50-liter fermentation with MBD sparging at 150 rpm.	69
Figure 4.10 50-liter fermentation with MBD sparging at 500 rpm.	70
Figure 4.11 Comparison of yeast growth profiles in 50-liter cell cultivation.	72
Figure 4.12 Comparison of oxygen profiles in 50-liter cell cultivation.	73
Figure 4.13 Comparison of volumetric oxygen transfer coefficient, specific growth rate, and oxygen uptake rate in 1-liter fermentation	77
Figure 4.14 Comparison of volumetric oxygen transfer coefficient, specific growth rate, and oxygen uptake rate in 50-liter fermentation	79
Figure 4.15 Comparison of volumetric oxygen transfer coefficient of air sparging system at agitation rates 144, 150, 476, and 500 rpm	84

Figure 4.16 Growth profiles of air sparging system at agitation rates 144, 150, 476, and 500 rpm. 85

Figure 4.17 Comparison of volumetric oxygen transfer coefficient of MBD sparging system at.....86
agitation rates 144, 150, 476, and 500 rpm

Figure 4.18 Growth profiles of MBD sparging system at agitation rates 144, 150, 476, and 500 rpm..... 88

LIST OF TABLES

	<u>Page</u>
Table 2.1 Products of microbial activity	5
Table 2.2 Industrial uses of yeast and yeast products	6
Table 2.3 Scale-up Criteria in Fermentation Industries	40
Table 4.1 Cell mass concentration, dissolved oxygen concentration, cell mass yield, and specific growth rate of 1-liter and 50-liter fermentations.	58
Table 4.2 Volumetric oxygen transfer coefficient and oxygen uptake rate.....	76
Table 4.3 Power consumption calculated from the 1-liter fermentations.	81
Table 4.4 Power consumption calculated from the 50-liter fermentations.....	81

CHAPTER 1

INTRODUCTION

Fermentation is the process of using microorganisms to produce valuable products such as antibiotics, industrial enzymes, food, and chemicals. Baker's yeast (*Saccharomyces cerevesiae*) is one of the oldest products of industrial fermentation. It is still one of the most important fermentation products based on volume of sales and its use for bread-making, a staple food for large section of world's population. Baker's yeast production is an aerobic fermentation process whose efficiency is strongly dependent on the transfer of oxygen and nutrients to the microorganisms. On a small scale, oxygen transfer is normally very efficient; however, as the volume of the reactor increases to 10,000 liters or more, oxygen transfer becomes a limiting factor in the production of yeast.

Unlike soluble compounds such as glucose or ammonia, the solubility of oxygen in water is very low, but utilization is very high. The situation is further exacerbated by the lowering of the solubility of oxygen in water by the presence of dissolved salts in the fermentation medium. The transfer of oxygen to the microorganisms involves the transport of the oxygen from the gas to the liquid phase. This process is influenced by several parameters, which are discussed below.

Oxygen is normally supplied to the fermentor by bubbling air up through the broth. The oxygen in the air bubbles is transferred into the media containing the microorganisms. The oxygen transfer rate is calculated from the oxygen transfer coefficient (k_L), the gas-liquid interfacial area (a), and the driving force, which is the oxygen concentration difference ($C^* - C$) between saturated dissolved oxygen concentration (C^*), and the existing oxygen concentration (C). The volumetric oxygen transfer coefficient (k_La) is used more than the two separate parameters (Doran, 1995). The oxygen transfer rate also depends on power input per unit volume, which is related to agitation speed, fluid and dispersion rheology, sparger characteristics, and gross flow pattern in the vessel.

The gas-liquid interfacial area and the bubble residence time are the limiting steps of oxygen delivery to the microorganisms. The gas-liquid surface area can be manipulated by changing interfacial tension, but this factor is difficult to adjust. Thus, an increase in interfacial surface may be better achieved by increasing mechanical agitation. The increase in interfacial area gained by a decrease in bubble size also results in a concomitant increase in bubble residence time. Ahmad *et al* (1994) found that the volumetric oxygen transfer coefficient for *Candida utilis* fermentation increased with increasing agitation rate.

The agitation rate of the fermentor affects the coalescence and breakup of bubbles, bubble-size distribution, and bubble residence time (Bailey and Ollis, 1986). For large-scale systems, power consumption during aeration and agitation is a significant fraction of the total operating cost. To increase agitation rate, the power of the impeller motor must be increased. The increase in agitation rate produces higher shear stress in the broth, which may cause a decrease in the growth of shear-sensitive microorganisms.

The scale-up of aerobic cultures from flask to jar fermentor and from jar fermentor to pilot plant, and subsequently to industrial tank, have been generally based on the volumetric oxygen transfer coefficient. Although the volumetric oxygen transfer coefficient constant is the common method in fermentation scale-up, the microbial growth kinetics observed in laboratory-scale experiments often does not agree with the kinetics observed in pilot-scale or industrial-scale fermentation. There are many factors other than the oxygen transfer rate to consider during scale-up: heat transfer, surface-to-volume ratio, and quality of mixing, shear, and superficial air velocity. Additionally, the type of microorganisms, time of inoculum transfer, operating time of the fermentation, and age and stability of culture can cause complications in the scale-up. To improve the oxygen transfer rate in large-scale fermentation, a more efficient method to supply oxygen must be found.

One of the techniques, which have been proposed for increasing oxygen transfer rate in aerobic fermentation, is the microbubble dispersion unit (Kaster *et al*, 1990 and Hensirisak, 1997). Kaster *et al* (1990) found that a microbubble dispersion increased the volumetric oxygen transfer coefficient in a 2-liter baker's yeast fermentation by 30 % compared to sparged air. In a 20-liter baker's yeast fermentation, Hensirisak (1997)

found that the volumetric oxygen transfer coefficient for a microbubble dispersion operated at 150 rpm was equivalent to the coefficient achieved with air sparging at 500 rpm. Unlike a gas sparger, the increase in the volumetric oxygen transfer coefficient was not correlated with agitation speed.

The objective of this research is to investigate the effect of a microbubble dispersion on oxygen transfer in a 50-liter baker's yeast fermentation unit. In this study, a yeast growth pattern and oxygen profile obtained by ordinary air sparging will be compared with those obtained by a microbubble dispersion at two different agitation speeds. The power consumption per volume of fermentation broth for each experiment will be estimated.

CHAPTER 2

LITERATURE REVIEW

2.1 Baker' s yeast

Industrial microbiology deals with microorganisms that have an economic value. The economic criterion implies that microorganisms have some specific type of growth or metabolic activity to produce one or more products. These considerations make it apparent that industrial microbiology is a very broad area for study. Industrial microbiology also deals with the isolation and description of microorganisms from natural environments, such as soil or water, and cultural conditions required for obtaining specific products from these organisms in the laboratory and in large scale culture vessels commonly known as fermentors. Thus, the ability of microorganisms to convert inexpensive raw materials (substrates) to economically valuable organic compounds obviously is of considerable interest.

The valuable organic compounds (fermentation products) may be components of the microbial cells, the cells themselves, intracellular or extracellular enzymes, or chemicals produced or converted by the microorganisms. Some commercially important products of microbial activity are shown in Table 2.1 (Casida, 1968). Yeasts are the most important and the most extensively used microorganisms in industry. They are cultured for the cell mass, cell components, and products that they produce during the fermentation. Table 2.2 shows the utilization of yeast and yeast products in industry (Brock and Madigan, 1991).

Industrial production of yeast cells and production of alcohol by yeast are two quite different processes. The first process, an aerobic process, requires oxygen for maximum production of cell, whereas the alcoholic fermentation process is anaerobic and takes place only in the absence of oxygen. The yeast widely used for both industrial processes is *Saccharomyces cerevisiae*.

Table 2.1 Product of microbial activity

-
1. Antibiotics: streptomycin, penicillin, tetracycline, erythromycin, polymyxin
 2. Organic solvents: acetone, butanol, amyl alcohol
 3. Gases: carbon dioxide and hydrogen
 4. Beverage: wine, beer, and distilled beverage
 5. Foods: cheese, fermented milks, pickles, sauerkraut, soy sauce, bread, vinegar
 6. Flavoring agents: monosodium glutamate and nucleotides
 7. Organic acids: lactic, acetic, citric, gluconic, butyric, fumaric, itaconic
 8. Glycerol
 9. Amino acids: L-glutamic acid and L-lysine
 10. Steroids
 11. Wide range of compounds used as chemical intermediates for further chemical synthesis of economically valuable products
 12. Bakers' yeast
 13. Food and feed yeast
 14. Legume inoculant
 15. Bacterial insecticides: *Bacillus thuringiensis*
 16. Vitamins and other growth stimulants: B12, riboflavin, vitamin A and the gibberellins
 17. Enzymes: amylase, proteases, pectinases, invertase
 18. Fats
-

From: L. E. Casida, Jr, Definition and scope of industrial microbiology, In *Industrial Microbiology*, John Wiley & Son, Inc, New York, 1968, pp.4

Table 2.2 Industrial uses of yeast and yeast products

Production of yeast cells

Baker' s yeast for bread making

Dried food yeast for food supplements

Dried feed yeast for animal feeds

Yeast products

Yeast extract for culture media

B vitamins, Vitamin D

Enzymes for food industry; invertase, galactosidase

Biochemicals for research; ATP, NAD, RNA

Fermentation products from yeast

Ethanol

Glycerol

Beverage alcohol

Beer

Wine

Distilled beverages

Whiskey

Brandy

Vodka

Rum

From: T. D. Brock and M. T. Madigan, Microbial biotechnology, In: *Biology of Microorganisms* sixth edition, Prentice Hall, Englewood Cliffs, New Jersey, 1991, pp. 376

Baker's yeast, *S. cerevisiae*, is still one of the most important biotechnological products because it has several industrial applications. Baker's yeast as a commercial product has several formulations that can be grouped into two main types: compressed yeast, called fresh yeast, and dried yeast (Beudeker et al, 1990). Compressed yeast is the traditional formulation of baker's yeast, and is ready for immediate use. Dried yeast is available in two forms: active dry yeast (ADY) and instant dry yeast (IDY).

Active dry yeast (ADY) is normally sold in airtight packages, vacuum seal or filled with an inert gas such as nitrogen. It is not a problem to maintain quality, but it should be rehydrated before use. Unlike ADY, instant dry yeast (IDY) does not have the cell damage during rehydration. IDY is the most expensive among the three types of baker's yeast.

2.2 Characteristics of baker's yeast fermentation

Selected strains of baker's yeast, *S. cerevisiae*, are used for industrial-scale production. These strains are selected for stable physiological characteristics, vigorous sugar fermentation in dough, cellular dispersion in water, no autolysis during the fermentation, rapid growth and high cell yields, and easy maintenance during storage. The fermentation of baker's yeast has to produce a product with minimum variation in yeast performance, maximum yield on raw material, and minimum production of undesirable side products.

Under aerobic conditions, *S. cerevisiae* uses sugars such as glucose to grow cell mass rather than produce alcohol (Reed and Peppler, 1973; Orłowski and Barford, 1987; Barford, 1990). Barford (1990) studied a general model for aerobic yeast growth in batch culture. This model was developed by comparing the rate of sugar transport into the cell and the rate of transport of respiratory intermediates (pyruvate) into the mitochondrion. If the rate of sugar uptake is higher than the transport rate of respiratory intermediates into the mitochondrion, the metabolism favored ethanol production and limited the specific oxygen uptake rate. If the respiratory intermediates transport rate into the mitochondrion was equal the transport of sugar into the cell, carbon dioxide (CO₂) was

the major metabolite with little or no ethanol produced and a much higher specific oxygen uptake rate occurred.

In aerobic batch fermentation, *S. cerevisiae* can only produce a limited amount of respiration enzymes. If the glucose concentration is more than 5% in the medium, the respiratory intermediate enzymes are suppressed and the ethanol mechanisms dominate. A concentration of glucose at 0.1 g L^{-1} is the maximum growth condition for cell growth (Furukawa *et al*, 1983).

In continuous fermentation, the dilution rate is equal to the growth rate when steady state is achieved. At steady state, the glucose concentration in the fermentor will be near zero. The low glucose concentration in the fermentor causes the yeast to completely oxidize all the glucose it consumes. A high glucose concentration in the feed stream decreases cell growth. In the presence of excess glucose, the yeast converts some glucose to ethanol, thereby reducing the cell mass yield. To get the high conversion of glucose to cell mass, the glucose concentration in the fermentation had to remain near zero and new glucose has to be added continuously.

In fed batch fermentation, the nutrients (glucose) are fed intermittently during the production phase (log phase). This technique has been found to be particularly effective for processes in which substrate inhibition, catabolic repression, and product inhibitions are important (Modak *et al*, 1986). The glucose is fed to the yeast at a rate almost equal to the glucose consumption rate. There is no inhibition effect due to high glucose concentration in fed-batch fermentation. It is not easy to equilibrate the glucose feed rate with the consumption rate by the yeast.

Since the yeast cell number is growing, the glucose feed rate should increase as the yeast cell number increase, but in a practical fermentation there is only one feed rate. This effect has the major disadvantage in large-scale fed-batch fermentation. Although the batch system has many limitations, this system is still used for industrial-scale production.

2.3 Oxygen transfer in fermentor

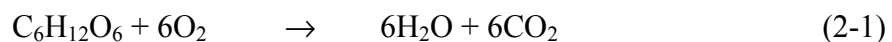
For aerobic fermentation, oxygen transfer is a key variable. Oxygen transfer is a function of aeration and agitation. Aeration is the supply of oxygen-containing air into

the fermentor. Agitation is the stirring of the broth to achieve improved distribution of the air bubbles rising from the sparging ring in the bottom of the fermentor. The aeration and agitation altogether are used to enhance oxygen transfer from gas (air) to liquid medium for the optimal cell mass production or product formation. In shake flask cultivation, there is no oxygen limitation. In pilot-scale and product-scale fermentation, oxygen transfer operation is a critical factor in the promotion of cell mass production.

Oxygen has low solubility in aqueous solutions. Many chemical and physical factors affect the oxygen transfer rate. These factors are interfacial area of gas bubbles, stirrer speed, medium compositions, and oxygen partial pressure. Since the rate of oxygen transfer from gas bubbles to liquid medium becomes the rate-limiting step, many studies to increase the efficiency of oxygen transfer have been done. These studies have investigated the effect of chemical and physical factors on oxygen transfer (Richards, 1961).

2.3.1 Oxygen transfer

Glucose and oxygen are major factors in aerobic fermentation. When oxygen is limited, glucose is metabolized to ethanol, and less cell mass is produced. When the objective is the production of cell mass such as baker's yeast or single cell protein (SCP), oxygen is the most important determinate of cell mass yield. The stoichiometry of glucose oxidation for single-cell organism respiration is



Respiration requires 192 grams of oxygen to oxidize 180 grams of glucose. Both glucose and oxygen must be dissolved in the liquid before microorganisms can use them for cell replication. The solubility of oxygen in liquid media is 6000 times lower than that of glucose (Stanbury *et al*, 1995). Oxygen must be supplied to the liquid by aeration and agitation so that cell growth remains aerobic.

Oxygen is normally introduced into the reactor by supplying compressed air through a circular ring (sparging ring). The resulting air bubbles are distributed by

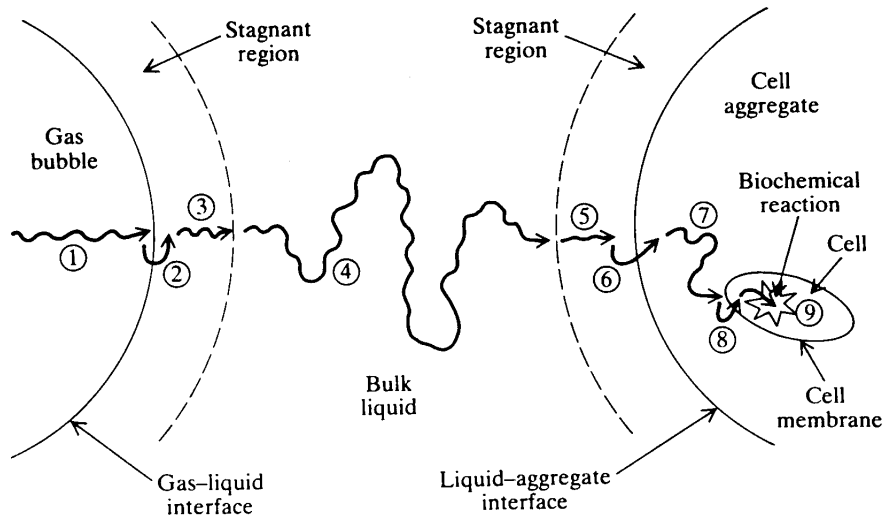


Figure 2.1 Schematic diagram of oxygen transport from a gas bubble to inside a cell (Baily, 1986).

agitating the broth with an impeller powered by an external motor. The oxygen transfer from an air bubble to the cell is represented in Figure 2.1 (Baily, 1986). Oxygen diffuses from an air bubble to the gas-liquid interface. It diffuses through the stagnant liquid layer surrounding the air bubble, and it is transported through the bulk liquid medium by liquid movement. It then diffuses through the liquid layer surrounding the cell. It is transported across the cell membrane to the reaction site.

The oxygen transfer mechanisms in gas and liquid are different. At steady state, the oxygen transfer rate through the gas-liquid interface equals the rate through the stagnant liquid layer. Since the oxygen dissolves poorly in liquid, the liquid-phase mass-transfer dominates the gas-liquid interface resistance. The rate-limiting step for oxygen transfer is the diffusion through the liquid layer around the air bubble. Therefore, the oxygen mass transfer rate equation at the liquid layer in a fermentation broth is described by:

$$N_A = k_L a \Delta C \quad (2-2)$$

where

- N_A = the rate of oxygen transfer per unit volume of fluid ($\text{mol m}^{-3} \text{s}^{-1}$),
- k_L = the liquid-phase mass transfer coefficient (m s^{-1}),
- a = the gas-liquid interfacial area per unit volume of fluid ($\text{m}^2 \text{m}^{-3}$), and
- ΔC = concentration driving force (mol m^{-3}).

ΔC is the difference between saturated dissolved oxygen concentration, C^* , and the oxygen concentration in the liquid medium, C . $\Delta C = C^* - C$

Therefore,

$$N_A = k_L a (C^* - C) \quad (2-3)$$

From the Eq. (2-3), it is clear that three parameters are involved in the oxygen transfer rate: the liquid-phase mass transfer coefficient (k_L), the gas-liquid interfacial area per unit volume of fluid (a) and the concentration driving force ($C^* - C$). Typically, the first two parameters are combined into one parameter: the volumetric mass transfer coefficient

($k_L a$). Because of the low solubility of oxygen, the difference between oxygen concentrations ($C^* - C$) is quite small.

The $k_L a$ value will depend on the design and operation of the fermentor. Some chemical and physical variables affect the $k_L a$ value such as gas flow rate, speed of agitation, oxygen partial pressure in the aeration gas, and the addition of an antifoam agent. The oxygen transfer rate from an air bubble to the liquid medium has to be higher than the oxygen consumption rate by the microorganisms; otherwise, their metabolism will shift to the anaerobic mechanism. To increase the oxygen transfer rate, factors affecting the oxygen transfer rate must be optimized.

2.3.2 Factors in oxygen transfer

The rate of oxygen transfer in fermentation broth is influenced by several physical and chemical factors that change either the value of k_L or the value of a , or the driving force, ($C^* - C$). If the gas bubble diameter is above 2-3 mm, k_L is relatively constant and insensitive to other conditions in the fermentor (Doran, 1995). To substantially improve mass transfer rate, it is necessary to increase the interfacial area. The driving force, oxygen concentration, is difficult to increase because of the low solubility of oxygen. The volumetric mass transfer coefficient ($k_L a$) is widely used to measure the oxygen transfer rate. Operating conditions in fermentors are discussed based on their effect on oxygen transfer.

Bubble size

The efficiency of gas-liquid mass transfer depends on the characteristics of the bubbles in the liquid medium. Bubble characteristics strongly affect the value of $k_L a$. In stirred fermentors, oxygen is supplied to the medium by sparging air bubbles underneath the impeller. The impeller then creates a dispersion of gas throughout the vessel. In laboratory-scale fermentation, all of the liquid is close to the impeller surface; bubbles in these systems are subjected directly to the high turbulent region in the vessel. Bubbles in most industrial stirred tank fermentors spent a large proportion of their time floating

free and unimpeded through the liquid after initial dispersion at the impeller. Liquid in large fermentors is far from the impeller surface and does not possess sufficient energy for break the bubbles. Most laboratory fermentors operate with stirrer power between 10-20 kW m⁻³, whereas large agitated vessels operate at 0.5-5 kW m⁻³ (Doran, 1995). The large-scale stirred fermentors operate with more of the volume in free bubble rise regime.

The size of air bubbles is the most important variable (Motarjemi and Jameson, 1978). Small air bubbles have more interfacial area a than large air bubbles. However, there are other important benefits associated with small bubbles, for example, slow rising velocity and high gas hold-up. Slow rising velocities keep air bubbles in the liquid longer, allowing more time for the oxygen to dissolve. Small bubbles create high gas hold-up, defined as the fraction of the fluid volume in the reactor occupied by gas:

$$\varepsilon = \frac{V_G}{V_L + V_G} \quad (2-4)$$

where

ε = the gas hold-up

V_G = the volume of gas bubbles in the reactor (m³), and

V_L = the volume of liquid in the reactor (m³)

The total interfacial area for oxygen transfer depends on the total volume of gas in the system as well as on the average bubble size. High gas hold-up gives a high oxygen transfer rate because the total volume of the air bubbles in the fermentor is greater. The bubble size is one of the major factors in the total interfacial area of the gas bubbles. Kaster *et al* (1990) and Hensirisak (1997) found that a microbubble dispersion increased oxygen transfer rate in aerobic fermentation of yeast. For a given volume of gas, more interfacial area, a , is provided if the gas is dispersed into many small bubbles rather than a few large ones. Since the efficiency of oxygen transport is approximately proportional to the ratio of the bubble surface area to the bubble volume, the smaller size bubbles increases oxygen transfer rate in the fermentor.

Sparging, Stirring and Medium Properties

The physical processes that determine bubble size in fermentors are aeration and agitation. These processes, and certain medium properties, have an important influence on the oxygen transfer rate. The sparger ring normally is positioned centrally under the impellers. The impellers provide mechanical agitation and distribute the air in small bubbles throughout the fermentor. When gas is present in stirred liquids, it is drawn into low-pressure cavities behind the impeller blades (Rushton and Oldshue, 1953). These cavities reduce the resistance to fluid flow and decrease the drag coefficient of the impeller. As the impeller blades rotate at high speed, small gas bubbles are thrown out from the back of the cavities into the bulk liquid under the influence of dispersion processes.

A schematic representation of airflow rate (aeration) and impeller speed (agitation) is shown in Figure 2.2. Different gas flow patterns develop depending on the relative rates of gas input and stirring. If the agitator speed N_i is low and the gas feed rate F_g is high; the gas flow pattern is dominated by airflow along the axis of the stirrer as shown in Figure 2.2 (a). This flow pattern is called impeller flooding, and represents poor mixing and minimal gas dispersion. As the impeller speed increases, gas is captured behind the agitator blades and is dispersed into the liquid. Figure 2.2 (b) shows the minimum stirrer speed required to completely disperse the gas. With further increases in stirrer speed, small recirculation patterns start to emerge as indicated in Figures 2.2 (c) and (d). The desired dispersion pattern is shown in Figure 2.2 (e).

Coalescence of small bubbles is generally undesirable because it reduces the total interfacial area and gas hold-up. Coalescence depends mainly on the liquid properties (Oolman and Blanch, 1986, Junker *et al*, 1990). A fermentation broth consists of many chemicals, including microbial cells and products from the microbial cells. Therefore, the fermentation broths vary in their properties depending on the desired product. Also, the broth rheology may change during the fermentation.

Under typical fermentor operating conditions, increasing the stirrer speed improves the value of $k_L a$. Ahmad *et al* (1994) found that an increase in oxygen transfer

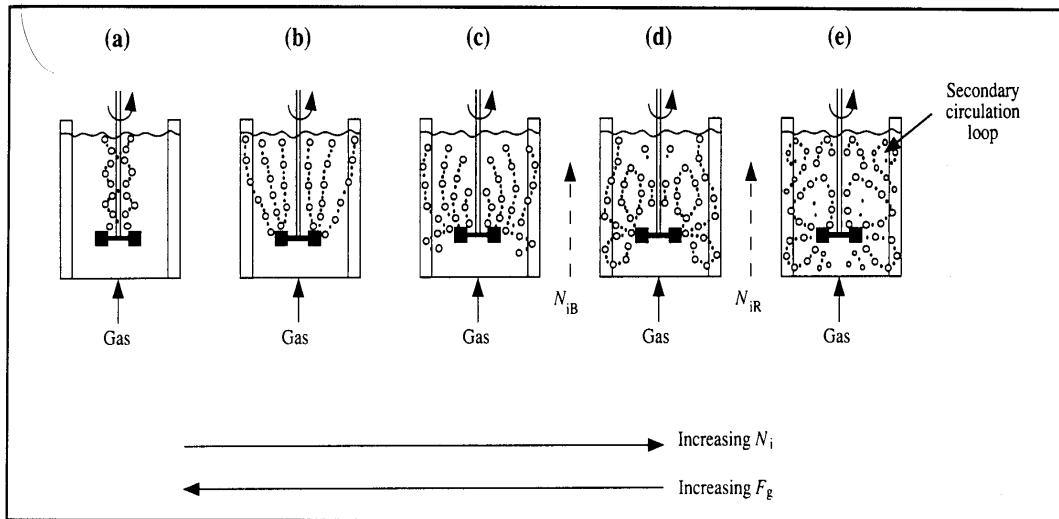


Figure 2.2 Different patterns of gas bubble dispersion in a stirred-tank reactor (Doran, 1995).

rate from 8.94 to 38.63 mmol O₂ L⁻¹ h⁻¹ is obtained as the agitation speed is increased from 300 to 600 rpm. In addition, by increasing the air flow rate from 0.21 L min⁻¹ to 1.05 L min⁻¹, the oxygen transfer rate increased from 5.7 mmol O₂ L⁻¹ h⁻¹ to 20.5 mmol O₂ L⁻¹ h⁻¹. Increasing the agitation rate is the traditional approach used to enhance the oxygen transfer rate. More agitation produces more gas dispersion, and more gas dispersion produces more mass transfer.

Antifoam Agents

Nutrients in culture medium induce a variety of foam-producing and foam-stabilizing agents, such as proteins, polysaccharides and fatty acids. Foam built-up in fermentors is very common, particularly in aerobic systems. The foam may overflow from the top of the fermentor via the air outlet or sample port resulting in a contamination and blockage of outlet gas lines. Liquid and cells trapped in the exiting foam represent a loss of medium and products. The presence of foam may actually decrease the oxygen transfer rate by coalescing the air bubbles.

Addition of special antifoam compounds to the medium is the most common method to collapse the foam, but these additives sometimes cause the coalescence of air bubbles (Onodera *et al*, 1993). Most antifoam agents are strong surface-tension-lowering substances. A decrease in surface tension causes the coalescence of air bubbles. Lowering the surface tension increases the average bubble diameter, and the volumetric oxygen transfer coefficient is decreased. This effect occurs because of a reduction in mobility of the gas-liquid interface, and this lowers the value of k_L . With most silicon-based antifoam, the reduction in k_L is generally larger than the increase in a so the net effect is a reduction in $k_L a$.

Mechanical methods of disrupting foam are used because these methods produce no change in medium properties. Mechanical foam breakers, such as high-speed rotating discs or centrifugal foam destroyers, are suitable; however, these methods need high power to operate. Their limited foam-destroying capacity is also a problem with high-foaming cultures. In many cases, use of chemical antifoam agents is unavoidable.

Temperature

The temperature of an aerobic fermentation affects both the solubility of oxygen and the mass transfer coefficient. The solubility of oxygen drops when the temperature increases; thus the driving force for oxygen transfer is reduced. At the same time, the mass-transfer coefficient (k_L) increases because diffusivity of oxygen in the liquid film is increased. The net effect of temperature on oxygen transfer depends on the range of temperature considered. The oxygen transfer rate will increase when the temperature increases from 10°C to 40°C (Doran, 1995). Above 40°C the solubility of oxygen drops significantly, adversely affecting the driving force and rate of oxygen transfer.

Gas Pressure and Oxygen Partial Pressure

Total pressure and partial pressure of oxygen affect the solubility of oxygen. Assuming the concentration of oxygen in liquid is low, the relationship between the solubility of oxygen and oxygen partial pressure is given by Henry's law:

$$P_{AG} = P_T Y_{AG} = H C_{AL}^* \quad (2-5)$$

where

P_{AG} = the partial pressure of component A in the gas (Pa),

P_T = total gas pressure (Pa),

Y_{AG} = the mole fraction of A in the gas (mol A mol^{-1}),

H = Henry's constant which is a function of temperature,

C_{AL}^* = the solubility of component A in the liquid (mol m^{-3}).

In Eq. (2-5), the two variables, total gas pressure (P_T) and the concentration of oxygen in the gas (Y_{AG}), affect the solubility of oxygen. At constant temperature, if either P_T or Y_{AG} is increased, the solubility of oxygen and the oxygen transfer driving force also are increased.

To increase the concentration of oxygen in the gas, oxygen enriched air or pure oxygen can be used. Alternatively, sparging compressed air at high pressure increases

oxygen solubility. Both strategies increase the operating cost of the fermentor. In some cases, there may be inhibitory effects from exposure to very high oxygen partial pressures.

Presence of Cells

Oxygen transfer is influenced by the presence of cells and their product in the fermentation broth. The species of microorganism, its morphology and concentration have an effect on liquid properties (Abel *et al*, 1994, Ju and Sandararajan, 1994, 1995, Sousa and Teixeira, 1996). Cells with complex morphology generally cause a lower transfer rate. Fungal and streptomycete fermentation present major difficulties in oxygen transfer. The viscosity of the liquid medium is increased during fermentation. Increasing the agitation rate of a viscous liquid requires high power and results in a high operating cost. The product formation may drop because fungus microorganisms are sensitive to the shear stress generated by the high agitation rate.

2.4 Measurement of oxygen transfer

There are two approaches to evaluating k_La : calculation using empirical correlation and experimental measurement. In aerobic fermentors, k_La is dependent on the hydrodynamic conditions around the gas bubbles. Relationships between k_La and parameters such as bubble diameter, liquid velocity, density, viscosity and oxygen diffusivity have been investigated extensively, and empirical correlations between mass transfer coefficients and important operating variables have been developed. The important correlation is the relationship between k_La and power consumption shown below:

$$k_La = k (P_g/V)^a (V_s)^b \quad (2-6)$$

where

P_g = the power absorption in an aerated system (W),

- V = the liquid volume in the fermentor (m^3),
V_s = the superficial air velocity (m s^{-1}), and
k, a and b = empirical factors specific to the investigated system.

Cooper *et al* (1944) investigated the relationship between k_La and power consumption in one impeller stirred tank using the sulfite oxidation technique. They found the values of a and b were 0.95 and 0.67, respectively. Figure 2.3 shows their results for volumetric oxygen transfer coefficient and power consumption. Van' t Riet (1983) summarized the above correlation in two systems: pure water and strong electrolyte solution. For pure water, the values of k, a, and b were 0.026, 0.4 and 0.5, respectively. For strong electrolyte solution, the values of k, a, and b were 0.002, 0.7 and 0.2, respectively.

Theoretically, the correlations allow prediction of mass transfer coefficients based on information gathered from a large number of previous experiments. In practice, however, the accuracy of published correlations applied to biological systems is strongly affected by the additives usually present in the fermentation media. Because fermentation liquids contain varying levels of substrates, products, salts, surface-active agents and cells, the surface chemistry of bubbles and therefore the mass transfer situation become very complex. Most available correlations for oxygen mass transfer coefficients were determined using pure air in water, and it is very difficult to correct these correlations for different liquid compositions. Prediction of k_La under these conditions is problematic.

Because of the difficulty in predicting k_La in bioreactors using correlations, mass transfer coefficients for oxygen are usually determined experimentally. Several methods have been developed to estimate the oxygen transfer rate in fermentors. The four most common methods are yield coefficient, dynamic technique, sodium sulfite oxidation, and direct method. The measurement conditions should match those in the fermentor during normal operation.

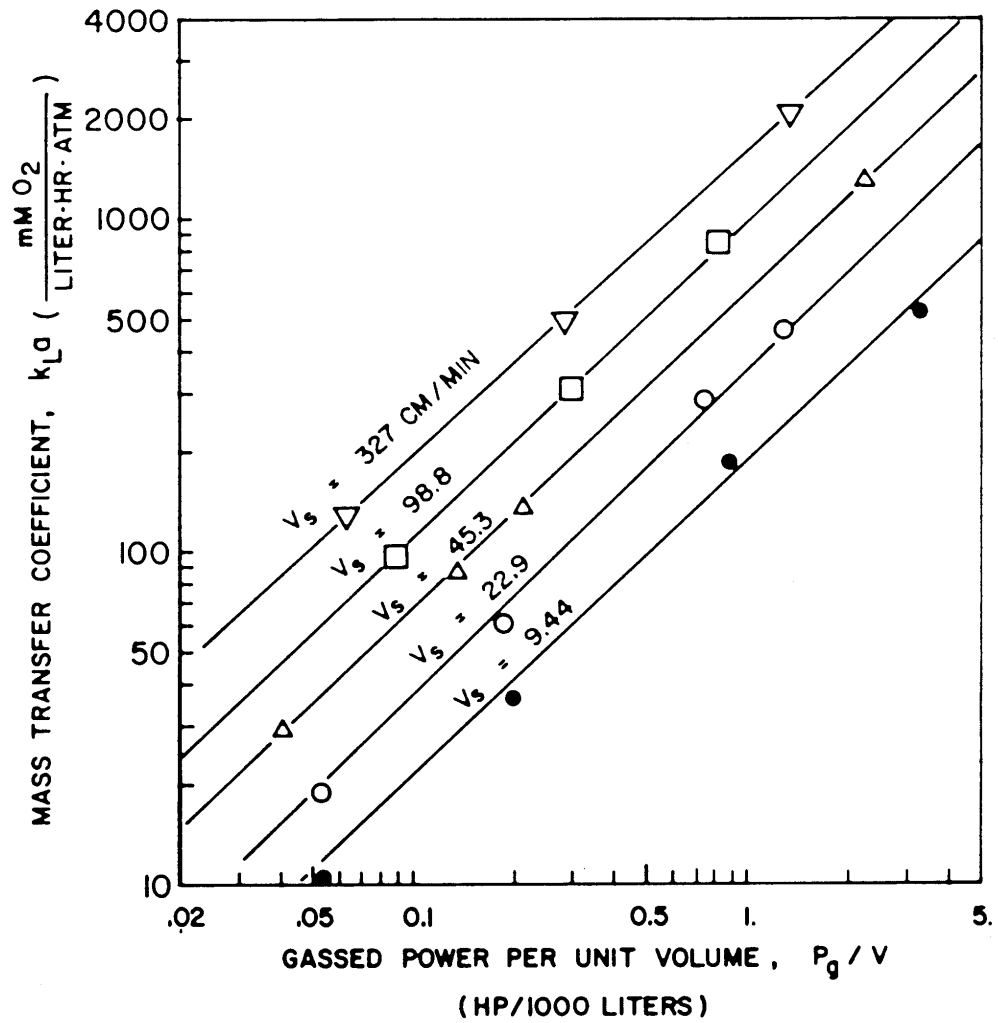


Figure 2.3 Oxygen transfer coefficient versus gassed power per unit volume at different superficial velocity (Cooper et al, 1944).

2.4.1 Yield coefficient method

This method gives the most accurate oxygen transfer rate because it measures the oxygen transfer rate under actual process conditions (Moser, 1996). This method measures the oxygen uptake rate by microorganisms during fermentation rather than the rate of depletion of oxygen in the gas-liquid phase. The oxygen uptake rate is the rate that microorganisms in fermentors consume oxygen during fermentation. This technique applies the stoichiometric relationships between oxygen and cell mass together with the kinetic data for growth. The oxygen uptake rate of microorganisms (Wang *et al*, 1979) is shown as:

$$Q_o = \mu X(K'/Y_o) \quad (2-7)$$

where

- Q_o = oxygen uptake rate (mmol O₂ L⁻¹ h⁻¹),
- μ = specific growth rate of microorganisms (h⁻¹),
- X = cell mass (g cell mass L⁻¹),
- K' = conversion factor = 31.25 (mmol O₂ g O₂⁻¹), and
- Y_o = yield coefficient on oxygen (g cell mass g O₂⁻¹).

In Eq. (2-7), the oxygen yield coefficient is the only unknown variable. The oxygen consumed to produce cell mass is difficult to measure. Mateles (1971) provided a generalized method to calculate the oxygen yield coefficient as a function of substrate yield coefficient, Y_s (gm of cell mass/gm of substrate consumed). Figure 2.4 is a graph of the relationship between the oxygen yield coefficient and the substrate yield coefficient for yeast on several substrates. At steady state, the rate of oxygen transfer from the bubbles is equal to the rate of oxygen uptake by the cells. By this assumption, the $k_L a$ value is calculated by setting these two oxygen rates equal, then the oxygen uptake rate is divided by the driving force of oxygen concentration. This method is a simple and easy to determine $k_L a$ but it is based on the assumption that the substrate is completely

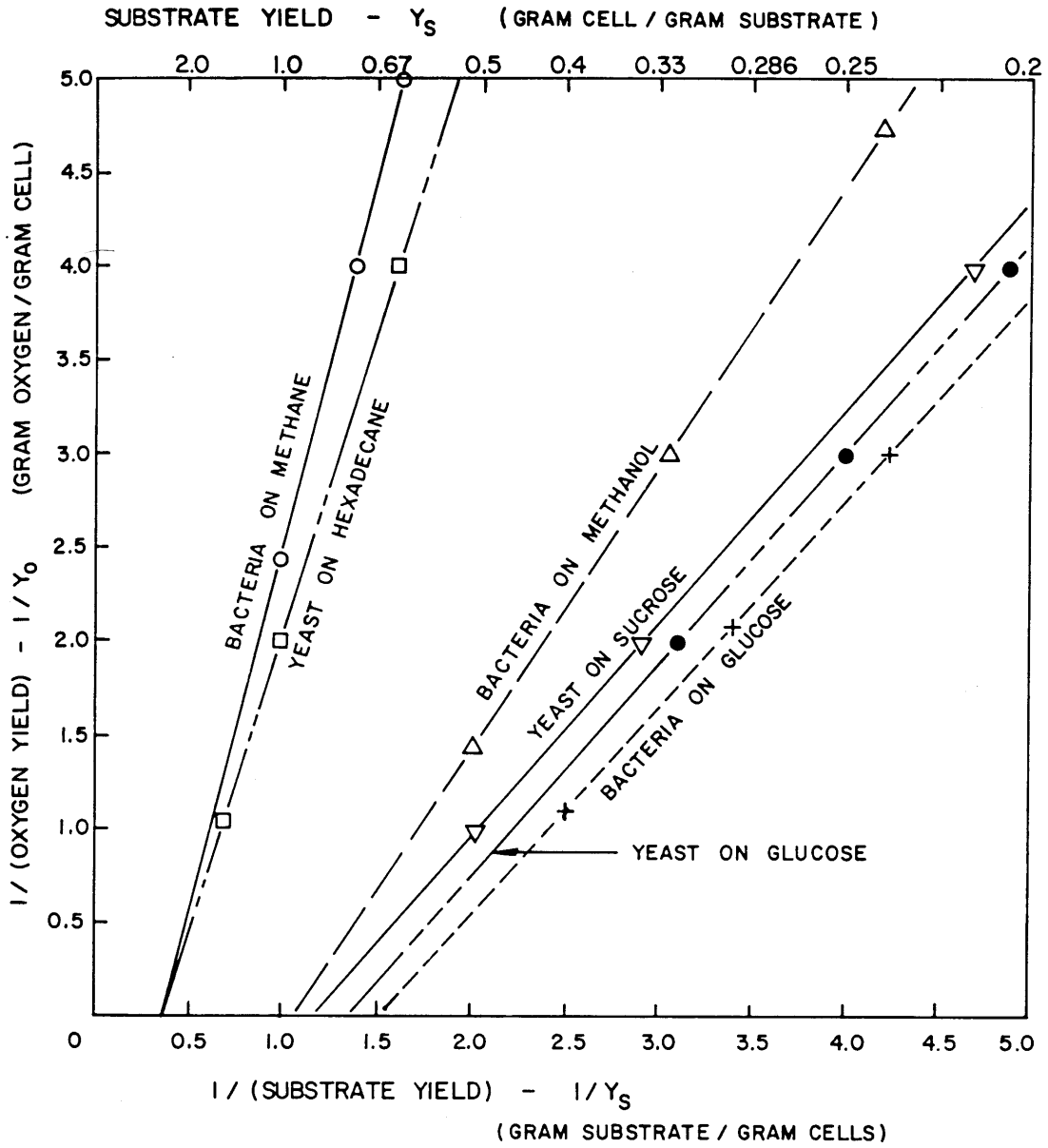


Figure 2.4 Relationship between substrate yields and oxygen yields on different substrate (Mateles, 1971).

converted into carbon dioxide, water, and cell mass.

2.4.2 Dynamic method

Taguchi and Humphrey (1966) first developed this method by using the respiratory activity of growing microorganisms in the fermentor. This method measures the k_La value based on an unsteady-state mass balance for oxygen. Although there are many different versions of the dynamic method, the fundamental calculation of the dynamic method developed by Taguchi and Humphrey (1966) is still used to determine the k_La value.

The calculation is based on the material balance of dissolved oxygen in a liquid medium. The relationship between the dissolved oxygen in liquid medium and time is shown in Figure 2.5 (Stanbury *et al*, 1995). After the starter is inoculated into the fermentor, the air supply is stopped. Due to the respiration of the culture, the dissolved oxygen concentration linearly declines as shown by the slope of line AB in Figure 2.5. The slope of line AB shows the respiration rate of the microorganisms. At point B, air is pumped into the culture and the dissolved oxygen concentration increases as a function of time. Assuming the re-aeration is fast enough not to have an effect on cell growth, the dissolved oxygen concentration will soon reach the steady-state value (point C). The curve BC represents the difference between the oxygen transfer rate and the oxygen uptake rate of the cells in the medium. The material balance of dissolved oxygen concentration in the liquid medium over the line ABC is expressed as:

$$\frac{dC}{dt} = k_La(C^* - C) - q_oX \quad (2-8)$$

where

$$q_o = \text{the specific oxygen uptake rate (mmol O}_2 \text{ g}^{-1} \text{ cell mass h}^{-1}\text{)}$$

The slope of the line AB gives the term q_oX . The equation can be rearranged as:

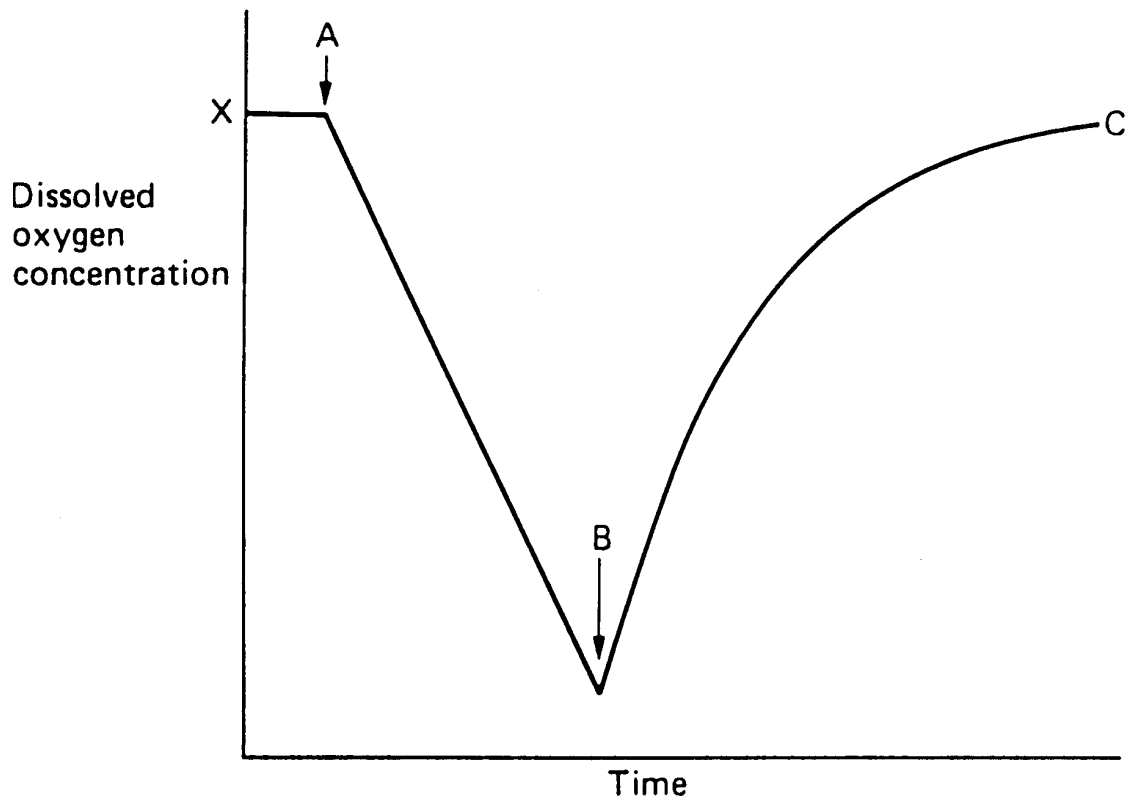


Figure 2.5 Relationship between dissolved oxygen concentration and time in dynamic gassing out method (Stanbury et al, 1995).

$$C = -\frac{1}{k_L a} \left[\left(\frac{dC}{dt} + q_o X \right) \right] + C^* \quad (2-9)$$

This equation is a linear equation between the term $(dC/dt + q_o X)$ and C . A plot with C on the y-axis and $(dC/dt + q_o X)$ on the x-axis will result in a straight line, which has a slope equal to $-1/k_L a$ and an intercept equal to C^* .

The advantage of this method is that it is easy to determine the $k_L a$ value by measuring the dissolved oxygen concentration as a function of time. However, there are two disadvantages of this method. First, when the air supply is turned off, the dissolved oxygen concentration at point B has to be above the critical dissolved oxygen concentration ($C_{critical}$). If the dissolved oxygen concentration is below $C_{critical}$, anaerobic metabolism will occur rather than the aerobic metabolism. Second, this method requires an oxygen probe with fast response time; otherwise the result will be less accurate.

2.4.3 Sodium sulfite oxidation method

Cooper et al (1944) presented the sodium sulfite oxidation method. This method uses the oxidation of sodium sulfite to sodium sulfate in the presence of catalyst (Cu^{++}). The oxidation reaction follows the equation



The reaction rate is independent of both sulfite concentration and oxygen concentration. Oxygen is fed into the solution and immediately consumed in the sulfite oxidation. The oxidation rate is faster than the oxygen transfer rate so the oxygen transfer rate is the limiting factor of this method and the concentration of oxygen in the liquid is zero at all time. The $k_L a$ value can be calculated from the equation:

$$N_A = k_L a (C^*) \quad (2-11)$$

To measure the oxygen transfer rate (N_A) in a fermentor, a 0.5 M sodium sulfite solution containing at least 10^{-3} molar Cu^{++} is added to the fermentor. Air is sparged into the stirred reactor for a given time interval (depending on the aeration and agitation). The aeration and agitation are stopped and a sample is taken. The sample is mixed with an excess of iodine reagent. After that, this sample is titrated with standard sodium thiosulphate solution ($\text{Na}_2\text{S}_2\text{O}_3$) to a starch indicator end point. The slope of a graph of the volume of the thio sulphate titration versus sample time is used to calculate the oxygen transfer rate. N_A divided by C gives the k_La value.

The sodium sulfite oxidation method is simple and eliminates some difference from reactor geometry for each fermentor. However, this method consumes time for the oxidation. Some chemicals such as amino acids, proteins, and fatty acids affect the accuracy of the results (Bell and Gallo, 1971). The rheology of the sodium sulfite solution is different from that of the fermentation broth. The k_La value determined with this method does not represent the true k_La value of fermentation.

2.4.4 Direct measurement method

The direct measurement method uses an oxygen-balance technique to measure the oxygen transfer rate based on the difference in oxygen concentration in the air entering and exiting the fermentor. This oxygen balance technique determines directly the amount of oxygen transported into the broth. From a mass balance at steady state, the oxygen transfer rate can be determined from the equation (Wang *et al*, 1979):

$$N_A = (7.32 \times 10^5 / V_L) (Q_i P_i y_i / T_i - Q_o P_o y_o / T_o) \quad (2-12)$$

where

- V_L = the volume of liquid in the fermentor (m^3),
- Q_i and Q_o = the volumetric air flow rate measured at fermentor inlet and outlet (L min^{-1}),
- P_i and P_o = the total pressure measured at fermentor inlet and outlet (atm absolute),

T_i and T_o = the temperature of gas measured at fermentor inlet and outlet (K),
 y_i and y_o = the mole fraction of oxygen measured at fermentor inlet and outlet (mol O₂ mol⁻¹), and
 $7.32 \cdot 10^5$ = the conversion factor equaling
 (60 min/h)[mol/22.41(STP)](273 K/1 atm)
 STP is standard temperature and pressure; T at 273 K, P at 1 atm.

To determine $k_L a$, the concentration of oxygen in the broth (C) is measured in the fermentor. For small-scale fermentors, there is no problem in determining where in the fermentor to measure C , because the content is well mixed. C^* is the equilibrium dissolved oxygen concentration at the outlet (C^*_{out}). The $k_L a$ value is calculated from the equation:

$$k_L a = N_A / (C^*_{out} - C) \quad (2-13)$$

For large-scale fermentors, C is the average value of dissolved oxygen concentration measured at many positions in the fermentor. The C^* measured at the gas outlet and gas inlet is different so a logarithmic mean value for the equilibrium dissolved oxygen concentration is used as shown:

$$k_L a = N_A / (C^* - C)_{\log \text{ mean}} \quad (2-14)$$

and

$$(C^* - C)_{\log \text{ mean}} = (C^*_{in} - C) - (C^*_{out} - C) / \ln [(C^*_{in} - C) / (C^*_{out} - C)] \quad 2-15$$

where C^*_{in} , C^*_{out} are the equilibrium dissolved oxygen concentration at the gas inlet and gas outlet, respectively.

This method is the most reliable procedure for measuring $k_L a$, and allows determination from a single point measurement. The important advantage is that it can be applied to fermentors during normal operation. This method is the most accurate, but

it requires accurate instrumentation for oxygen analysis, flow, pressure, and temperature measurements.

2.5 Microbubble Dispersion unit

In the early 1970s, Sebba (Chemical Engineering Department, Virginia Polytechnic Institute and State University, Blacksburg, Virginia) first described the term microfoam. Microfoam is a method of forming colloidal dispersions of gas in liquid. He hypothesized that microfoam could improve aeration. The microfoam is produced by using surfactant to diminish the bubble size and to prevent the coalescence of air bubbles. Since the capacity of his initial microfoam generator was not sufficient to supply large-scale production, the colloidal gas aphrons (CGA) generator was developed (Sebba, 1985). The term microbubble dispersion has been used instead of CGA because the generator produced a mixture of CGA-size bubbles (20-70 μm) and large bubbles (3-5 mm) (Kaster, 1988). The microbubble dispersion generator was sequentially used to supply very small bubbles with good stability for an aerobic fermentation (Bredwell *et al*, 1995, Kaster, 1988).

2.5.1 Characteristics of Colloidal Gas Aphrons

According to Sebba (1987), “an aphron is made up of a core which is often spherical, but is not necessarily so, of an internal phase, usually liquid or gas, but not excluding solid, encapsulated in a thin aqueous shell”. The thin liquid shell (film) is a body of liquid which has two surfaces separated by a short distance measured in nanometres. Surfactant molecules at the thin film give aphrons colloid properties. Because of the surfactant effects in water, a colloidal gas aphron (CGA) produces an effective barrier against coalescence with adjacent aphrons. The characteristics of CGA are compared to those of a normal sparged gas bubble in Figure 2.6.

A CGA consists of an inner gas phase surrounded by a soapy shell. The soapy shell has an inner and outer surfaces. The inner surface of the shell contacts the gas bubble; whereas, the outer surface of shell contacts the bulk liquid. These two surfaces

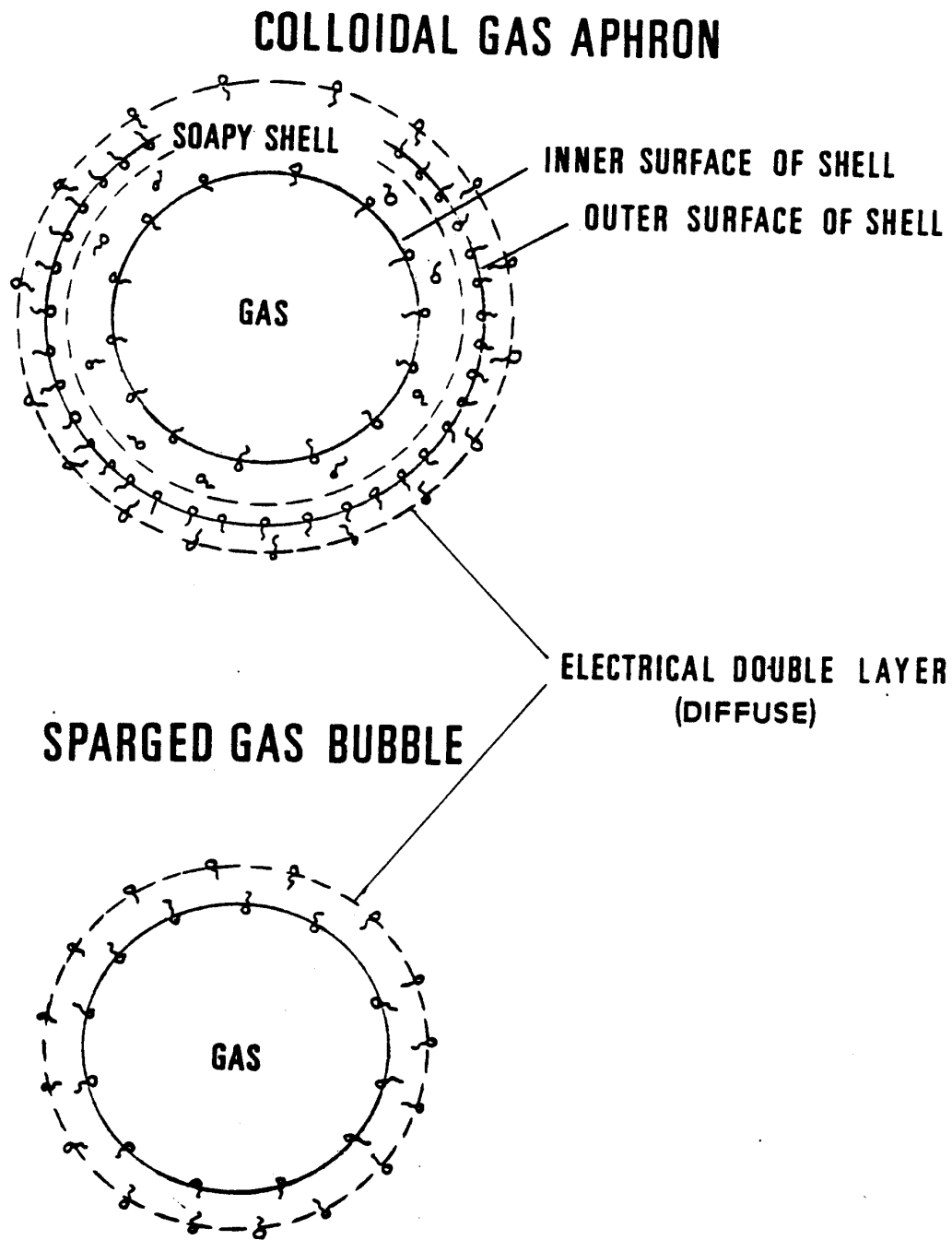


Figure 2.6 Colloidal gas aphron and sparged air bubble structures (Kaster, 1988).

have surfactant monolayers absorbed on them. Water near the two surfaces is different from the bulk water because the water near the surfaces has more hydrogen bonds than the bulk water. This water phase positions the surfactant molecules with the hydrophilic hydrocarbon head pointing inwards and the hydrophobic hydrocarbon tail pointing outwards as shown in Figure 2.6. With this orientation, the CGAs are prevented from coalescing. An electric potential gradient is induced by the orientation of the hydrophilic hydrocarbon heads at the interface of the air bubble. CGAs created with the same surfactant will have similar surface charges and will not collide together. The CGAs have a long half-life of 5 minutes. The combination of these two effects results in foam that can be pumped in a pipe.

The first device for generating micron bubbles (Sebba, 1971) was based upon rapid flow of the surfactant solution through a venturi throat, at which point air was admitted through a fine orifice (Figure 2.7). Although this method could produce a dispersion of bubbles ranging from 25 to 50 μm in diameter at a concentration of 65% volume of gas in the water, the production was comparatively slow as it required recycling of the dispersion to build up the concentration. The venturi device required large recirculation velocities in order to form a uniform bubble size distribution. This created problems for scale-up.

In 1985, Sebba introduced an improved CGA generator design shown in Figure 2.8. A spinning disk approximately 5 cm in diameter is mounted horizontally about 2-3 cm below the surface of the surfactant solution. Dimension of the generator and concentration of surfactant solution are not critical. The disk needs to rotate at approximately 4000 RPM to produce an average bubble size of 25 μm .

Based on the benefit of the CGA properties, the CGA is utilized in many applications: fermentation, stripping of dissolved gases from water, and removal of ash forming materials from coals (Sebba, 1987). To apply the technique to fermentation, the CGA generator had to be modified because direct contact with the fermentation broth in an open environment led to contamination by microorganisms in the surrounding air.

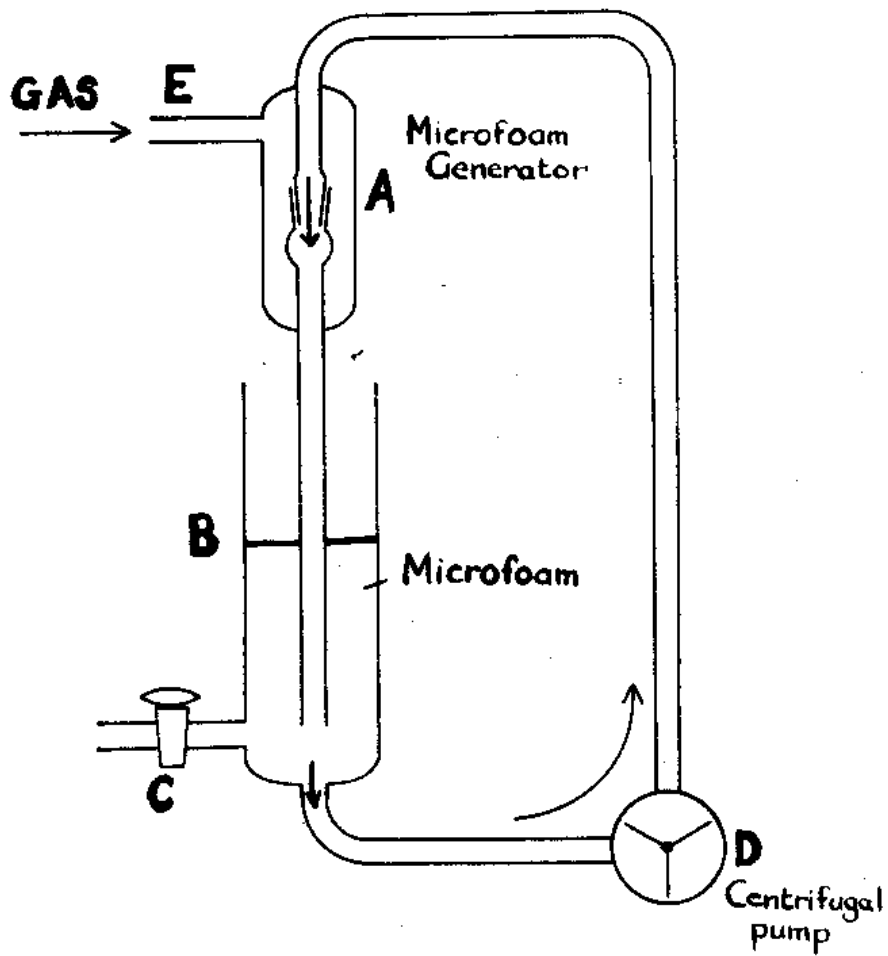


Figure 2.7 The microfoam generator (Sebba, 1971).

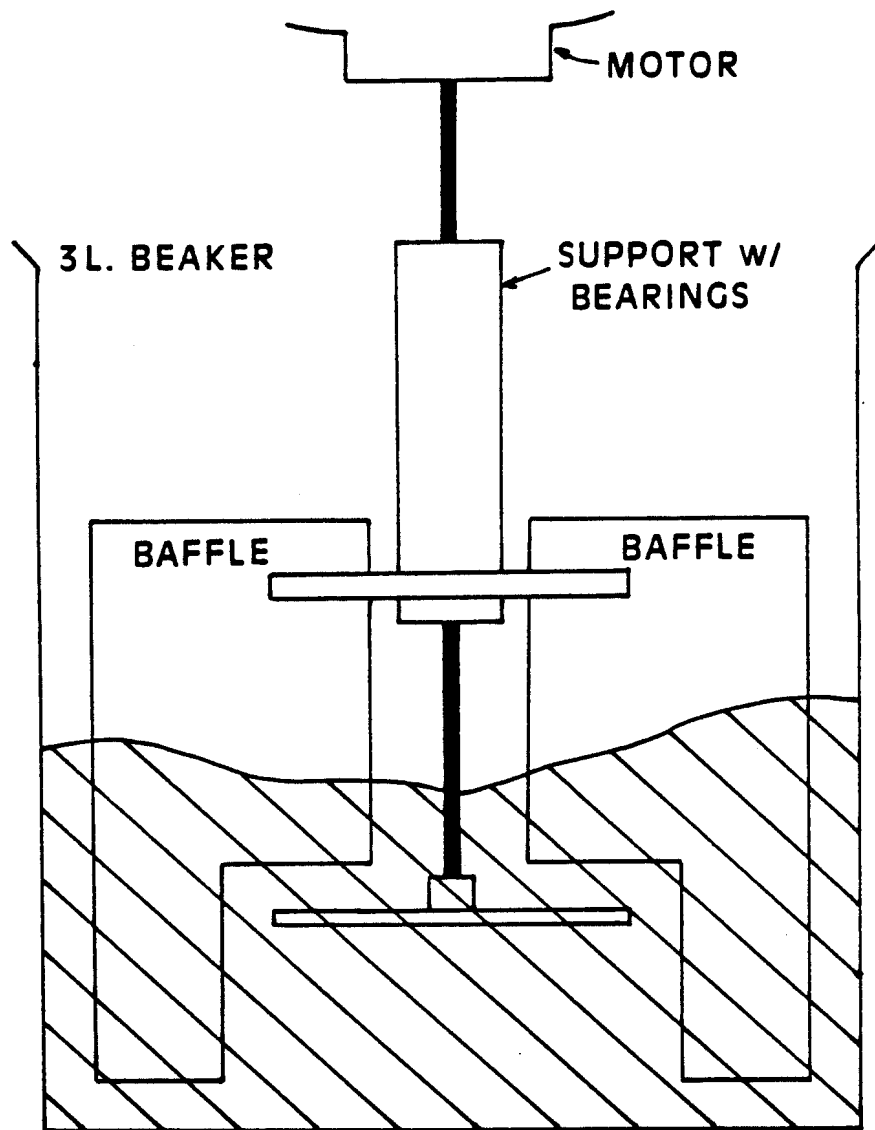


Figure 2.8 The spinning disk CGA generator (Sebba, 1985).

2.5.2 Microbubble dispersion in fermentation

The many possible applications of colloidal gas aphrons (CGA) depend upon their properties: the buoyancy of the encapsulated gas, adherence of particles to the encapsulating shell, low viscosity of the system to pump from the CGA dispersion unit, and the large surface area produced by the very small bubbles. For an aerobic fermentation, the rate at which oxygen can be provided to the growing microorganisms determines the rate of fermentation. Oxygen can be provided by sparging, but the residence time of larger bubbles is quite short. Much of the filtered air introduced into fermentor exits without contributing to the growth of microorganism; it is wasted. Because of CGA properties, it is hypothesized that the oxygen transfer rate can be improved by incorporating CGA dispersion instead of normal air sparging system.

Kaster (1988) used the term microbubble dispersion (MBD) instead of CGA dispersion when he grew Baker's yeast in a 1-liter fermentor. His generator produced a mixture of CGA-size bubbles (20-70 μm) and some large bubbles (3-5 μm). Kaster (1988) modified the CGA generator to protect the foam from contamination (Figure 2.9). The volumetric oxygen transfer coefficient (k_{La}) apparently increased when the MBD generator (operated at 100 RPM) was used to supply oxygen to a 1-liter fermentor. Hensirisak (1997) used the MBD generator to supply oxygen to a 20-liter fermentor and reported that the oxygen transfer rate increased relative to air sparging. For an anaerobic fermentation, Bredwell and Worden (1998) applied the MBD to increase the mass transfer of synthesis gas to produce ethanol and butanol.

2.6 Scale-up in fermentation

Scale-up means increasing the volume of fermentation. The scale-up of bioprocesses is divided into three stages: laboratory scale (also referred to as bench scale), pilot plant and plant scale (also referred to as production scale) (Wang *et al*, 1979; Ju and Chase, 1992). Basic screening procedures and all operating conditions for cell culture in shake flasks and 1 or 2 liter fermentor are referred to as laboratory scale (bench

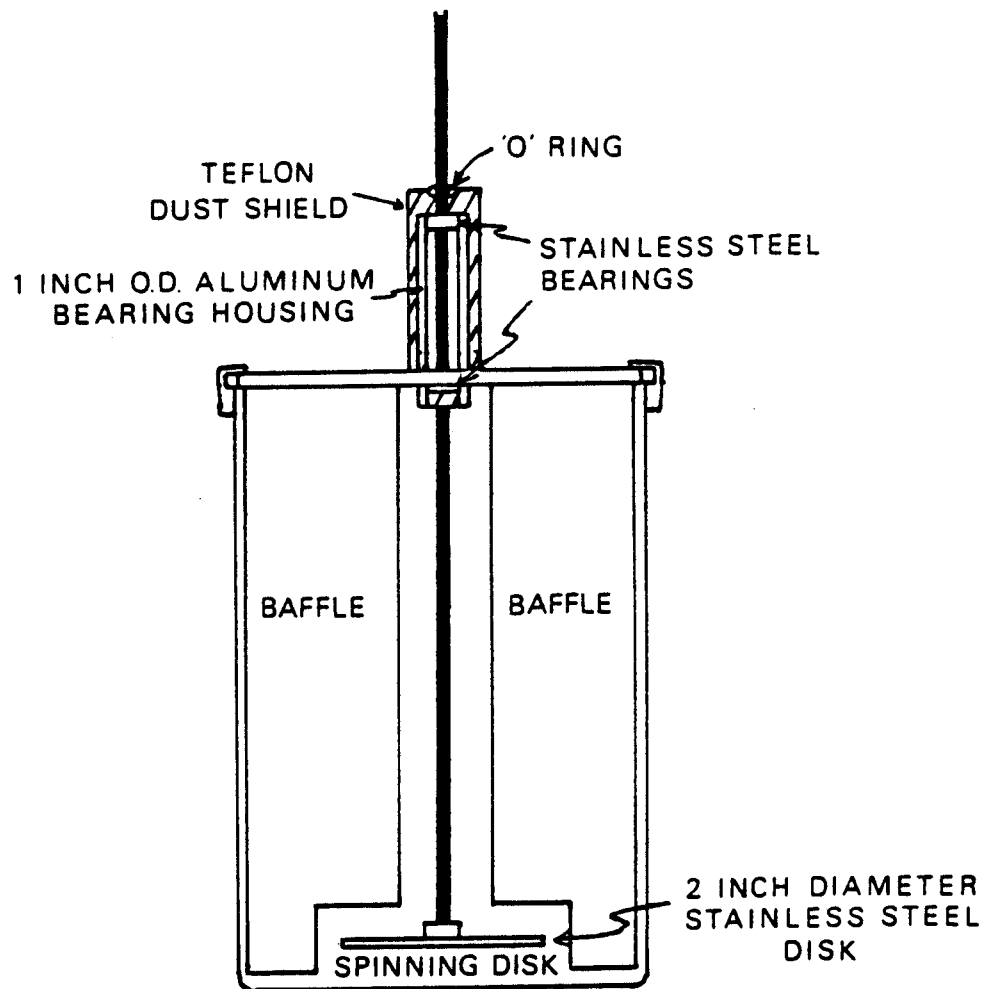


Figure 2.9 The microbubble dispersion generator (Kaster, 1988).

scale). Pilot plant scale, where the optimal conditions of process operation are determined, varies from 40 – 1000 liters. In plant scale or production scale, the fermentors and all of the auxiliary service facilities such as sterilization equipment are designed and tested with close attention to the economics of the process. The objective of scale-up is to increase the size of the equipment without reduction in yield per unit volume.

2.6.1 Scale-up consideration

The problems in process scale-up result from the increased size of each unit. The major factors involved in scale-up are inoculum development, sterilization, and environmental parameters. Inoculum medium for production scale is different from the medium utilized in laboratory scale or pilot-plant scale. Since the production medium is used in large volumes, the cost of the medium should be low. The design of production medium is determined not only by the cell mass production but also by the maximum product formation. Chemical properties in the production medium differ from those in the laboratory medium and may change the cell mass production and the product formation as compared to the product formation achieved in the laboratory-scale tests.

After the medium is blended for use in production-scale run, it must be sterilized to prevent contamination. Steam normally is used to sterilize the fermentation medium. The sterilization of a large volume of medium takes more time than a small volume of medium. During the longer sterilization time, the quality of the medium may be changed because of nutrient degradation during the sterilization. The sterilization regime often has to be adjusted to give the best quality medium.

The increase in scale also affects the environmental parameters in fermentors. The change in environmental parameters such as dissolved oxygen concentration, shear condition, and temperature may increase or decrease the cell mass production and the product formation. The environmental parameters deal with transport phenomena (momentum, heat and mass transport). There are three different phenomena involved in fermentor design: thermodynamic phenomena, microkinetics (intrinsic) phenomena, and transport phenomena (Mavituna, 1996). Transport phenomena is dependent on scale but

thermodynamic and microkinetics are scale-independent phenomena. Transport phenomena tend to dominate in scale-up.

2.6.2 Scale-up method for fermentor

Agitation and aeration directly influence transport phenomena in the fermentor; therefore, the study of scale-up is based on the agitation and aeration of the fermentor (Maxon and Johnson, 1953). To solve the scale-up problems, the principal environmental parameters affected by aeration and agitation (oxygen concentration, shear, bulk mixing) are identified and studied. The process variables (airflow rate and agitation speed) are calculated for the large-scale fermentor to give the same environmental parameters as in the small-scale fermentor.

Ju and Chase (1992) suggest that the following environmental parameters should be kept constant during scale-up:

- reactor geometry;
- volumetric oxygen transfer coefficient;
- maximum shear rate;
- power input per unit volume of liquid;
- volumetric gas flow rate per unit volume of liquid;
- superficial gas velocity;
- mixing time;
- impeller Reynolds number;
- momentum factor.

The standard geometry is assumed to be the optimum geometry for reactors. The standard geometry is shown in Figure 2.10 (Tatterson, 1991). All scale-up studies of fermentors are developed experimentally using geometrically similar reactors of different sizes. Instead of using geometrically similar reactors, the constant mixing time is used in a viscous non-Newtonian system. This criterion is unnecessary for normal fermentations and requires more power. Impeller Reynolds Number and momentum factor criteria are

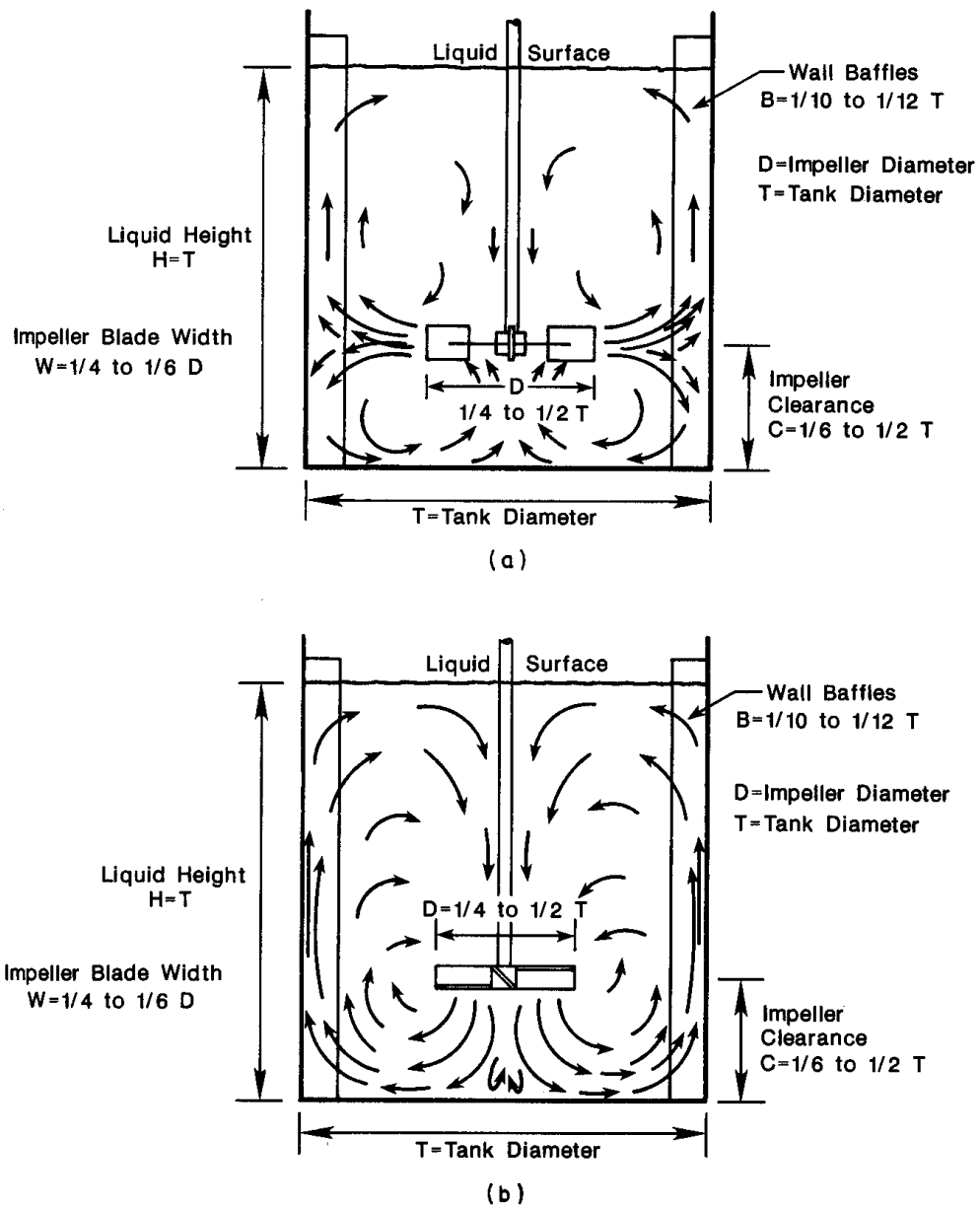


Figure 2.10 The standard geometry of mixing tank (Tatterson, 1991).

not considered in calculating the effect of aeration on the process.

The most important problem in aerobic fermentations is oxygen transfer. To maintain the oxygen transfer rate as vessel size increases, scale-up of aerobic fermentations is typically done with a constant volumetric oxygen transfer coefficient (Karow *et al*, 1953, Andrew, 1982). The criterion to keep power input per unit volume of liquid and maximum shear constant is important when growing shear-sensitive microorganisms. The volumetric gas flow rate per unit volume of liquid (VVM) criterion and the superficial gas velocity (V_s) criterion are contradictory to each other when applied to geometrically similar fermentors. If the VVM is maintained constant, the superficial gas velocity will increase directly with the scale ratio. The choice between the volumetric gas flow rate per unit volume of liquid criterion and the superficial gas velocity criterion has to be carefully considered for the process.

Scale-up rules generally used in the fermentation industries are constant power input per unit volume of liquid (P/V), constant k_La , constant impeller tip speed (v_{tip}), and constant dissolved oxygen concentration (Mavituna, 1996). Frequency of use of the various rules is given in Table 2.3. For scale-up of aerobic fermentation, the oxygen transfer rate is the important factor (Hubbard, 1987; Humphrey, 1998).

After the fermentation has been accomplished successfully in a laboratory-scale reactor, a scale-up procedure (Hubbard, 1987) can be calculated as follows.

For the plant-scale fermentor:

- choose the required volume
- calculate the dimensions based on geometric similarity
- establish the scale-up strategy to be used $(k_La)_{plant} = (k_La)_{lab}$
- calculate air flow rate (Q) and agitation rate (N) with either method 1 or 2 (see below)
- estimate power consumption

Method 1:

- determine Q using VVM constant
- calculate N from power and k_La correlation.

Method 2:

- determine N using πND constant (v_{tip} constant)

-calculate Q from power and k_La correlation.

The accuracy of this procedure depends on the relationship between k_La and power consumption. This procedure is used widely in scale-up aerobic fermentation. However, poor mixing and hidden auxotrophy are two factors still uncertain on scale-up (Humphrey, 1998). Success in scale-up of aerobic fermentation requires the preliminary calculation of environmental parameters and then trial and error testing to achieve the same results as in the laboratory scale

Table 2.3 Scale-up Criteria in Fermentation Industries

Scale-up criterion used	Percentage of industries
Constant P/V	30
Constant $k_L a$	30
Constant v_{tip}	20
Constant pO_2	20

From: F. Mavituna, Strategies for bioreactor scale-up, In: *Computer and Information Science Application in Bioprocess Engineering* (A. R. Moreira and K. K. Wallace), Kluwer Academic Publishers, Dordrecht, Netherlands, 1996, pp.129.

CHAPTER 3

MATERIALS AND METHODS

3.1 Laboratory-scale fermentor

The one-liter fermentation tests were conducted in a 1.6-liter bench top, Bioflo III fermentor (New Brunswick Scientific Co. Inc., NJ). The fermentor can be used for both batch and continuous culture. The fermentor is equipped with four baffles and two 6-flat-blade disc-turbine impellers. The stainless steel headplate, bottom dish, and penetrations are polished to a mirror finish to minimize contamination. The system is equipped with built-in controllers for pH, dissolved oxygen (DO), foam/level, agitation, and temperature. It also includes pumps for acid, base, antifoam, and nutrient addition.

The pH is measured by a glass electrode (Ingold) and controlled by a Proportional/Integral/Derivative (PID) controller. The pH controller operates two peristaltic pumps to maintain the pH value. Sterile air was supplied to the broth through the ring sparger and was controlled by the needle valve of the flowmeter. A DO electrode (Ingold) was used to measure the dissolved oxygen concentration. A PID controller controlled the agitation speed with an optical encoder coupled to the motor shaft. The medium temperature was measured with platinum Resistance Temperature Detector (RTD) and controlled by a PID controller. Foam was controlled during the fermentation by the antifoam probe (conductivity probe), which was located in the headplate and adjustable in height from the medium surface. The Bioflow III unit cannot be sterilized in place, but must be disassembled and sterilized in an autoclave.

3.2 Pilot-scale fermentor

The 50-liter fermentations were run in a 72-liter fermentor (BIOSTAT[®] U 50, Braum Company, Germany). This fermentor consists of a basic unit, a stirrer drive unit, a culture vessel, and a measurement and control system. The basic unit is a sturdy basic frame accommodating all energy and supply systems and related installations including

pipng as well as temperature control and air/gas supply systems. The stirrer drive system is designed as a bottom drive. The culture vessel is mounted with four baffles and the stirrer shaft is equipped with three 6-flat-blade disc-turbine impellers. The culture vessel can be sterilized *in situ* by steam heated jacket. The measurement and control system is contained in a compact 19-inch cabinet integrated into an open stainless steel frame.

A pressurized closed-loop hot water system was used to control the temperature of the culture medium in the fermentor. The temperature was measured by a Pt-100 resistance thermometer and controlled by PD-PID controller with pulsewidth-modulated outputs for heating and cooling. Air was supplied into the bottom of the vessel via a sparger and was measured by a rotameter with manually operated valve. A polarographic pO₂ electrode (Ingold) was used to measure the dissolved oxygen. The agitation speed was measured by a DC tachogenerator integrated into the motor and controlled by PI controller with cascade control of armature current. The pH of the culture medium was measured by a combination electrode (InFit 764-50[®], Ingold) and maintained by PI controller for acid and alkali pumps.

3.3 Organism and medium

Baker's yeast, *Saccharomyces cerevisiae* ATCC 4111, was used in this study. Stock culture was maintained on a Difco Yeast-Malt (YM) agar medium at 4°C and was subcultured every month to maintain viability. Difco YM broth was used to prepare preculture and fermentation media. The YM broth consisted of yeast extract, 3 g, malt extract, 3 g, peptone, 5 g, and dextrose, 10 g. The YM broth is suitable for yeast growth and has natural surfactant property, which can stabilize the microbubbles (Kaster, 1988). The YM broth used in this study was laboratory grade purchased from Fisher Scientific (Pittsburg, PA). The fermentation medium consisted of 21 g of YM broth dissolved in 500 mL deionized water and then deionized water was added to increase the volume to 1000 mL.

1 M ammonium hydroxide (NH₄OH) was prepared by measuring 71.43 mL concentrated NH₄OH (14 M) and made up to 1000 mL with deionized water. 0.5 M HCl

was prepared by measuring 29.74 mL concentrated HCl and made up to 1000 mL with deionized water. Both NH₄OH and HCl were reagent grade chemicals purchased from the chemical stock room at the Chemistry Department of Virginia Polytechnic Institute and State University.

3.4 Fermentation

3.4.1 Preliminary experiments

Preliminary experiments using baker's yeast were conducted in 500-mL Erlenmeyer flasks to provide the growth pattern of the yeast. The YM broth solution (100 mL) was sterilized at 121°C for 15 minutes in an autoclave (C2260, Barnstead in Sybron Co, MA). Three loops of the stock culture were transferred to 100 mL of sterilized YM broth solution and the inoculum was incubated at 35°C on a platform shaker (Innova 2000, New Brunswick Scientific Co Inc) agitated at 130 rpm for 24 hours. During the shake-flash fermentation, 2 mL-samples were taken with Eppendorf pipette (series 2000, Brinkmann Instruments) every hour. The optical density (OD) of the sample was measured at 620 nm with a Spectronic 1001 instrument (Milton Roy, NY). The fermentation was continued until the stationary phase of the microorganism was reached. A growth curve for the baker's yeast was developed and the mid-log phase was determined. Additionally, a calibration curve was developed by first measuring the OD of the sample and then drying the sample to a constant mass at 80°C in a Thelco laboratory oven (Model 70, Precision Scientific Co, IL). The mass of the oven-dried yeast was plotted against the OD. This curve was subsequently used to determine the cell mass concentration of starter culture and the fermentation broth.

3.4.2 1-liter fermentation with ordinary sparger air

YM broth (1.05 g) was dissolved in 50 mL deionized water and then sterilized at 121°C for 15 min in the C2260 autoclave. After sterilization, 8 mL of sterilized water was added to the flask to make up the sterilized YM broth to 50 mL. Starter culture was

prepared by transferring three loops of the stock culture to a 250 mL Erlenmeyer flask containing 50 mL of sterilized YM broth. Starter culture was incubated at 35°C for 18 hours (mid-log phase) on the platform shaker at 130 rpm. The OD of the starter culture was determined and it was then used to inoculate the fermentation medium to an initial cell concentration of 0.13 g L⁻¹.

The YM broth was prepared for the 1.0 L fermentation as described in section 3.3 (21 g of YM broth in 1000 mL of deionized water). The pH probe was calibrated before the sterilization. The pH measuring system was calibrated using two buffer solutions of known pH (4 and 7). The selector switch and the mode switch were set to pH and ZERO, respectively. The pH probe was immersed into a pH 7 buffer solution and the display was adjusted to read pH 7 with INC/DEC switch. The pH probe was then immersed into a second buffer solution (pH 4) and the mode switch was set to SPAN. The display was set to read pH 4 with the INC/DEC switch. The complete fermentor assembly with medium was sterilized at 121°C for 25 minutes in an autoclave (AMSCO, American Sterilizer Company, PA). After the sterilization, about 200 mL of sterilized water was added to the fermentor through the inoculum port to make up the volume to 1.0 liter. When the medium cooled down to 35°C, the dissolved oxygen (DO) probe was calibrated as follows. The DO probe cable was removed from the DO probe and the selector switch was set to DO and the mode switch was set to ZERO. The display was adjusted to read zero with the INC/DEC switch. The DO probe cable was connected to the DO probe and the mode switch was set to SPAN. Air at 1.0 L min⁻¹ was introduced into the vessel and the agitation speed was set to 500 rpm. When the DO value stabilized after 30 min, the DO value was adjusted to 100 % saturation with the INC/DEC switch. The DO value at 100 % saturation of YM broth at pH 6 and 35°C was assigned a value of 0.19 mmol O₂ L⁻¹ (Kaster, 1988), which was assumed to be the saturated dissolved oxygen concentration (C^*).

About 49 mL of starter culture (concentration 8.5 g L⁻¹ measured by OD method) was prepared for inoculation. The cap of the inoculum port was screwed off and the starter culture was introduced into the fermentor. The inoculum port screw was wiped with ethanol-soaked paper towel and screwed back on. The fermentation was conducted at 35°C at pH 6. The temperature of the fermentor was controlled by cooling/hot water in

the jacket of the fermentor. The pH of the broth was adjusted with automatic periodic addition of 1.0 M ammonium hydroxide. A peristaltic pump, which was connected to the pH probe, was used to add the ammonium hydroxide to the fermentation broth. The agitation speeds were set at 144 rpm or 476 rpm depending on the parameter being measured. Air was supplied to the fermentation medium through the sparger ring under the six-blade impeller. The air flow rate was set at 100 mL min^{-1} using a rotameter. This flow rate was equivalent to 0.1 volume of air per volume of medium per minute (0.1 VVM).

Aliquotes were taken from the sample port every hour for 24 hours. A 10-mL plastic syringe attached to the sampling port facilitated the sampling procedure. A 4-drum (15 mL) vial was tightened to the sampling port and the sample valve was opened and the syringe was slowly released. When the desired volume of sample was obtained (5 mL), the sample valve was closed. The cell mass concentration for 2 mL samples were measured in the Spectronic 1001 spectrophotometer using the calibration curve previously determined. About 1.5 mL of the sample was centrifuged ($20000 \times g$ for 10 min) and the supernatant was used for glucose analysis. The dissolved oxygen saturation values (DO) were recorded immediately after taking the sample.

3.4.3 1-liter fermentation with natural surfactant-stabilized microbubble

For the microbubble dispersion tests, the fermentation conditions were the same as the air sparging system except that a microbubble dispersion (MBD) generator was used to supply air instead of the normal air supply. To maintain the broth volume (1 L) in the fermentor, the MBD generator was filled with 200 mL sterilized YM broth solution (4.2 g YM broth in 200 mL of deionized water). The MBD generator containing the YM broth solution was sterilized at 121°C for 15 min in an AMSCO autoclave. The experimental set-up for a MBD experiment is shown in Figure 3.1. The peristaltic recycle pump was used to transfer the fermentation broth to the MBD generator at approximately 40 mL min^{-1} . Air at 100 mL min^{-1} was introduced into the MBD generator and the agitation speed of the MBD generator was set at 4000 rpm to create the

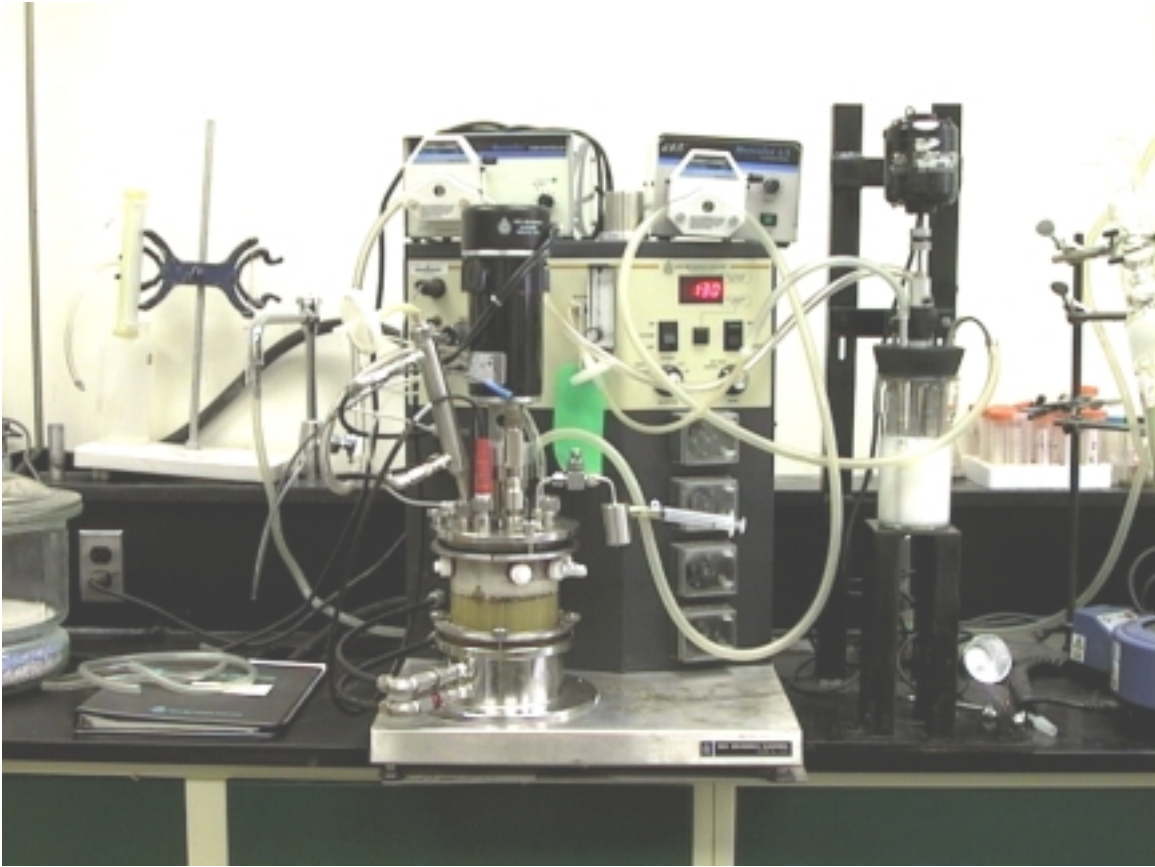


Figure 3.1 1-liter fermentation with microbubble dispersion unit

microbubble dispersion. The microbubble dispersion was delivered by the MBD pump at 100 mL min^{-1} to the fermentor and introduced through the ring sparger.

3.4.4 50-liter fermentation with ordinary sparger air

Fermentation was carried out at 50 liters working volume in a 72-liter fermentor. Yeast starter culture was prepared in proportion to the scale-up volume. In order to speed up the fermentation, the starter culture was prepared in two stages. In the first stage, a 100-mL culture was prepared and this was used as the starter for the second stage (4 L). The 4-L starter culture was used to inoculate the 50-L fermentor. The YM broth (2.1 g) was dissolved in 50 mL of deionized water and made up to 100 mL with deionized water. The 100-mL YM broth solution was put in a 500 mL Erlenmeyer flask and sterilized at 121°C for 15 min in the C2260 autoclave. After sterilization, 20 mL of sterilized water was added to make up the volume to 100 mL. The starter culture was prepared by transferring three loops of the stock culture to the flask containing 100 mL of sterilized YM broth solution. The starter culture was incubated at 35°C for 18 hours (mid-log phase) on the platform shaker at 130 rpm.

The 2-L YM broth solution was prepared by dissolving 4.2 g YM broth in deionized water and made up to 2 L. The YM broth solution was sterilized at 121°C for 15 min in the AMSCO autoclave and the sterilized water was added to make up the volume to 2 L. The second starter culture was commenced by adding the 100-mL starter culture to a 4 L Erlenmeyer flask containing the sterilized YM broth solution. The second starter culture was incubated at 35°C for 18 hours (mid-log phase) on the platform shaker at 130 rpm.

The pH electrode was calibrated before filling the vessel. For calibration, the temperature compensation was set to manual mode and the temperature of the buffer solution was set at 35°C on the temperature potentiometer. The pH electrode was rinsed with the deionized water and dipped into the pH 7 calibration buffer. When the pH value was steady, the pH was set to 7 using the pH potentiometer. The pH electrode was rinsed with deionized water and dipped into the pH 4 calibration buffer. When the pH was steady, the value was adjusted to 4 using the slope potentiometer.

The display modules, the stirrer speed control, and the thermostat were switched on. The vessel was filled with 50 liters of deionized water and 1050 g of YM broth was added. The sterilization temperature was set at 121°C using the sterilization temperature potentiometer. The agitation speed was set at 200 rpm (Motor Speed Module). The thermostat module was set to the sterilization-operating mode. The sterilization cycle operated automatically. After the fermentor temperature was cooled down to 35°C, the pO₂ electrode was calibrated. In this calibration, the pO₂ electrode cable was disconnected from the pO₂ electrode, and the pO₂ value was adjusted to 0% oxygen saturation using the zero potentiometer. This method was 97% accurate because almost all of air was gassed out of the fermentation medium by the sterilization (the operating manual of BIOSTAT U50, Braum Company, Germany). The pO₂ electrode cable was reconnected and air at 5.0 L min⁻¹ was bubbled through the fermentation medium until the pO₂ value was stable. The pO₂ value was set to 100% oxygen saturation using the slope potentiometer. The 100% oxygen saturation of YM broth solution at 35°C and pH 6 was equal the maximum oxygen concentration of 0.19 mmol O₂ L⁻¹ (C*) (Kaster, 1988).

Because the objective of these series of experiments in the 72-liter fermentor was to scale-up the 1-liter fermentor, the Hubbard scale-up method (1987) was used to set up the air flow rate. The air flow rate was set at 5.0 L min⁻¹ that was equivalent to 0.1 VVM and the agitation rate was set at 150 and 500 rpm. The temperature of the fermentation medium was maintained at 35°C. The pH of the fermentation medium was set at 6 and maintained automatically with 1 M NH₄OH. The inoculation port was cleaned with ethanol and the blind plug was removed and a plastic funnel was used to add 2.1-L starter culture (8.2 g/L) to the fermentor. Fermentation samples were taken through the lower outlet valve of the fermentor every hour for 24 hours. Each sample was stored in a 4-drum (15 mL) vial in a fridge for 24 hours before analysis. The samples were analyzed for cell mass and glucose concentration using the OD and DNS methods (section 3.5.1 and 3.5.2). About 1.5 mL of the sample was centrifuged at 20000×g for 10 minutes and the supernatant was decanted and used for glucose analysis. The dissolved oxygen saturation (DO) values at 35°C were recorded immediately after taking each sample.



Figure 3.2 50-liter fermentation with microbubble dispersion unit.

3.4.5 50-liter fermentation with natural surfactant-stabilized microbubble

The MBD experiments were set up in the pilot-scale fermentation unit shown in Figure 3.2. The volumetric flow rate of the microbubble dispersion was set at 5.0 L min⁻¹ (0.1 VVM). To deliver the MBD through the sparger ring, the original air connection of the fermentor was disassembled and the brass hose barb was connected to the air connection as shown in Figure 3.3. The MBD was introduced into the sparging ring through the hose barb. Plastic tubing connected the MBD generator to the hose barb. For the recycle system, the sampling port at the bottom of the fermentor was modified by using a polypropylene fitting. A three-way splitter valve was used to divide the broth into sampling and recycle streams. The liquid flow rate in the recycle loop was 1.1 liters/min. The broth samples were taken from the three-way splitter every hour for 24 hours.

3.5 Assays

3.5.1 Dry cell mass concentration

Biomass concentration (grams of dry cell per liter) was determined from the optical density (OD) measurement at 620 nm on a Spectronic 1001 spectrophotometer (Milton Roy, NY). The OD values of samples were measured and the samples were transferred into 10-mL centrifugal tubes. The samples were centrifuged at 4307×g for 10 min and decanted. They were washed, recentrifuged, and decanted. The washed samples were dried at 80°C for 24 hours and weighed. The dry cell mass concentration was calculated using the equation below:

$$C_x = \frac{X_2 - X_1}{V_L} \quad (3-1)$$

where

C_x = the dry cell mass concentration (g L⁻¹),

X_1 = centrifuge tube weight (g),

X_2 = centrifuge tube and cell dry weight (g),



Figure 3.3 The brass hose barb connected to the air connection.

V_L = the culture volume (L)

The culture volume was determined by measuring with 10-mL cylinder. Absorbance at 620 nm was plotted against the dry cell mass. The curve was linear within the OD value of 0 to 0.8. The slope of the curve was 0.85 and the r^2 was 0.9996. When OD values exceed 0.8 absorbance, the sample was diluted to fit into the calibration range and the cell mass concentration was multiplied by the dilution factor.

3.5.2 Glucose concentration

The glucose concentration in the fermentation broth was determined by the dinitrosalicylic acid (DNS) method (Miller, 1959). In this method, DNS reagent was prepared from Rochelle salt, 306g, phenol, 8.132 g, sodium metabisulfite, 8.3 g, phenolphthalein, 3 mL, NaOH, 19.8 g, and 0.1 N HCl. Standard glucose solutions were prepared in concentrations of 0.2, 0.4, 0.6, 0.8, and 1.0 g L⁻¹. 1 mL of standard glucose solution was pipetted into a test tube and 3 mL of DNS reagent was added to it. The mixture was placed in boiling water for 5 minutes to develop color. After 5 minutes, the sample was cooled to room temperature. About 2 mL of the sample was placed in a cuvette and the absorbance at 550 nm was measured. Deionized water was used as a reference. The absorbance of the standard glucose solutions were all measured and plotted against the concentration of glucose. The plot was linear with a slope of 2.48 and the correlation coefficient (r) was 0.9989. To determine the glucose concentration in the fermentation broth, the sample (1.5 mL) was centrifuged at 20000×g for 10 min and decanted. The glucose content of the supernatant solution was measured by the DNS method using the glucose calibration curve determined above.

3.5.3 The major metabolic parameter calculation

The specific growth rate (μ) was calculated from the log phase of the growth curve of the baker's yeast (*Saccharomyces cerevisiae* ATCC 4111). The growth yield of baker's yeast, $Y_s = -(\Delta x/\Delta S)$, was defined as the amount of yeast cells produced per gram of dextrose consumed. The oxygen yield coefficient (Y_o), the amount of cells produced

per gram of oxygen consumed, was obtained from the correlation between the oxygen yield coefficient and growth yield coefficient (Mateles, 1971). The $1/Y_s$ was calculated from the reciprocal of Y_s . From the $1/Y_s$ value, the $1/Y_o$ was calculated from the line of yeast on glucose in Fig 2.4. The Y_o value was determined from $1/Y_o$.

3.5.4 Determination of the k_La values

The volumetric oxygen transfer coefficient (k_La) was determined by the yield coefficient method (Wang et al, 1979). At steady state, the oxygen uptake rate by the cells is equal to the oxygen transfer rate. The k_La value was then calculated from this assumption (see details in section 2.4.1) and shown below:

$$k_La = \frac{\mu X (K' / Y_o)}{(C^* - C)} \quad (3-2)$$

where

- k_La = volumetric oxygen transfer coefficient (h^{-1}),
- μ = specific growth rate (h^{-1}),
- X = cell mass (g L^{-1}),
- K' = conversion factor = 31.25 ($\text{mmol O}_2 \text{ g O}_2^{-1}$),
- Y_o = yield coefficient on oxygen ($\text{g cell mass g O}_2^{-1}$),
- C^* = saturated dissolved oxygen concentration ($0.19 \text{ mmol O}_2 \text{ L}^{-1}$), and
- C = dissolved oxygen concentration ($\text{mmol O}_2 \text{ L}^{-1}$).

To find Y_o , the Y_s had to be determined first. Cell mass concentration at time 0 and late log phase were calculated (see details in section 3.5.1). The cell mass concentration at late log phase subtracted from the cell mass concentration at time 0 was equal to Δx . Glucose concentrations at time 0 and late log phase were determined (see details at section 3.5.2). The $1/Y_s$ and $1/Y_o$ were calculated from the line of yeast on glucose in Figure 2.4. The Y_o value was determined from $1/Y_o$. The dissolved oxygen concentration (C) was determined from the DO value (% saturation dissolved oxygen) interpolated with

the OD value at 100%. For YM broth solution at 35°C and pH 6, the 100% DO was 0.19 mmol O₂ L⁻¹.

CHAPTER 4

RESULTS AND DISCUSSION

4.1 Small scale fermentation

The small-scale fermentation was conducted in a Bioflo III fermentor (New Brunswick Scientific Co. Inc., NJ) using 1-liter working volume. The pH and temperature of fermentation medium were maintained at 6 and 35°C, respectively. The air sparging system and MBD sparging system were used to supply oxygen in the fermentor. Both aeration systems were operated at low (144 rpm) and high (476 rpm) agitation rates. The cell mass, dissolved oxygen, and glucose profile were investigated.

4.1.1 Air sparging system

The cell mass, dissolved oxygen, and glucose profiles of the air sparged fermentation at both agitation speeds (144 and 476 rpm) are shown in Figures 4.1-4.2. The lag phase of both agitation speeds was about 1 hour followed by 8 hours of log phase. The difference between the two fermentations was the cell mass concentration at the stationary phase and the specific growth rates of the two systems. The cell mass concentration at 476 rpm was 2.19 times greater than that at 144 rpm (Table 4.1). The specific growth rate at 476 rpm was also 1.15 times greater than ($p < 0.05$) that at 144 rpm (Table 4.1). The cell mass yield increased 2.2 times as the agitation rate increased from 144 to 476 rpm. The oxygen profiles of both agitation speeds were much different ($p < 0.05$).

The dissolved oxygen concentration at 144 rpm decreased rapidly to almost zero after 8 hours; whereas, the dissolved oxygen concentration at 476 rpm decreased slowly to a steady state value of 16 % saturation after 18 hours. The dissolved oxygen concentration at 476 rpm was 53 times greater than that at 144 rpm (Table 4.1). The high

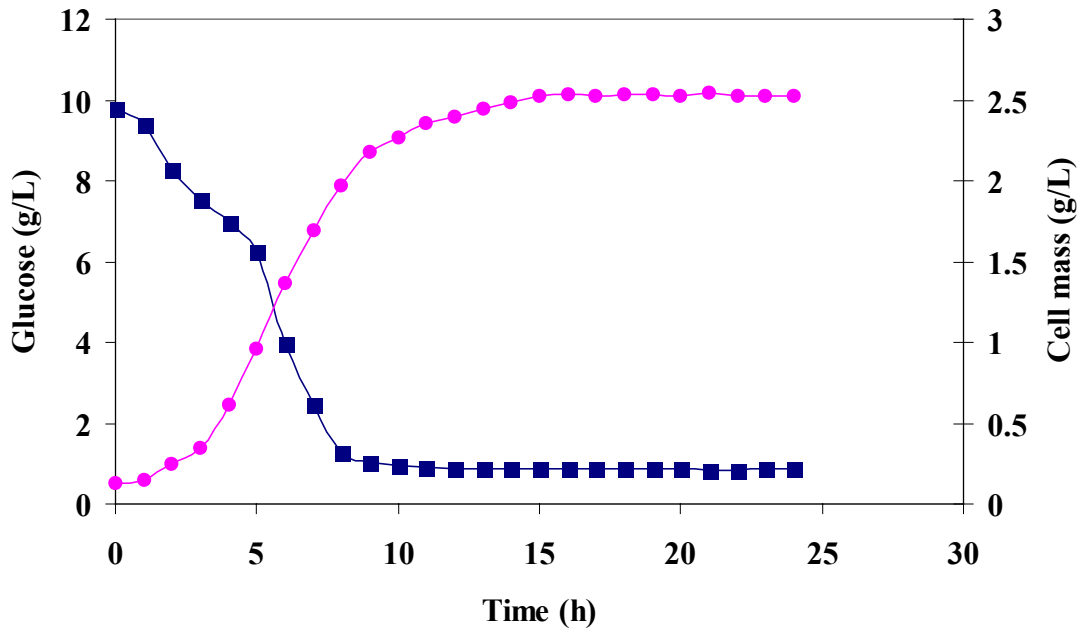
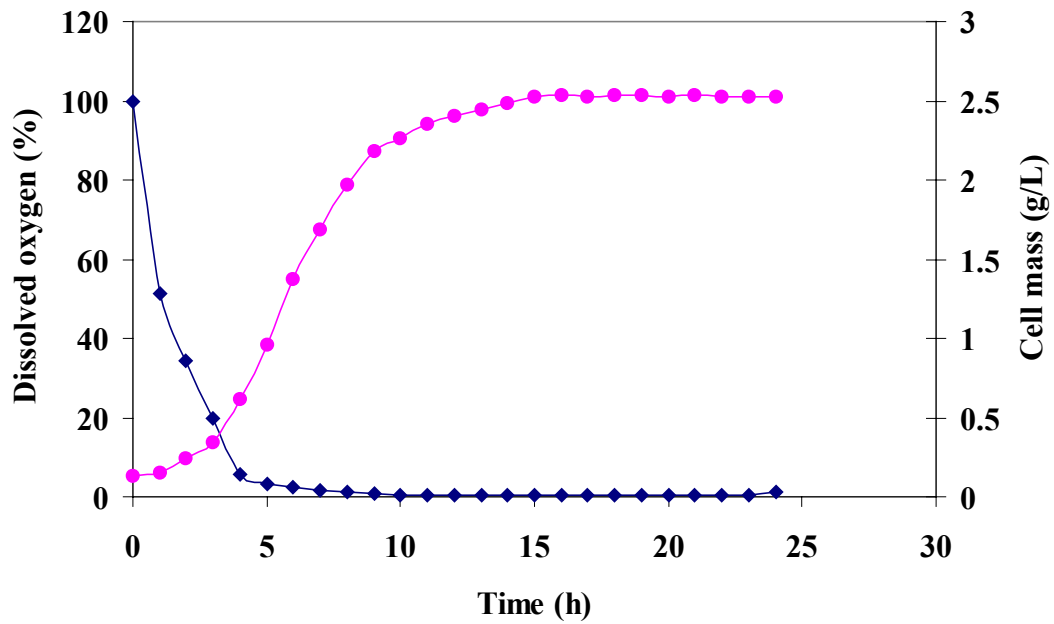


Figure 4.1 1-liter fermentation with air sparging at 144 rpm.

Cell mass concentration (●), dissolved oxygen concentration expressed as % saturation (◆), and glucose concentration (■).

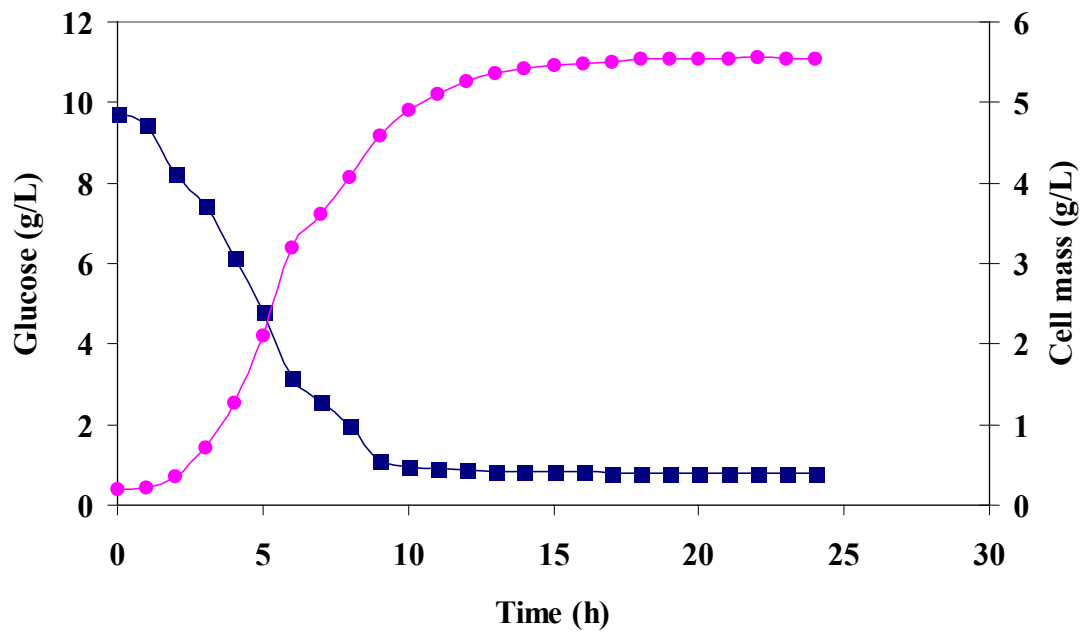
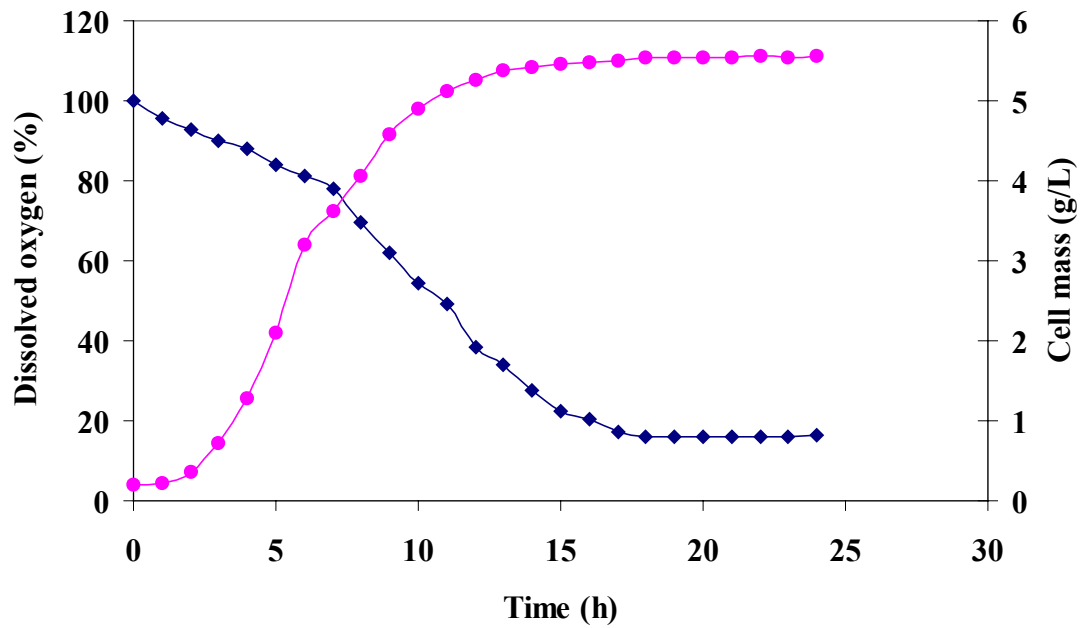


Figure 4.2 1-liter fermentation with air sparging at 476 rpm. Cell mass concentration (●), dissolved oxygen concentration expressed as % saturation (◆), and glucose concentration (■).

Table 4.1 Cell mass concentration, dissolved oxygen concentration, cell mass yield, and specific growth rate of 1-liter and 50-liter fermentations.

Volume (L)	Air supply	Agitation Speed(rpm)	X ^a (g L ⁻¹)	Y _s ^b	DO ^c (%)	μ ^d (h ⁻¹)
1.6	Air	144	2.54±0.08	0.27±0.01	0.3±0.05	0.47±0.02
1.6	MBD	144	3.82±0.14	0.40±0.02	2.2±0.16	0.52±0.01
1.6	Air	476	5.56±0.12	0.60±0.01	16.0±1.17	0.53±0.02
1.6	MBD	476	6.17±0.12	0.66±0.01	30.1±0.40	0.56±0.01
72	Air	150	2.46±0.11	0.26±0.02	1.3±0.26	0.39±0.01
72	MBD	150	4.22±0.18	0.43±0.02	5.4±0.14	0.52±0.01
72	Air	500	5.08±0.07	0.53±0.01	20.8±0.45	0.56±0.01
72	MBD	500	5.57±0.08	0.59±0.01	30.0±0.21	0.59±0.01

^a X = cell mass concentration.

^b Y_s = cell mass yield, no unit (g cell mass L⁻¹/g substrate L⁻¹).

^c DO = dissolved oxygen concentration.

^d μ = the specific growth rate.

agitation speed increased the oxygen transfer because the air sparging system had insufficient gas distribution at low agitation speed (Doran, 1995). As the agitation speed increased, the gas dispersion in the fermentation medium also increased.

4.1.2 MBD sparging system

The air sparging system was supplemented with the MBD sparging system. Figures 4.3-4.4 show the cell mass, dissolved oxygen, and glucose profiles of the fermentation at low and high agitation speeds (144 and 476 rpm). The effect of different agitation rates (144 and 476 rpm) on the above parameters was less pronounced in the MBD relative to the air sparging system. The cell mass concentration and specific growth rate at high agitation rate were greater than that at low agitation rate ($p < 0.05$). The cell mass concentration at 476 rpm was 1.61 times greater than that at 144 rpm, while the specific growth rate at 476 rpm was only 1.08 times greater than that at 144 rpm. From these effects, the cell mass yield increased 1.6 times higher than that at low agitation rate. At 144 rpm, the dissolved oxygen concentration was steady at 2.2 % saturation after 15 hours. The dissolved oxygen concentration at 476 rpm was 13.68 times greater than that at 144 rpm.

Although the dissolved oxygen concentration was increased significantly, the corresponding increases in the cell mass concentration and the specific growth rate were not one-to-one. This was probably because the DO value of the yeast was close to the critical value, and substrate was depleted. The MBD system was more effective at low agitation speed (144 rpm) than at high agitation speed (476 rpm). The MBD enhanced the oxygen transfer by increasing the interfacial area of air bubbles and preventing the coalescence of air bubbles (Kaster, 1988). Therefore the high agitation speed did not increase the oxygen transfer as much as in the air sparging system.

4.1.3 Comparison between air sparging system and MBD sparging system

The growth profiles of the four systems including sparged air at 144 and 476 rpm

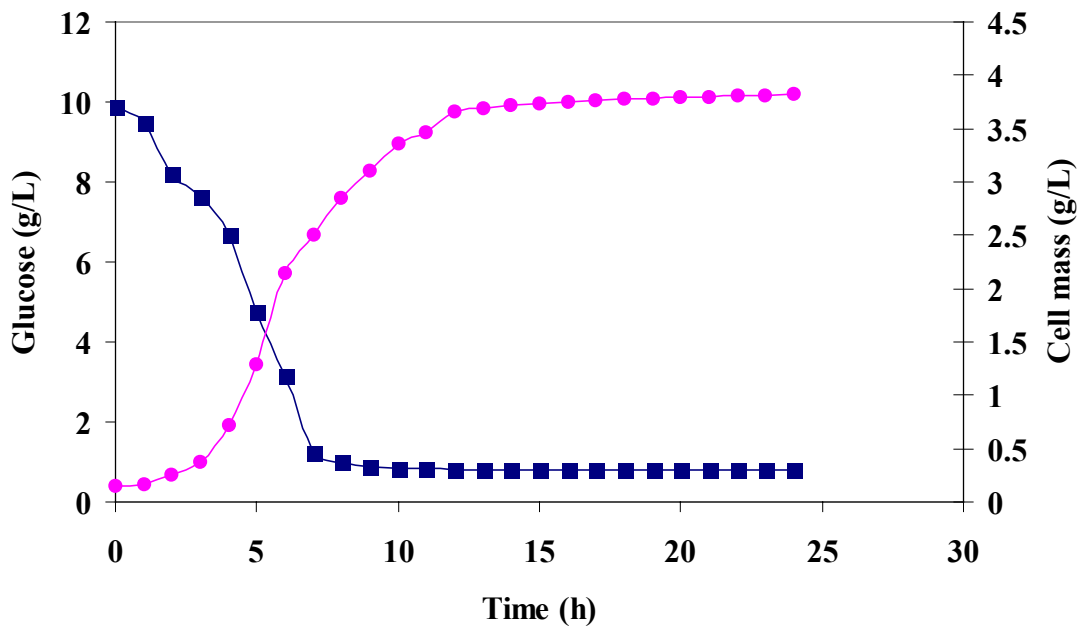
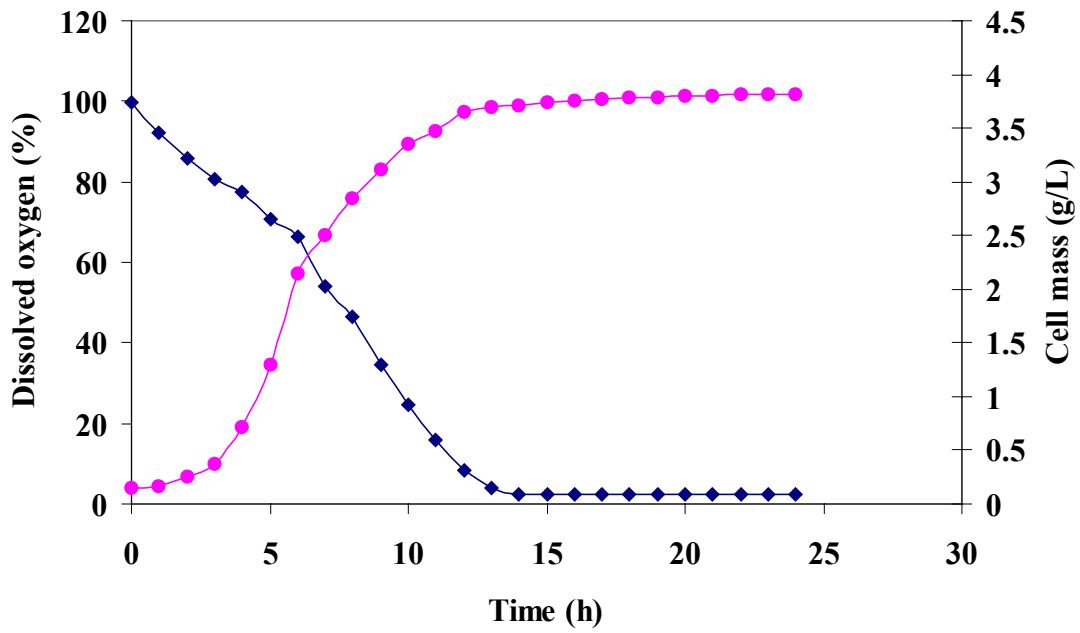


Figure 4.3 1-liter fermentation with MBD sparging at 144 rpm. Cell mass concentration (●), dissolved oxygen concentration expressed as % saturation (◆), and glucose concentration (■).

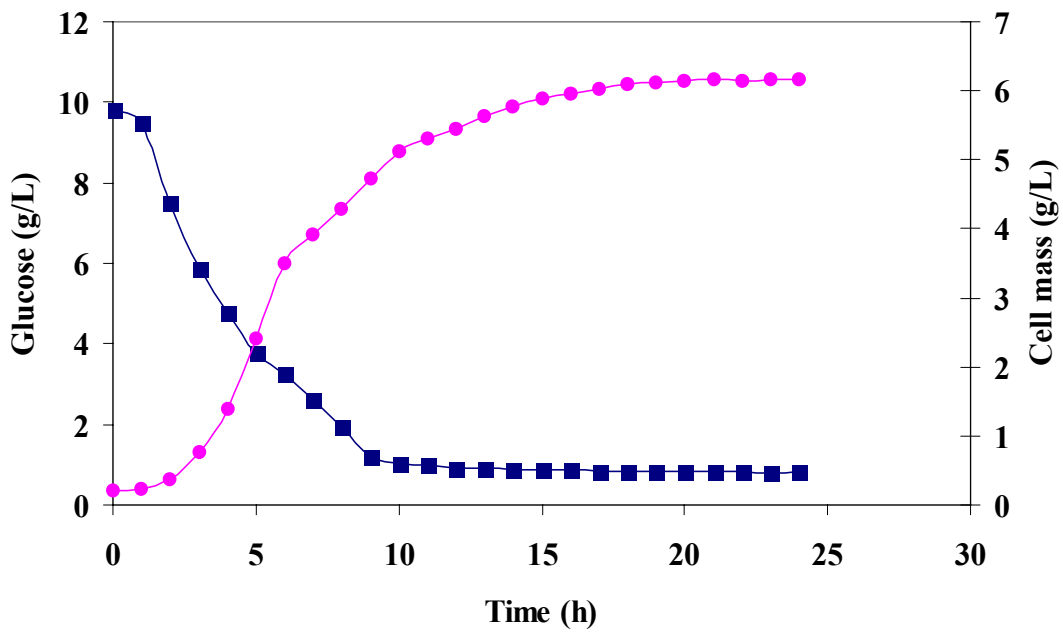
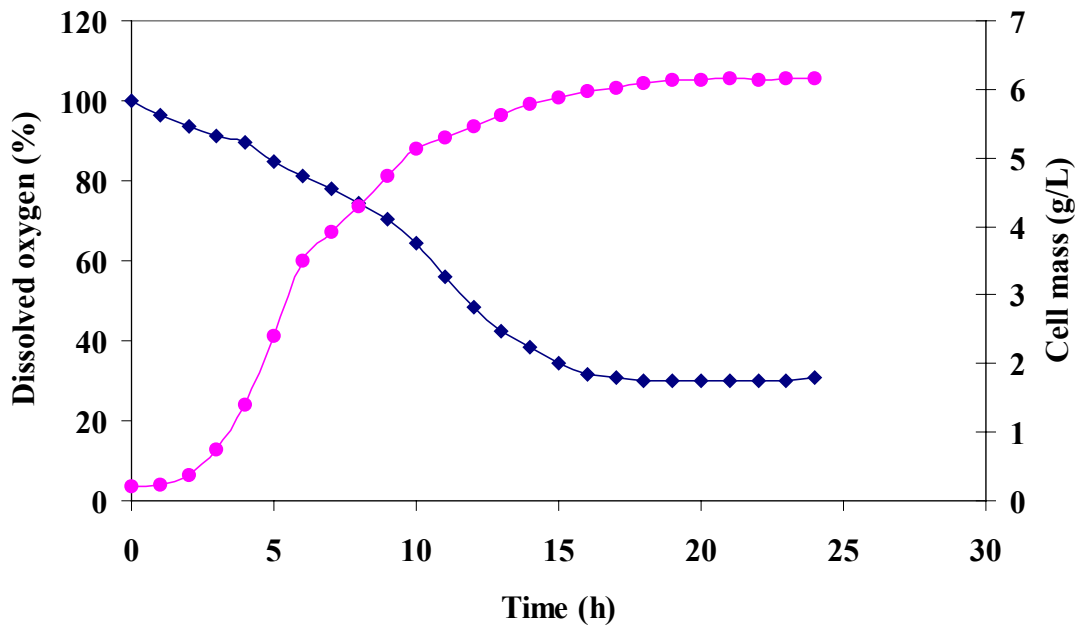


Figure 4.4 1-liter fermentation with MBD sparging at 476 rpm. Cell mass concentration (●), dissolved oxygen concentration expressed as % saturation (◆), and glucose concentration (■).

and MBD at 144 and 476 rpm are presented in Figure 4.5. The cell cultivation with sparged air at 144 rpm gave the lowest cell mass concentration (2.54 g L^{-1}). The growth profiles of sparged air and MBD at 476 rpm were similar. The oxygen profiles of the four different systems are presented in Figure 4.6. The oxygen profiles of both sparged air and MBD at 476 rpm were very similar between 0 to 8 hours but there were differences after 8 hours.

The MBD affected oxygen transfer at low agitation speed more than at high agitation speed. At high agitation rate (476 rpm), the dissolved oxygen concentration in the MBD system was 1.9 times higher than that in the air sparging system. However, at low agitation rate the dissolved oxygen concentration in the MBD system was 7.3 times higher than that in the air sparging system. Thus, at low agitation speeds, the MBD system significantly improved the oxygen transfer rate. Because of the improved dissolved oxygen concentration in the medium, the cell mass concentration increased significantly ($p < 0.05$). The cell mass concentration in the MBD system was 1.5 times higher than that in the corresponding air sparging system.

At higher agitation rates, the difference in cell mass concentration of the MBD and air sparging system was smaller than at low agitation rates. In the MBD system, cell mass concentration was 1.1 times higher than the air sparging system probably because the DO values for both systems were above the critical value. It has been shown that above the critical DO value, the specific growth rate of an aerobic microorganism is constant (Shuler and Kargi, 1992). For yeast and bacteria, this has been shown to be 10-20 % of the saturated DO concentration. For the MBD system, the DO concentration was 30 % of the saturated value while the air sparging system was 16 %. Although the critical DO concentration was not determined for this microorganism, the levelling-off of the specific growth rates ($\mu = 0.56 \text{ h}^{-1}$ for the MBD, $\mu = 0.54 \text{ h}^{-1}$ for air sparging) indicated that perhaps the critical DO concentration was exceeded in both systems.

The results from the air sparging system at high agitation speed (476 rpm) were compared with those from the MBD sparging system at low agitation speed (144 rpm). The high agitation speed had much more effect on the cell mass concentration and cell mass yield than the MBD ($p < 0.05$). The increase in the specific growth rate due to the

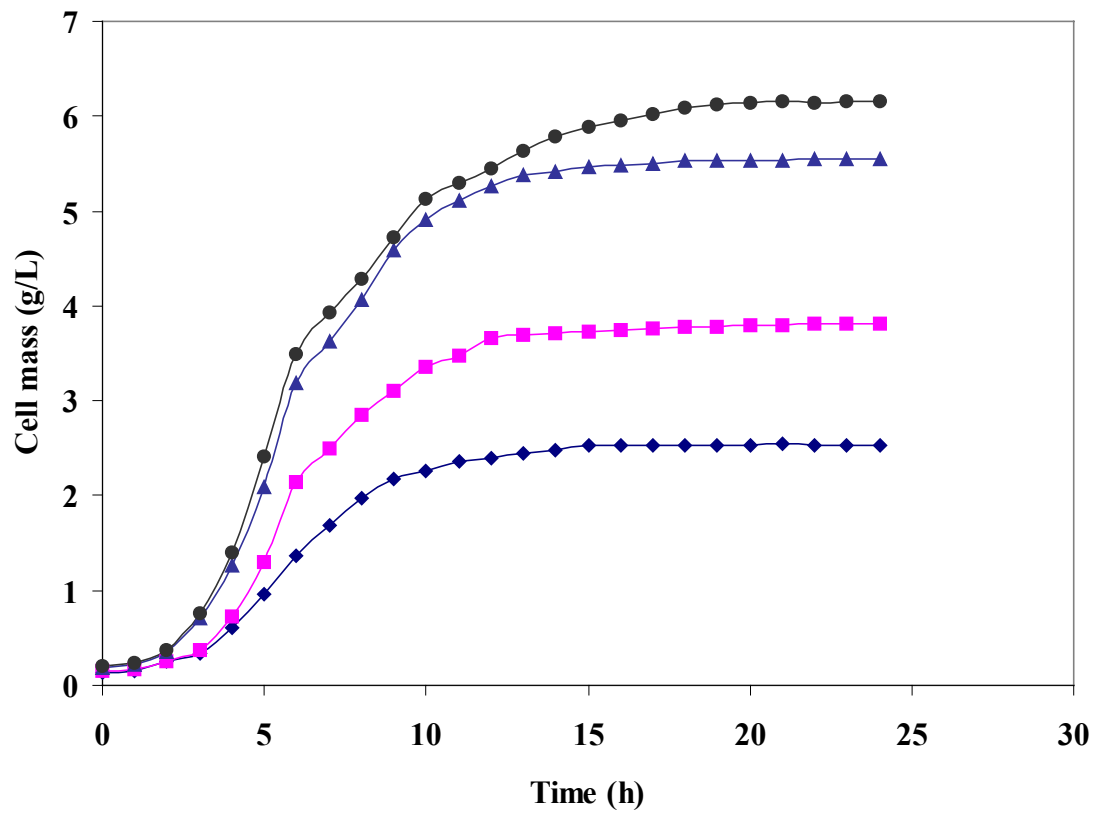


Figure 4.5 Comparison of yeast growth profiles in 1-liter cell cultivation. 144 rpm agitation, air sparging (◆), 144 rpm agitation, MBD sparging (■), 476 rpm agitation, air sparging (▲), 476 rpm agitation, MBD sparging (●).

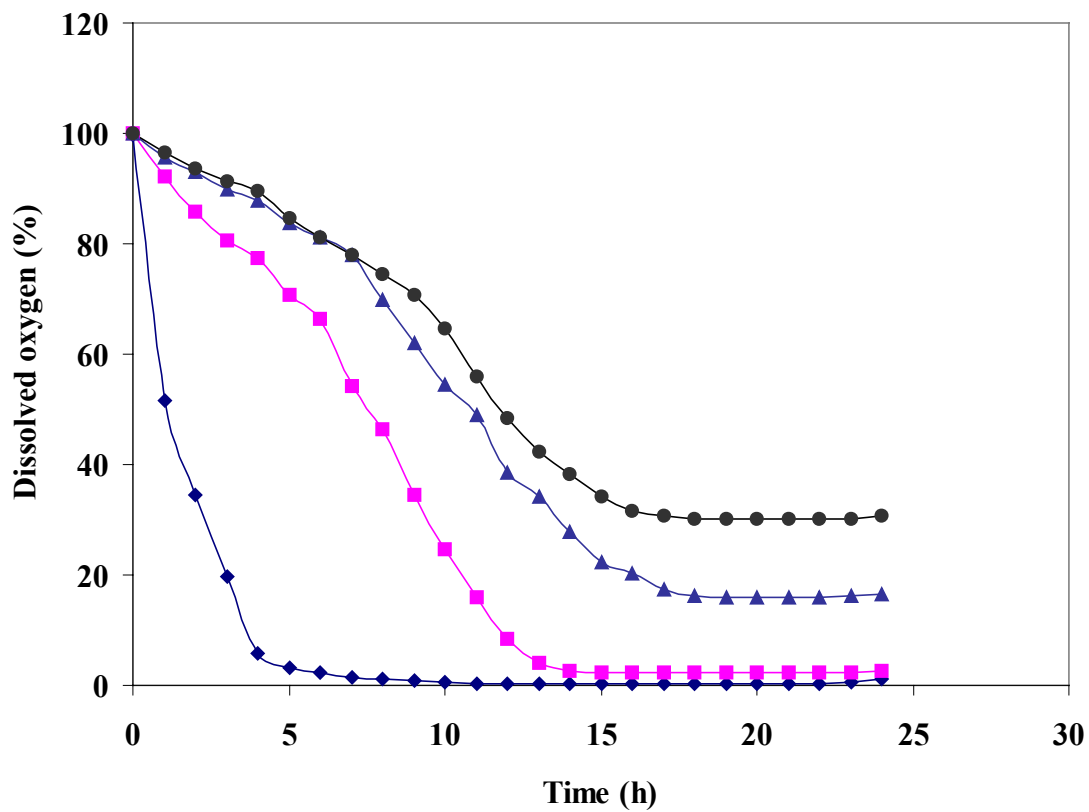


Figure 4.6 Comparison of oxygen profiles in 1-liter cell cultivation. 144 rpm agitation, air sparging (◆), 144 rpm agitation, MBD sparging (■), 476 rpm agitation, air sparging (▲), 476 rpm agitation, MBD sparging (●).

MBD was not statistically significantly different from the high agitation rate ($p > 0.05$). The major difference between the two systems (the MBD at 144 rpm and the sparged air at 476 rpm) was the dissolved oxygen concentration. With sparged air at high agitation rate, the dissolved oxygen concentration was 53.3 times more than that at the low agitation rate. The dissolved oxygen concentration with MBD at 144 rpm increased 7.3 times more than the sparged air at the same agitation speed. For the air sparging system, the high agitation speed increased the oxygen transfer because insufficient oxygen dispersion occurred at low agitation speed. The MBD had more interfacial area and prevented coalescence of air bubbles (Kaster, 1988), therefore even at low agitation speed the oxygen transfer was high.

4.2 Large scale cell cultivation

The 72-liter fermentor (BIOSTAT[®] U 50, Braum Company, Germany) was used to conduct the 50-liter fermentation. The operating conditions were the same as in the small-scale fermentation except the agitation rates. The low agitation rate was 150 rpm and the high agitation rate was 500 rpm. The different agitation rates was due to the scale-up methodology used (Hubbard, 1987). The cell mass, dissolved oxygen, and glucose profiles for the 50-liter fermentation are shown in Figures 4.7 -4.10. The cell mass, dissolved oxygen, and glucose concentrations at the stationary phase as well as the specific growth rate are reported in Table 4.1.

4.2.1 Air sparging system

Figures 4.7-4.8 show the growth, dissolved oxygen, and glucose profiles at low (150 rpm) and high (500 rpm) agitation rates. The high agitation rate strongly affected the cell cultivation in the air sparging system. The cell mass concentration at 500 rpm with sparged air was 2.1 times greater than that at 150 rpm, whereas the specific growth rate increased by 1.45 times. The cell mass yield at high agitation rate was 2.1 times greater than that at low agitation rate. The oxygen profile at 150 rpm decreased rapidly

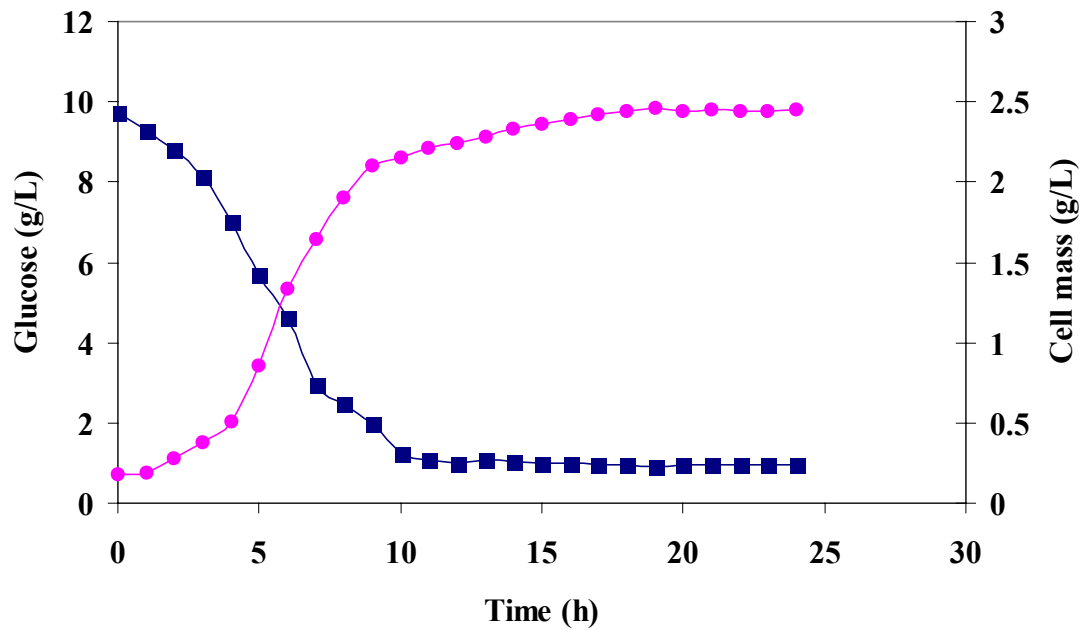
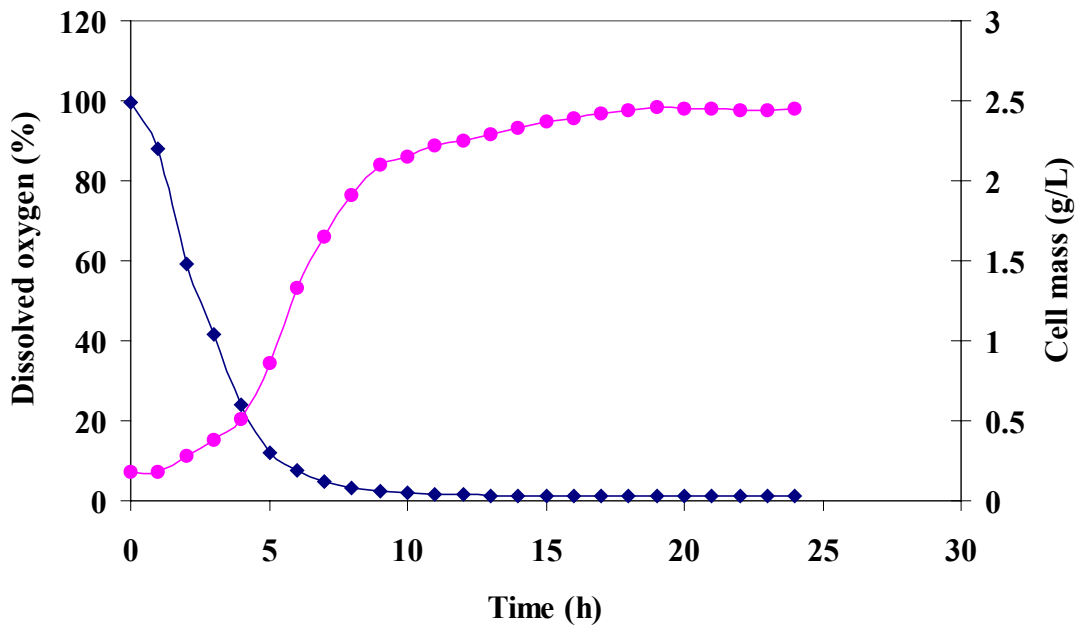


Figure 4.7 50-liter fermentation with air sparging at 150 rpm. Cell mass concentration (●), dissolved oxygen concentration expressed as % saturation (◆), and glucose concentration (■).

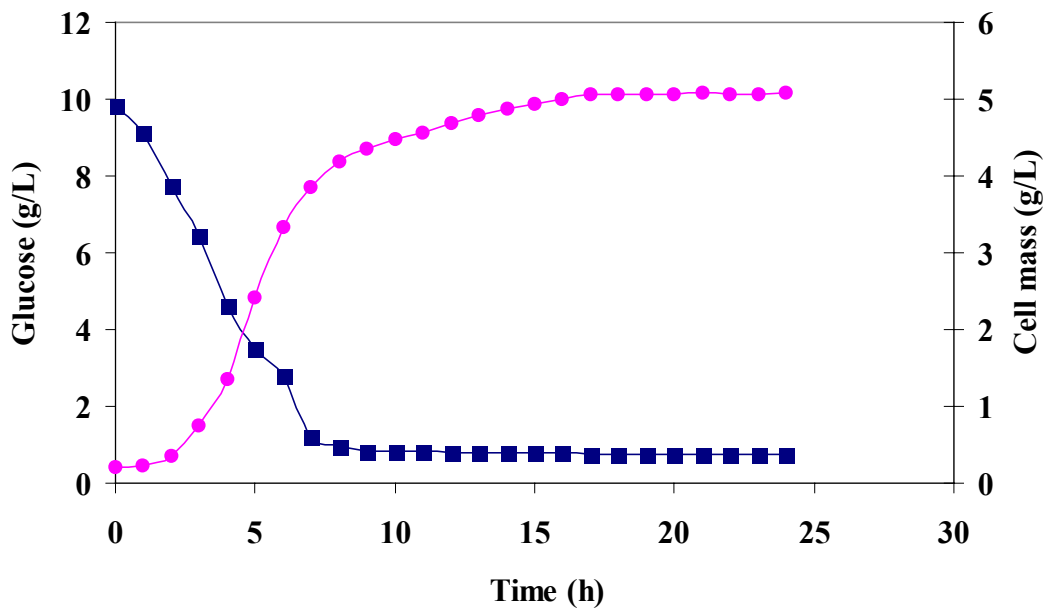
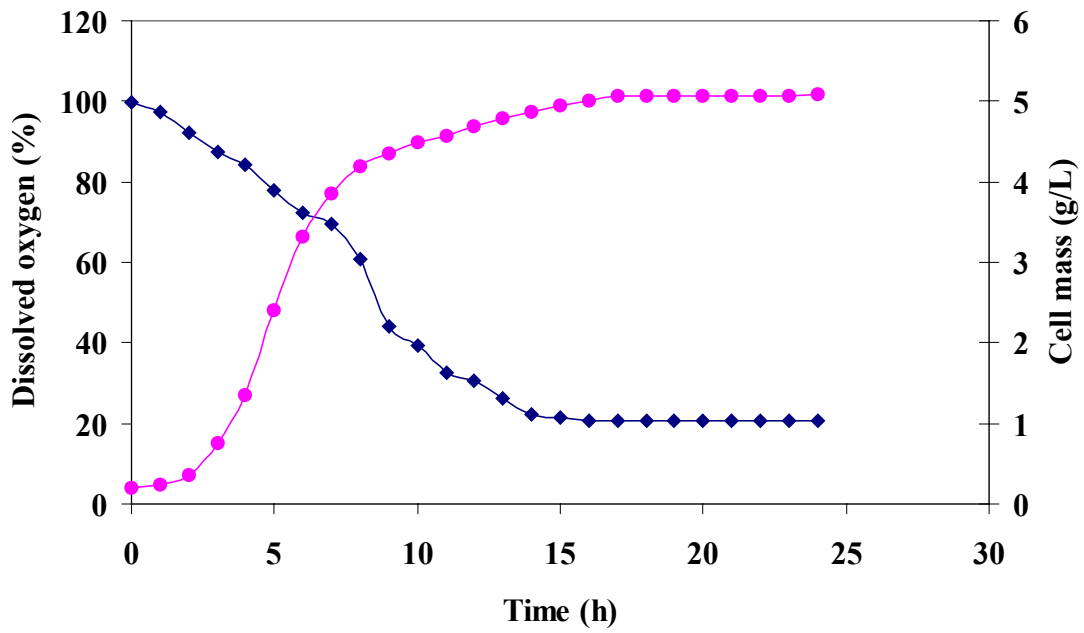


Figure 4.8 50-liter fermentation with air sparging at 500 rpm. Cell mass concentration (●), dissolved oxygen concentration expressed as % saturation (◆), and glucose concentration (■).

to a constant value of 1.3 % saturation after 10 hours, while that at 500 rpm decreased slowly to a constant value of 20 % saturation after 15 hours. The high agitation rate improved the oxygen dispersion in the fermentation medium since the cell mass concentration, specific growth rate, and dissolved oxygen concentration increased.

4.2.2 MBD sparging system

The MBD sparging system was used to supply oxygen to the fermentor. The original design of this fermentor was not suitable for retrofitting with the MBD. The original air connection was disassembled and replaced with a brass hose barb as shown in Figure 3.3. This modification was very effective for transferring dispersed microbubbles from the MBD generator to the air sparger. The cell mass, dissolved oxygen, and glucose profiles of the cell cultivation with the MBD sparging system at 150 and 500 rpm are shown in Figures 4.9-4.10. The increase in the cell mass concentration when the agitation rate was changed from 150 to 500 rpm was 1.3 times ($p < 0.05$) compare to the sparging air system, which was 2.1 times. The specific growth rate due to the change in agitation rates for the MBD sparging system was less pronounced. The specific growth rate increased 1.1 times compared to the 1.45 times for the air sparging system. Similar to the 1-liter fermentation, the cell mass yield increased 1.4 times when the agitation rate was increased from 150 to 500 rpm.

The dissolved oxygen concentration showed a large difference between the air sparging system and MBD sparging when the agitation rates were changed from 150 to 500 rpm. The dissolved oxygen concentration with MBD at 500 rpm was 5.6 times greater than that at 150 rpm, while the dissolved oxygen concentration with sparged air increased 16 times. In the case of the MBD system, because of the large interfacial area created by the MBD generator, the increased agitation did not have a large effect on the dissolved oxygen concentration.

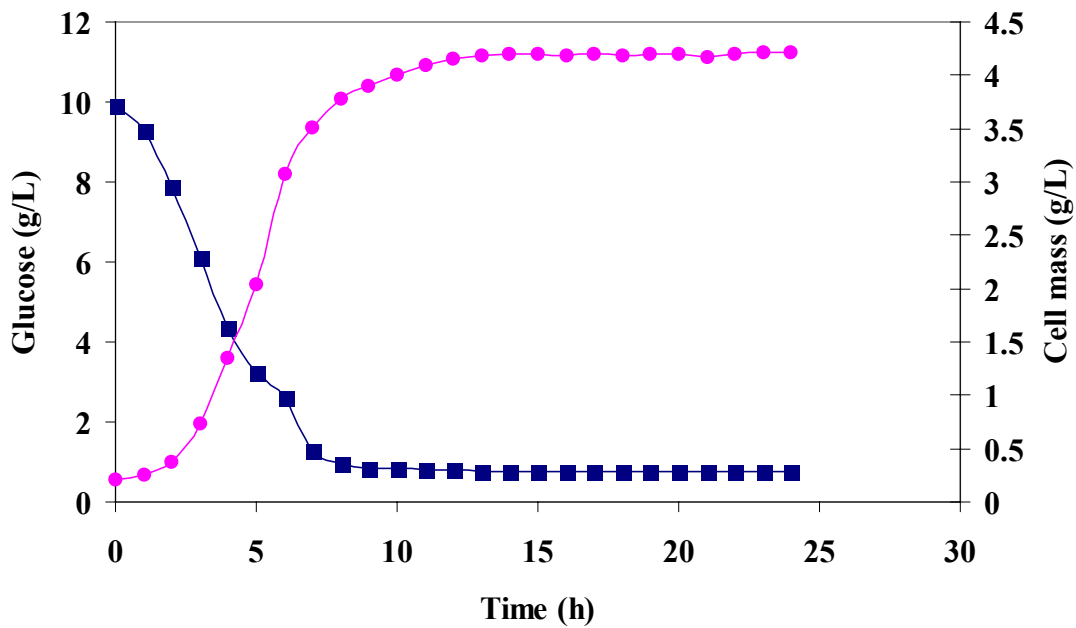
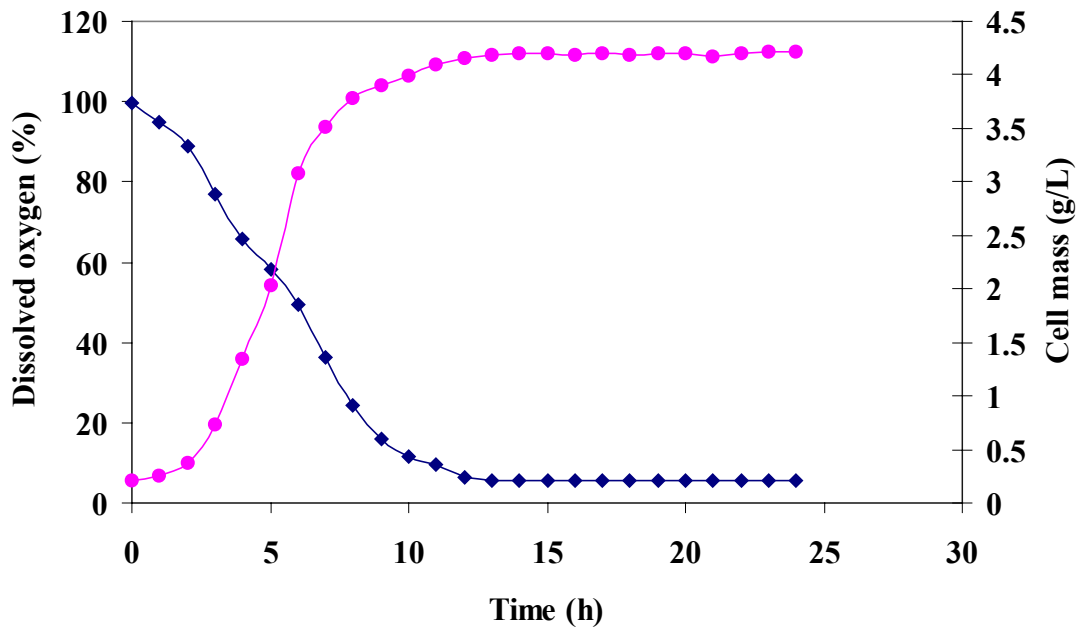


Figure 4.9 50-liter fermentation with MBD sparging at 150 rpm. Cell mass concentration (●), dissolved oxygen concentration expressed as % saturation (◆), and glucose concentration (■).

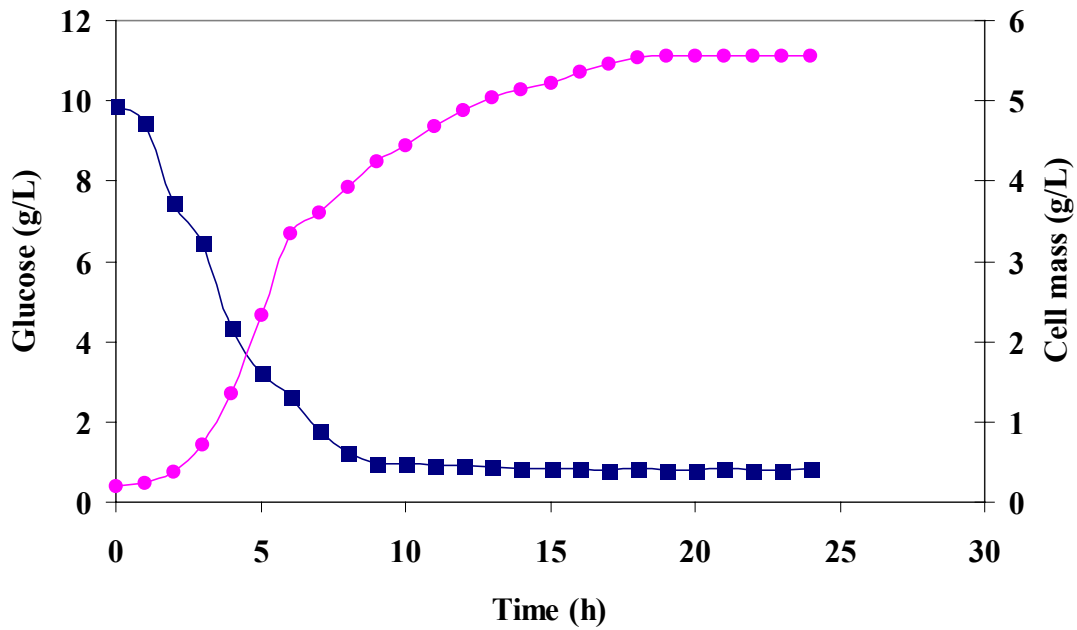
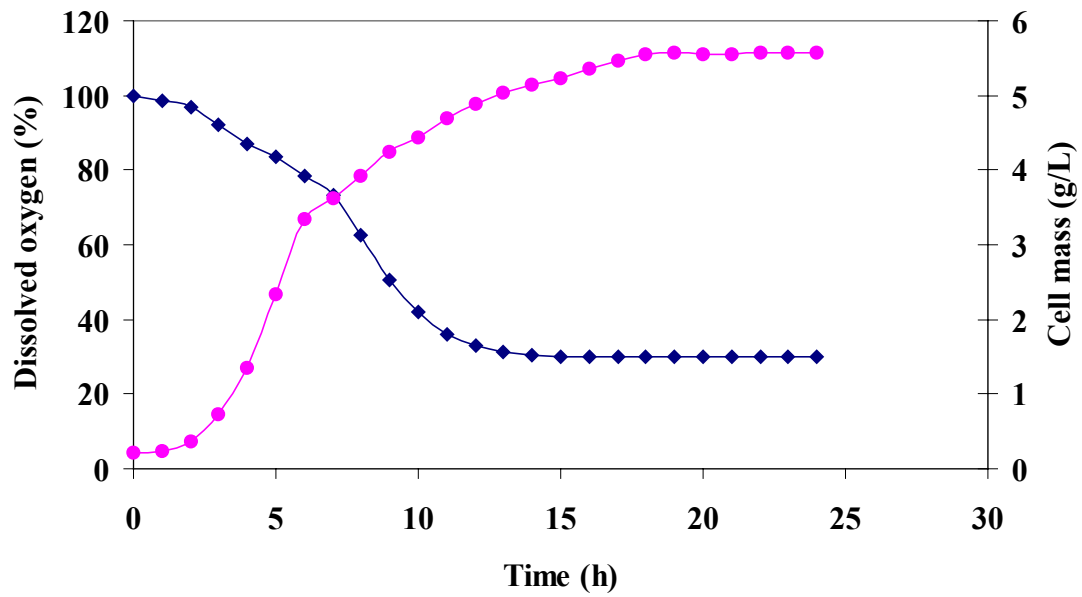


Figure 4.10 50-liter fermentation with MBD sparging at 500 rpm. Cell mass concentration (●), dissolved oxygen concentration expressed as % saturation (◆), and glucose concentration (■).

4.2.3 Comparison between air sparging system and MBD sparging system

The growth profiles of the four different systems are shown in Figure 4.11. The lag phase of the four profiles was about 1 hour followed by 10 hours of exponential growth phase. The stationary phase of yeast growth for sparged air and MBD at 150 rpm occurred after 12 hours; whereas, the yeast growth for sparged air and MBD at 500 rpm were in the stationary phase after 18 hours. The cell cultivation with the sparged air system at 150 rpm produced the lowest cell mass concentration and the specific growth rate (Table 4.1). The oxygen profiles of the four different systems are shown in Figure 4.12. At 150 rpm with sparged air, the dissolved oxygen concentration was steady at 1.3 % saturation after 10 hours. The dissolved oxygen concentration of yeast fermentation with MBD at 150 rpm was steady at 5.4 % saturation after 14 hours. The oxygen profiles between 0 to 12 hours of the sparged air and MBD at 500 rpm were very similar. In both the MBD and air sparged systems, the steady state DO values at the low agitation rates were several times higher than the corresponding systems at the 1-liter fermentator. This was probably because of the longer residence times of the bubbles in the media. However, at higher agitation rates the differences between the 1-liter and 50-liter fermentors were less pronounced probably because of the better dispersion of gas bubbles.

The effect of the MBD on the growth profile was compared with that of the sparged air at low and high agitation rates. At low agitation speed (150 rpm), the cell mass concentration with MBD was 1.7 times greater than that with air sparging. The cell mass concentration with MBD at 500 rpm was only 1.1 times that with air sparging. The effect of agitation speed on the specific growth rates of MBD sparging system showed no significant improvement. The specific growth rate with MBD at 150 and 500 rpm increased 1.35 and 1.05 times, respectively relative to the air sparging system at corresponding agitation rates. The dissolved oxygen concentration with the MBD at 150 rpm was 4.2 times greater than that with sparged air. At high agitation speed (500 rpm), the dissolved oxygen concentration with MBD was 1.4 times that with sparged air. It

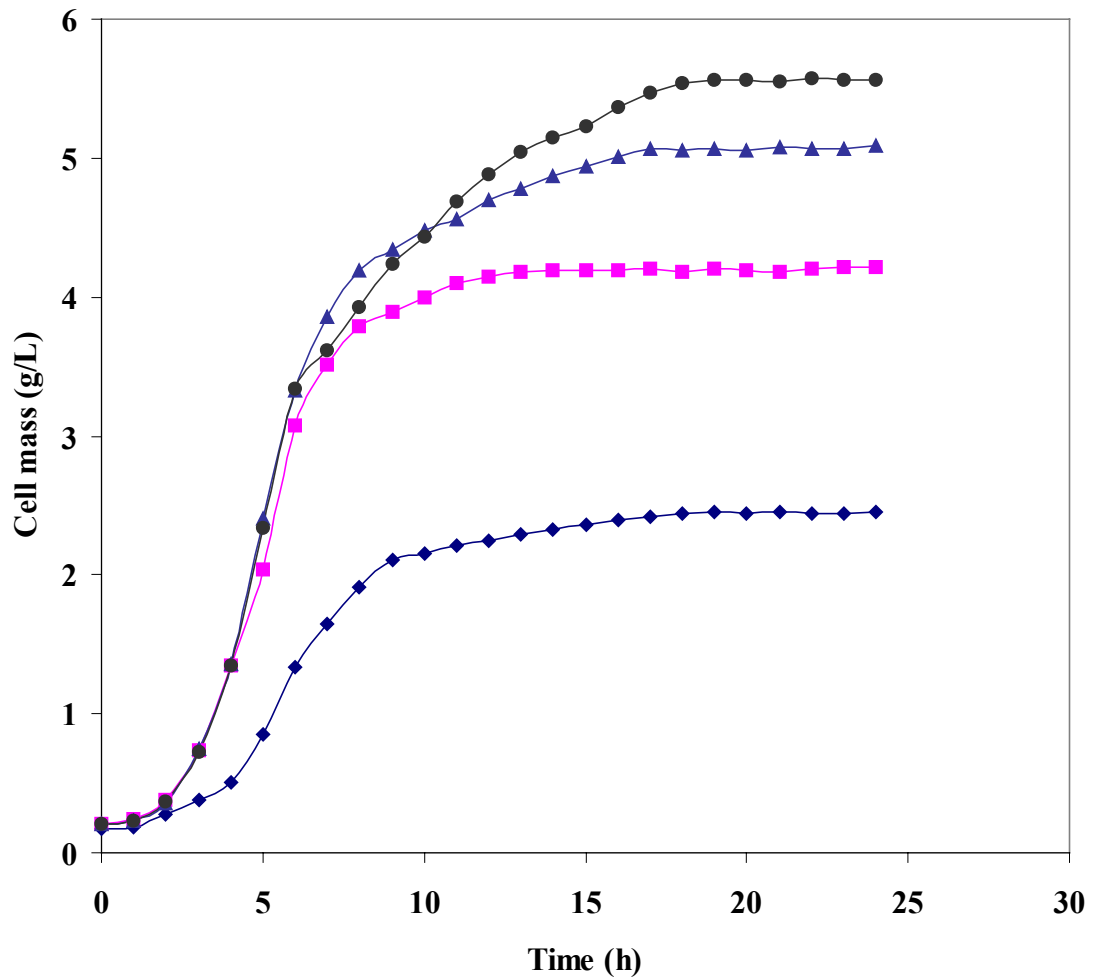


Figure 4.11 Comparison of yeast growth profiles in 50-liter cell cultivation. 150 rpm agitation, air sparging (♦), 150 rpm agitation, MBD sparging (■), 500 rpm agitation, air sparging (▲), 500 rpm agitation, MBD sparging (●).

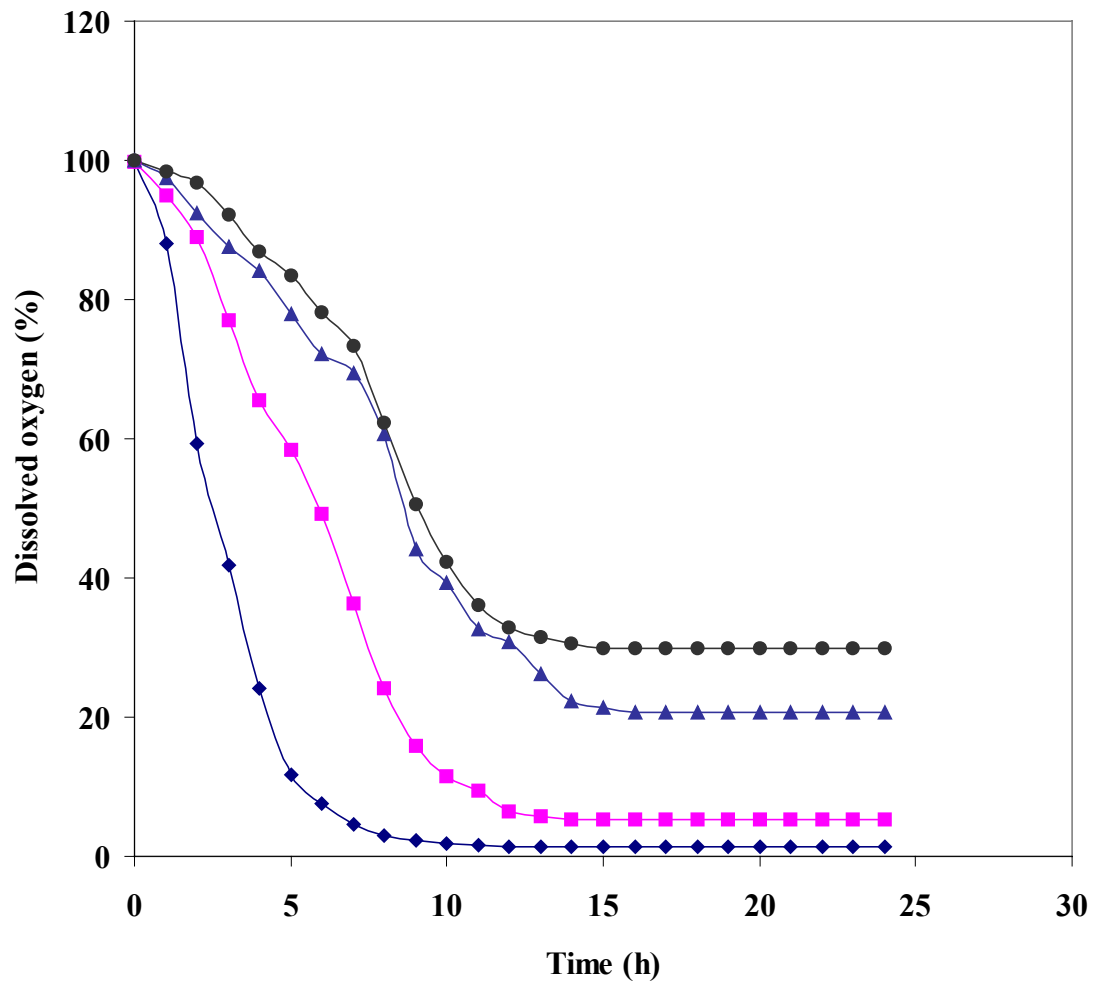


Figure 4.12 Comparison of oxygen profiles in 50-liter cell cultivation. 150 rpm agitation, air sparging (♦), 150 rpm agitation, MBD sparging (■), 500 rpm agitation, air sparging (▲), 500 rpm agitation, MBD sparging (●).

appears that at 500 rpm with air sparging system the dispersion of air bubbles was very high, consequently, microbubble dispersion did not have much impact of the DO concentration.

The results from the air sparging system at high agitation speed (500 rpm) were compared with those from the MBD sparging system at low agitation speed (150 rpm). The high agitation speed had much more effect on the cell mass concentration than the MBD. The cell mass concentration increased by 2.1 times with air sparging at 500 rpm compared to sparging 150 rpm, while the MBD sparging system at 150 rpm increased the cell mass concentration by 1.7 times. The increase in the specific growth rate due to the MBD was 1.35 times while that due to higher agitation rate was 1.45 times. The cell mass yield with sparged air at 500 rpm was 1.2 times greater than that with MBD at 150 rpm. However, the differences in cell mass concentration and cell mass yield between the sparged air at high agitation rate and the MBD at low agitation rate were not statistically significant ($p > 0.05$). The major difference between the two systems (the MBD at 150 rpm and the sparged air at 500 rpm) was the dissolved oxygen concentration. With sparged air at high agitation rate, the dissolved oxygen concentration was 16 times more than that at the low agitation rate. The dissolved oxygen concentration with MBD at 150 rpm was 4 times higher than the sparged air at the same agitation speed. For the air sparging system, the high agitation speed (500 rpm) increased the oxygen transfer because of improved oxygen dispersion compared to the low agitation speed (150 rpm). On the other hand, the MBD had more interfacial area and prevented coalescence of air bubbles (Kaster, 1988), and this enhanced the oxygen transfer at low agitation speed (Hensirisak, 1997).

4.3 Effect of MBD on the oxygen transfer of the fermentation

4.3.1 1-liter fermentation

The volumetric oxygen transfer coefficients (k_La) and oxygen uptake rates were the most important factors in the aerobic fermentation. The k_La and oxygen uptake rates of all experiments are shown in Table 4.2. In the 1-liter cell cultivation, the k_La value

increased 2.4 times as the agitation speed increased from 144 to 476 rpm in the air sparging system. The k_{La} value in the MBD sparging system at 476 rpm was 1.45 times greater than that at 144 rpm. The k_{La} values from the MBD sparging system were compared with those from the air sparging system at the same agitation rates (144 and 476 rpm). The increase in the k_{La} values at 144 rpm (2.0 times) due to MBD effect was more than that at 476 rpm (1.2 times). The high agitation speed had most significant effect on the k_{La} values by enhancing the oxygen dispersion in the fermentation medium (Doran, 1995). The MBD could increase the oxygen transfer with low agitation speed because of the smaller bubble sizes and their stability, which prevented coalescence.

In order to maintain aerobic condition, the oxygen transfer rate should be greater or equal to the oxygen uptake rate. The oxygen transfer rate of the air sparging system at 144 rpm was the lowest (Table 4.2). It showed insufficient oxygen dispersion in the medium. The oxygen uptake rates of the air sparging system at 476 rpm and the MBD sparging at 144 and 476 rpm were similar (Table 4.2). The dispersion of oxygen with MBD at 144 rpm was similar to that at 476 rpm for both the sparged air and the MBD. The oxygen uptake rate for the sparged air system at high agitation rate and the MBD system at low agitation rate were not significantly different ($p > 0.05$). The volumetric oxygen transfer coefficients, oxygen uptake rates, and specific growth rates in the 1-liter fermentation are shown in Figure 4.13.

For aerobic fermentation, the oxygen transfer is the major barrier to cell mass production and product formation. For baker's yeast fermentation, the k_{La} value and the cell mass production were used as indicators of oxygen transfer in the system. Agitation and bubble sizes have significant effects on the oxygen transfer, so the k_{La} and the cell growth profile were investigated by the effect of agitation and MBD. In the 1-liter fermentation, increasing the agitation speed from 144 to 476 rpm with air sparging system increased the k_{La} value and the cell mass concentration more than the other three systems. The MBD sparging system at 144 rpm significantly increased the k_{La} value and the cell mass concentration, but these increases were less than those achieved by increasing the agitation speed from 144 to 476 rpm in the air sparging system.

Table 4.2 Volumetric oxygen transfer coefficient and oxygen uptake rate.

Volume (L)	Air supply	Agitation speed (m ⁻¹)	OUR ^a (m mol O ₂ L ⁻¹ h ⁻¹)	<i>k_La</i> ^b (h ⁻¹)
1.6	Air	144	64.15±2.10	338.77±11.0
1.6	MBD	144	126.73±0.17	682.03±0.58
1.6	Air	476	127.72±2.02	800.57±4.13
1.6	MBD	476	131.51±0.59	990.24±1.68
72	Air	150	76.32±0.45	407.00±2.34
72	MBD	150	137.53±0.93	765.18±4.05
72	Air	500	141.08±0.64	937.14±1.92
72	MBD	500	144.85±0.89	1089.10±2.29

^a Oxygen uptake rate.

^b Volumetric oxygen transfer coefficient.

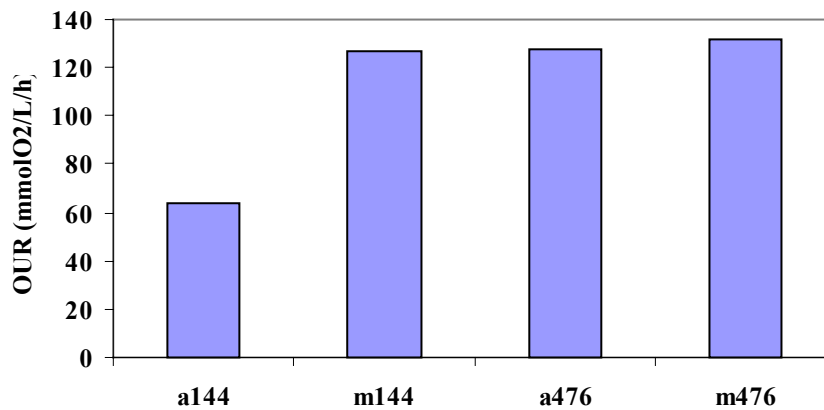
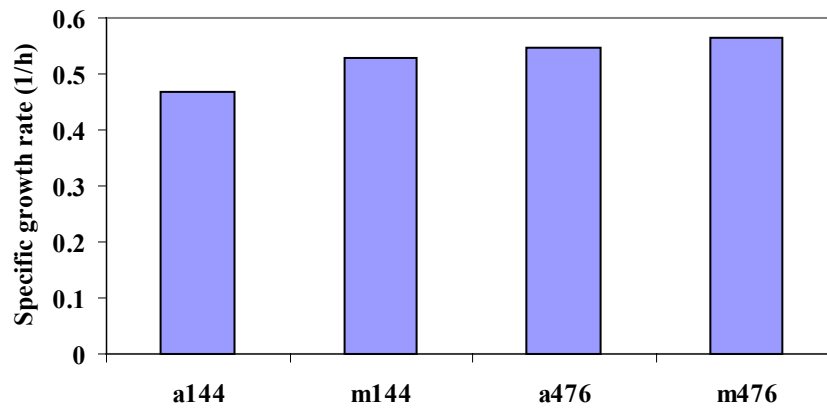
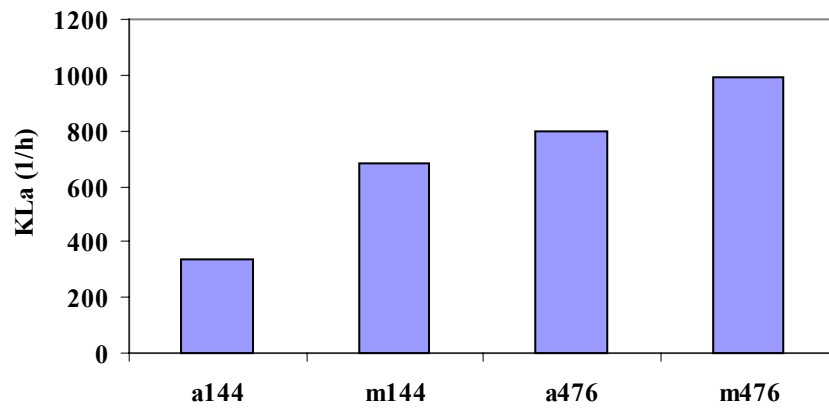


Figure 4.13 Comparison of volumetric oxygen transfer coefficient, specific growth rate, and oxygen uptake rate in 1-liter fermentation.

4.3.2 50-liter fermentation

In the 50-liter fermentation, when the agitation speed was increased from 150 to 500 rpm, the k_La values of the air sparging system increased 2.3 times. The effect of the MBD on k_La value at low agitation speed was more than that at high agitation speed. The k_La value with the MBD sparging system at 150 rpm was 1.9 times greater than that with the air sparging system at 150 rpm. The k_La value with the MBD sparging system at 500 rpm was 1.2 times higher than the air sparging system at the same agitation rate. The trends in the k_La values for the 50-liter fermentor were similar to those in the 1-liter fermentor.

The oxygen uptake rate of the MBD sparging system at 150 was slightly lower than the oxygen uptake rates of the air sparging system and MBD at 500 rpm (Table 4.2). The high agitation speed had more effect on the oxygen uptake rate than the MBD in the large volume fermentor. The values of the volumetric oxygen transfer coefficients, oxygen uptake rates, and specific growth rates in the 50-liter fermentation are shown in Figure 4.14. Although the k_La value and the cell mass concentration from the MBD at 144 rpm were not the same as those due to the high agitation speed with the sparged air, the MBD sparging system demonstrated the benefit of increased the oxygen transfer at low agitation speed (Kaster, 1988; Hensirisak, 1997).

In a 20-liter fermentation, the MBD sparging system at low agitation speed (150 rpm) was shown to produce similar k_La values and cell mass concentration as increasing the agitation speed from 150 to 500 rpm with the air sparging system (Hensirisak, 1997). In the 50-liter fermentation, the k_La value and the cell mass concentration for the MBD sparging at 150 rpm were 18.4 and 16.9 % respectively less than those from the sparged air at 500 rpm. Though the increase in the k_La value was less than that from the high agitation speed with the sparged air, there was no statistically significant difference in the cell mass concentration ($p > 0.05$) and oxygen uptake rate ($p > 0.05$) in the two systems. This was probably because the DO concentrations were above the critical value for this microorganism. Consequently specific growth rate did not increase inspite of the difference in k_La values.

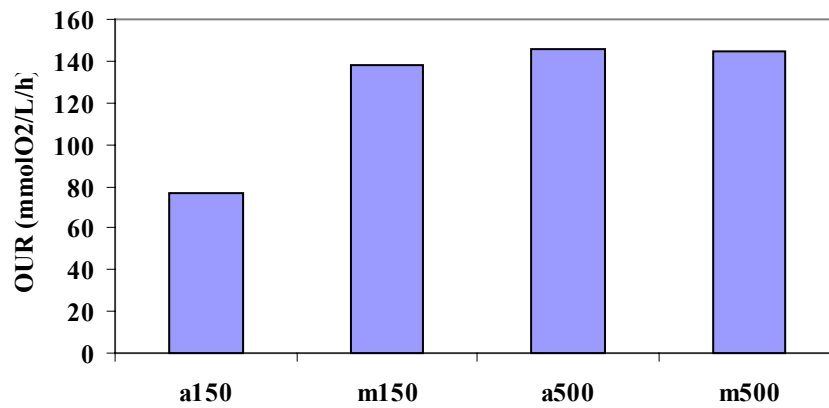
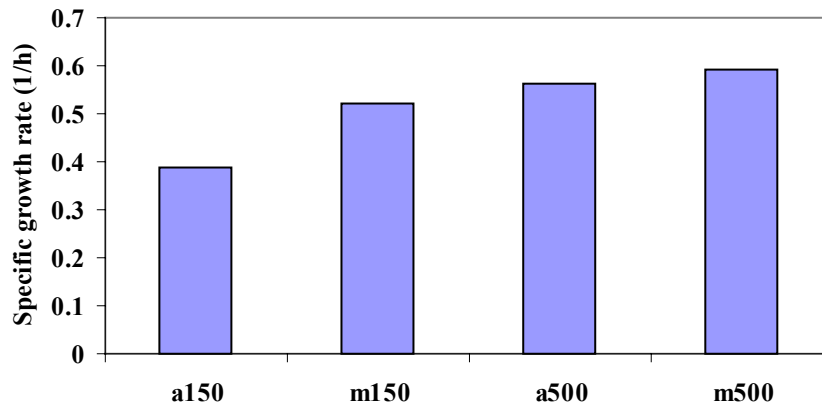
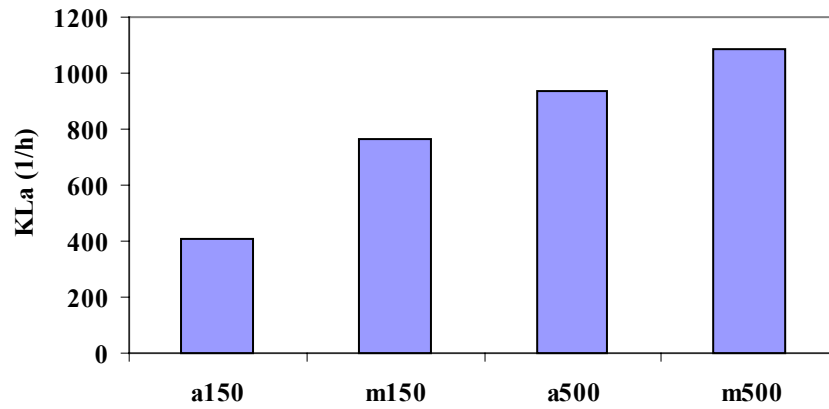


Figure 4.14 Comparison of volumetric oxygen transfer coefficient, specific growth rate, and oxygen uptake rate in 50-liter fermentation.

4.4 Power consumption

4.4.1 1-liter fermentation

The total power consumption for each run was the sum of the power from the fermentor agitator, air compressor, and MBD generator including MBD and recycle pump (for the MBD run). The estimated power consumption for the 1-liter and 50-liter fermentation are shown in Tables 4.3 and 4.4, respectively. In the 1-liter fermentation with sparged air, the power consumption per unit volume at 476 rpm was 35 times greater than that at 144 rpm. With MBD, the power consumption per unit volume increased by 1.1 times when agitation speed was increased from 144 to 476 rpm. At 144 rpm, the power consumption per unit volume with the MBD was 278 times greater than that with sparged air. At 476 rpm, the power consumption per unit volume with MBD was 8.8 times higher than the sparged air.

4.4.2 50-liter fermentation

In the 50-liter fermentation, the power consumption per unit volume with sparged air at 500 rpm was 12.9 times greater than that at 150 rpm. The power consumption per unit volume with the MBD system increased 3.9 times when the agitation rate was increased from 150 to 500 rpm. The power consumption per unit volume with MBD at 150 rpm was 4.1 times greater than that with the sparged air at the same agitation rate. At 500 rpm, the power consumption per unit volume with MBD was 1.2 times higher than that with sparged air. The significant difference in the power consumption per unit volume was due to power required by the MBD generator. The MBD generator consumed the most power in the 1-liter fermentation; whereas the estimated power from the agitator at high agitation speed was the major portion of the total power consumption per unit volume in the 50-liter fermentation.

The power requirement for the low agitation speed MBD and the high agitation speed sparged air were compared with respect to the k_La values and the cell mass

Table 4.3 Power consumption calculated from the 1-liter fermentations.

Device Consuming Power	Agitation,		Oxygen Supply	
	144 rpm, Air Power	144 rpm, MBD Requirement	476 rpm, Air (kW × 10 ⁻⁶)	476 rpm, MBD
Agitator	63.70	63.70	2750	2750
Air compressor	14.55	14.55	14.55	14.55
MBD generator	-	21611	-	21611
Total	78.25	21689	2765	24376
Total (kW × 10 ⁻⁶ L ⁻¹)	78	21689	2765	24376

Table 4.4 Power consumption calculated from the 50-liter fermentations.

Device Consuming Power	Agitation,		Oxygen Supply	
	150 rpm, Air Power	150 rpm, MBD Requirement	500 rpm, Air (kW × 10 ⁻⁶)	500 rpm, MBD
Agitator	2030	2030	89820	89820
Air compressor	5380	5380	5380	5380
MBD generator	-	23150	-	23150
Total	7410	30560	95200	118350
Total (kW × 10 ⁻⁶ L ⁻¹)	148	611	1904	2367

concentration. In the 1-liter fermentation, the power consumption per unit volume for the sparged air at 476 rpm was 87.2% less than that from the MBD at 144 rpm. Since the operating speed of the MBD generator was very high (4000 rpm), the power consumption from the MBD generator was the major contributing factor to the total power consumption. In the 50-liter fermentation, the power consumption for the sparged air at 500 rpm was 2.1 times greater than MBD at 150 rpm. The power consumption for the agitator was the greatest factor in the total power consumption because of the high power to drive the larger propeller in the larger volume.

For the 50-liter fermentation, the capacity of this MBD generator can increase the oxygen transfer at the air flow rate 5.0 L min^{-1} at low agitation rate (150 rpm) better than the air sparging system at high agitation rate (500 rpm). Increasing the oxygen transfer with the MBD had more effect on the large-scale fermentation than the laboratory-scale fermentation. On the industrial-scale, the major operating cost in the fermentation process is the power consumption used in the agitation and aeration (Bailey, 1986). It is hypothesized that a microbubble dispersion will demonstrate an economic benefit for increasing oxygen transfer in a large-scale fermentation at low agitation speed.

4.5 Effect of scale-up on oxygen transfer

The objective of scale-up was to increase the size of equipment without reduction in yield. For aerobic fermentation, a constant volumetric oxygen transfer coefficient (k_La) was used to scale-up in the laboratory-scale unit. In this research, a scale-up method (Hubbard, 1987) was used to scale down from 50 liters to 1 liter. The agitation speed at 150 and 500 rpm in 50-liter fermentation (Hensirisak, 1997) was used to calculate the agitation speeds in the 1-liter fermentor. The air sparging system was the normal aeration system used in the fermentation process. The k_La values and cell mass concentration from the fermentation with the air sparging system was determined to test the scale-up procedure. This scale-up method was also applied to the agitation speeds and the airflow rate in the MBD sparging system. However, the MBD generator itself was not scaled-up.

4.5.1 Air sparging system

For the low agitation speed, the k_La value for the 1-liter fermentor was 16.8% less than that for the 50-liter fermentor (Figure 4.15). For the high agitation speed, the k_La value for the 1-liter fermentor was 14.7% less than that for the 50-liter fermentor. The difference in the scale-up values might be due to the error in the empirical correlation used in the calculation (Stanbury, 1995). The empirical relationship between the k_La and power consumption was derived from coalescing air-water dispersion systems in 2 to 2600 liter fermentors (Van't Riet, 1983). The YM broth-air system used for this research may have significantly different properties from the air-water system.

The growth profiles of the air sparging system for 1-L and 50-L fermentation at low (144 and 150 rpm) and high (476 and 500 rpm) agitation speeds are shown in Figure 4.16. The cell mass concentrations at 144 and 150 rpm were almost the same (2.54 and 2.46 g L⁻¹). The growth profiles at 476 and 500 rpm were also similar between 0 to 8 hours. However, there were slight differences (1.09 times) in cell mass concentration in the stationary phase. The growth profiles of low and high agitation speeds differed significantly from each other because of the insufficient oxygen dispersion at low agitation speed. Significant differences ($p < 0.05$) were obtained for the k_La in the small and large scale fermentors. However, there was no statistically significant difference ($p > 0.05$) between the cell mass concentration and cell mass yield at low agitation rate in 1-L and 50-L fermentors.

4.5.2 MBD sparging system

The k_La values of the MBD sparging system in the two fermentors are shown in Figure 4.17. The k_La value in the 1-liter fermentor was 10.8% less than that in the 50-liter fermentor for the low agitation rate. At high agitation rate, the differences in the k_La values between the two systems were similar to those obtained for the low agitation rates. The differences at both low agitation speed and high agitation speed with the MBD sparging system were less pronounced than those with the air sparging system because

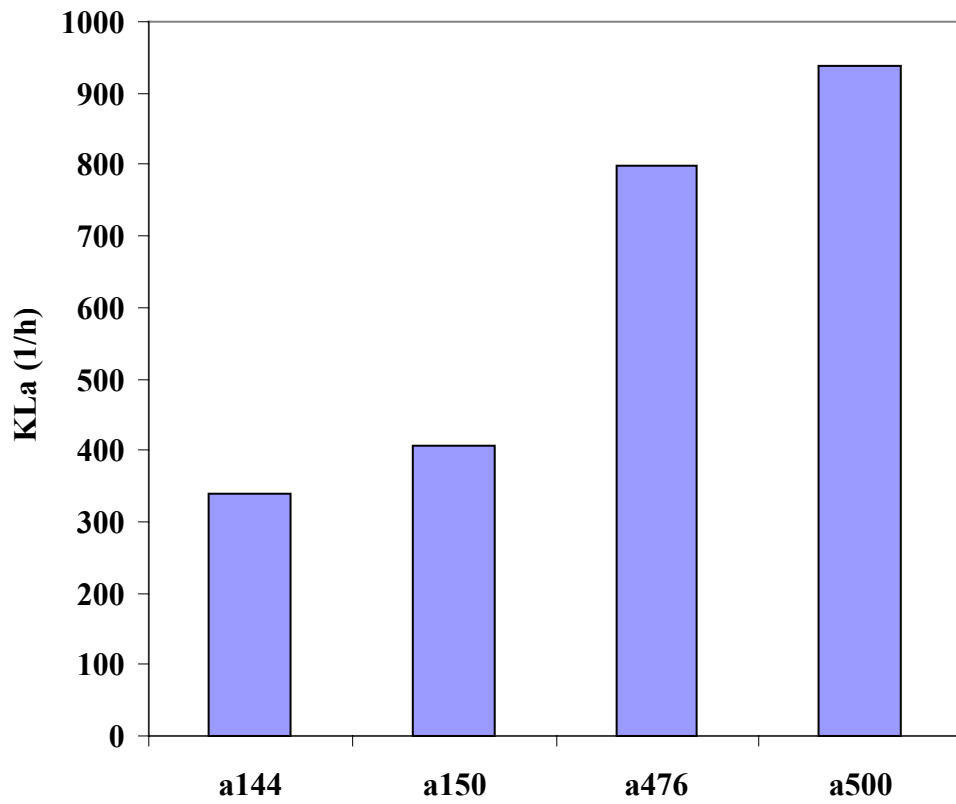


Figure 4.15 Comparison of volumetric oxygen transfer coefficient of air sparging system at agitation rates 144, 150, 476, and 500 rpm.

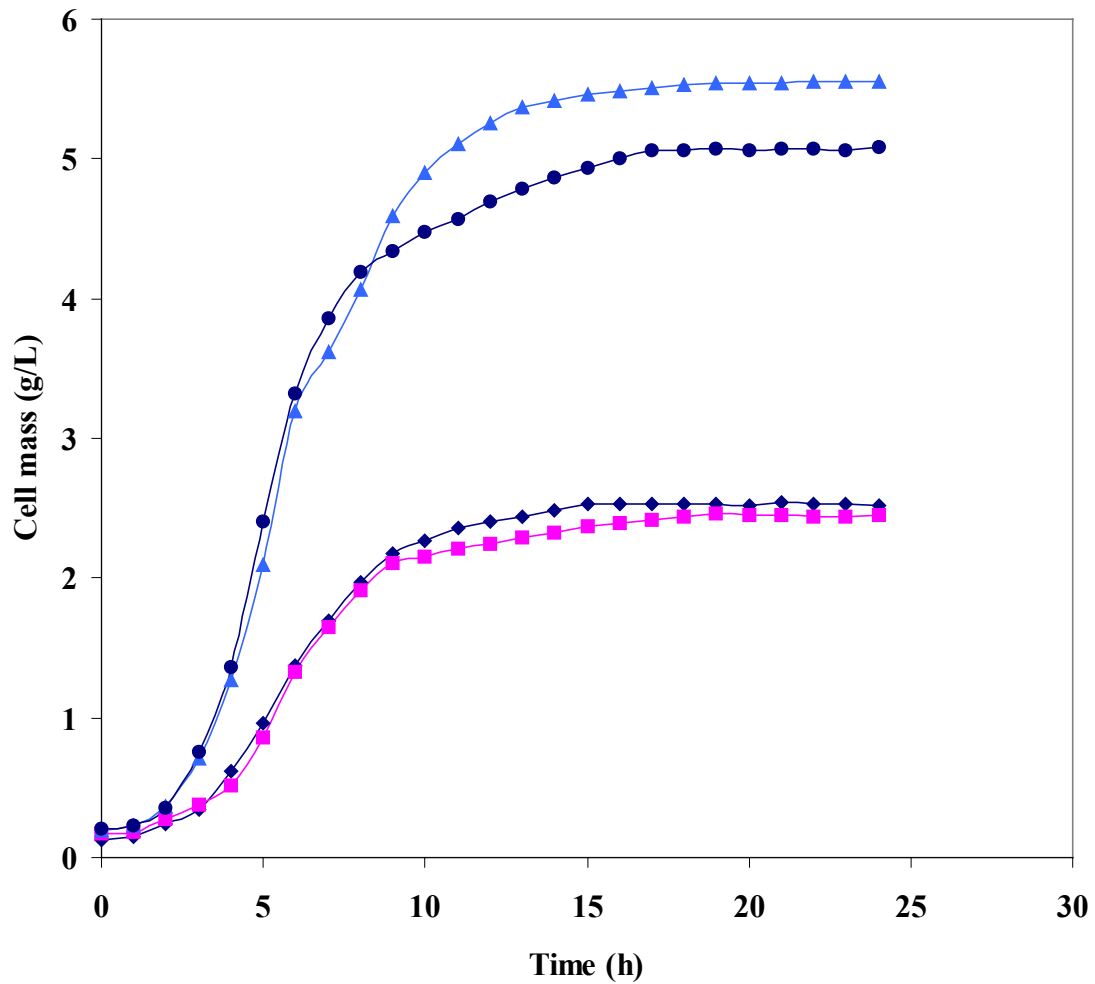


Figure 4.16 Growth profiles of air sparging system at agitation rates 144, 150, 476, and 500 rpm.
 144 rpm agitation, air sparging (◆), 150 rpm agitation, MBD sparging (■), 476 rpm agitation, air sparging (▲), 500 rpm agitation, MBD sparging (●).

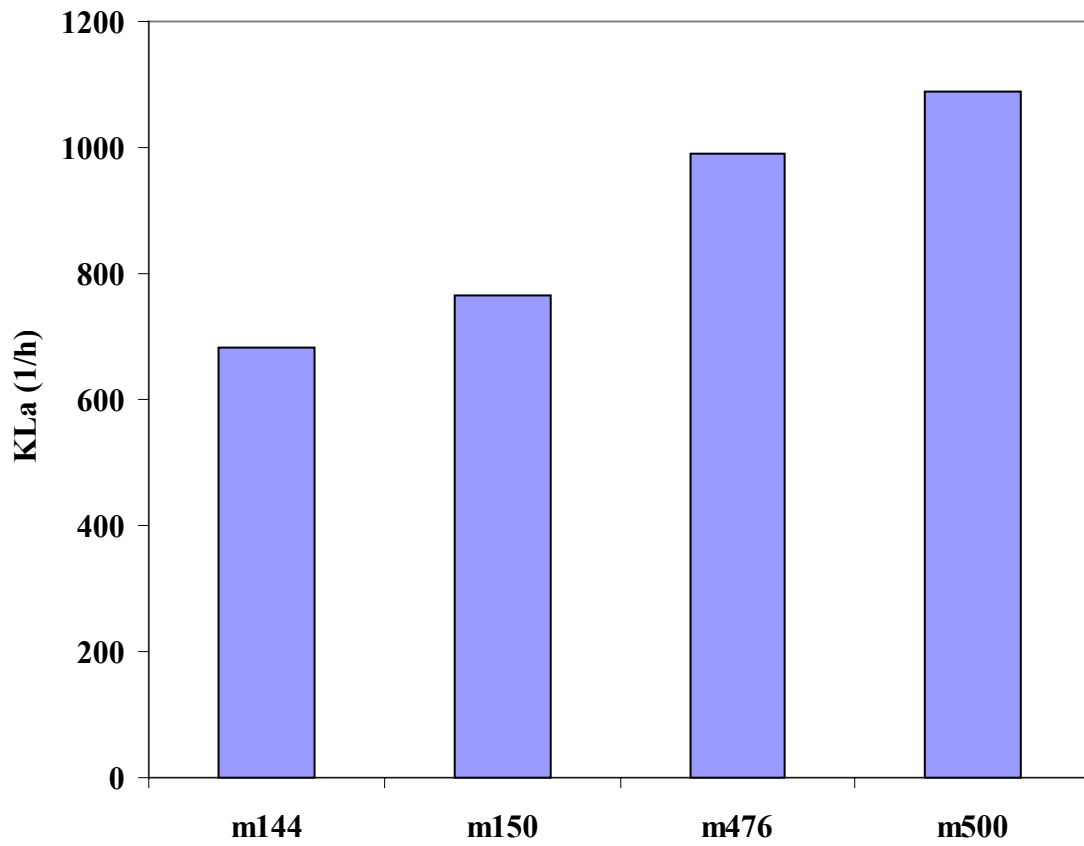


Figure 4.17 Comparison of volumetric oxygen transfer coefficient of MBD sparging system at agitation rates 144, 150, 476, and 500 rpm.

the oxygen transfer in the MBD was better than that in the sparged air.

The growth profiles of the 1-liter and 50-liter fermentation with the MBD at low and high agitation rates are shown in Figure 4.18. The growth profiles were similar between 0 to 7 hours. The cell mass concentration in the 50-liter fermentor was 1.10 times greater than that in the 1-liter fermentor for the low agitation rates. From this research, this scale-up method did not give the same k_La value at low and high agitation for the air and MBD sparging systems when the fermentation volume was scaled-down from 50-liter to 1-liter fermentation. The cell mass concentration and cell mass yield were not statistically different ($p > 0.05$) at the low agitation rate for both sparging systems, and there was no significant difference ($p > 0.05$) between the specific growth rate at the low agitation rate for the MBD sparging system.

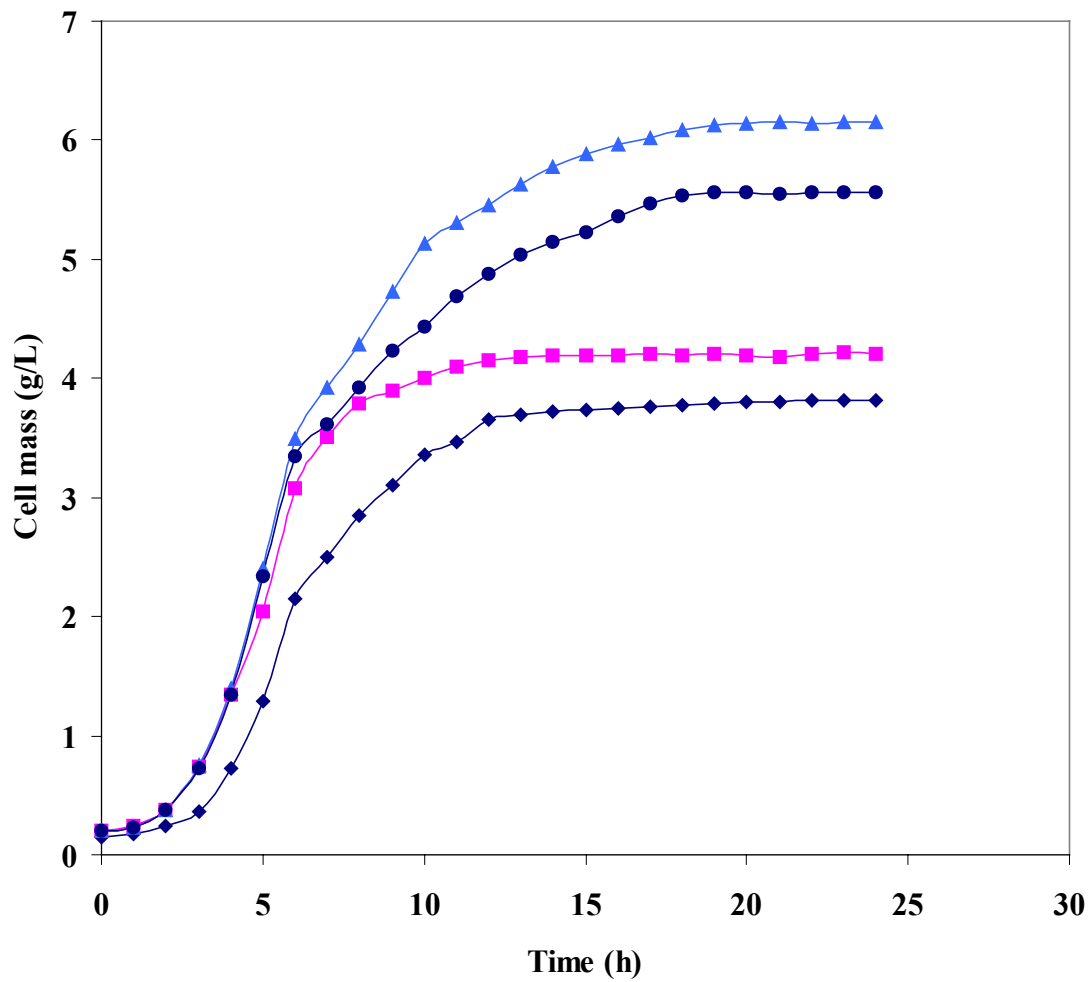


Figure 4.18 Growth profiles of MBD sparging system at agitation rates 144, 150, 476, and 500 rpm.
 144 rpm agitation, MBD sparging (◆), 150 rpm agitation, MBD sparging (■), 476 rpm agitation, MBD sparging (▲), 500 rpm agitation, MBD sparging (●).

CHAPTER 5

CONCLUSIONS AND RECOMMENDATIONS

Power input per unit volume, which is related to agitation speed, fluid and dispersion rheology, sparger characteristics, and gross flow pattern in the reactor tank, had some effect on the oxygen transfer to the baker's yeast (*Saccharomyces cerevisiae*). Increasing the agitation speed resulted in higher oxygen transfer, but more power was consumed and operating cost increased. Microbubble dispersion (MBD) could increase the oxygen transfer without increasing the agitation speed. The scale-up method used in this research was based on a constant volumetric oxygen transfer coefficient (k_La) (Hubbard, 1987). In this research, the scale-up method was performed inversely to scale down from a 50-L to 1-L fermentation. The lower agitation speed (150 rpm) in the 50-L fermentor was equivalent to 144 rpm in the 1-L fermentor, and the higher agitation speed (500 rpm) of the 50-L fermentor was equivalent to 476 rpm in the 1-L fermentor. For the air sparging system, the difference in the k_La values at higher agitation speeds was 14.8 % and that at low agitation speeds was 16.8 %. The differences in the k_La values for the MBD sparging system in low and high agitation were 10.8 % and 9.2 %, respectively.

In the 1-liter fermentation, the cell mass concentration with the MBD sparging system at 144 rpm was 31.3 % less than that with the air sparging system at 476 rpm. The volumetric oxygen transfer coefficient with the MBD sparging system at 144 rpm was 14.8 % less than the air sparging system at 476 rpm. The power consumption by the MBD generator was the major factor because of the very high speed (4000 rpm) of the MBD generator. The power consumption per unit volume of the air sparging system at 476 rpm was 87.2 % less than that of the MBD sparging system at 144 rpm. The increase in agitation speed was more effective than the MBD in the 1-liter fermentation.

In the 50-liter fermentation, the MBD sparging system at 150 rpm was comparable to the air sparging system at 500 rpm. The cell mass concentration of the MBD sparging system at 150 rpm was 16.9 % less than the air sparging system at 500 rpm. The volumetric oxygen transfer coefficient was 18.4 % less than the air sparging system at 500 rpm. However, the power consumption per unit volume of the MBD

sparging system at 150 rpm was 67.9 % lower than the air sparging system at 500 rpm. Because of the size of the fermentor, the power consumption from the agitator at 500 rpm dominated the overall power consumption. Although the MBD at 150 rpm produced volumetric oxygen transfer coefficient less than the sparged air at 500 rpm, there were no statistical differences in cell mass concentration ($p > 0.05$) and oxygen uptake rate ($p > 0.05$) between the two sparging systems. The sparged air at 500 rpm also consumed much more power than the MBD at 150 rpm. The MBD has a potential to increase the oxygen transfer with low power consumption per unit volume, especially for large-scale fermentations.

From this study, it was shown that the MBD could increase the oxygen transfer to a system operated with low agitation. This result suggests an economic advantage when the MBD is used for a large-scale process. Because of the limitations of the current MBD and recycle pump, the MBD flow rate was limited to 0.1 VVM. For future research, the 1-liter MBD generator should be investigated to determine the maximum MBD flow rate to give the highest cell mass concentration and the capacity of the 1-liter MBD generator to produce the MBD. Although the YM broth can produce natural surfactant-stabilized microbubbles, the cost of YM broth is high. This media is not suitable for the large-scale fermentation. The molasses widely used in industrial production of baker's yeast should replace the YM broth and the mechanisms to produce the MBD has to be investigated. It will be a great advantage for the MBD sparging system if the spinning disc of the MBD generator could be incorporated into a fermentor. Due to the high oxygen transfer at low agitation rate, the application of the MBD to shear-sensitive microorganisms should be investigated.

REFERENCES

- Abel, C., U. Huber, and K. Schugerl. 1994. Transient behaviour of Baker's yeast during enforced periodical variation of dissolved oxygen concentration. *J. Biotechnol.* 32 (1):45-57.
- Ahmad, M. N., C. R. Holland, and G. McKay. 1994. Mass transfer studies in batch fermentation: Mixing characteristics. *J. Food Eng.* 23:145-158.
- Andrew, S. P. S., 1982. Gas-Liquid mass transfer in microbiological reactors. *Trans AIChE. J.* 60:3-13.
- Bailey, J. E., and D. F. Ollis. 1986. *Biochemical Engineering Fundamentals*. 2d ed. New York: McGraw-Hill Book Company.
- Barford, J. P. 1990. A general model for aerobic yeast growth: Batch growth. *Biotechnol. Bioeng.* 35:907-920.
- Bell, G. H., and M. Gallo. 1971. Effect of impurities on oxygen transfer. *Process Biochem.* 6 (4):33-35.
- Beudeker, F. R., H. W. van Dam, J. B. van der Plaat, and K. Vellenga. 1990. Developments in baker's yeast production. In *Yeast Biotechnology and Biocatalysis*, ed. H Verachtert. New York: Marcel Dekker, Inc.
- Bird, R. B., W. E. Stewart, and E. N. Lightfoot. 1960. *Transport phenomena*. New York: John Willey & Sons.
- Bredwell, M. D., M. D. Telgenhoff, and R. M. Worden. 1995. Formation and coalescence properties of microbubbles. *Appl. Biochem. Biotechnol.* 51/52: 501-509.

- Bredwell, M. D., and R. M. Worden. 1998. Mass-Transfer properties of microbubbles. 1. Experimental studies. *Biotechnol. Prog.*14:31-38.
- Brock, T. D., and M. T. Madigan. 1991. *Biology of Microorganisms*. 6h ed. Englewood, N. J.: Prentice Hall.
- Casida, L. E. Jr. 1968. *Industrial Microbiology*. New York: John Wiley & Son.
- Cooper, C. M., G. A. Fernstorm, and S. A. Miller. 1944. Performance of agitated gas-liquid contractors. *Ind. Eng. Chem.* 36 (6):504-509.
- Doran, P. M. 1995. *Bioprocess Engineering Principles*. San Diego: Academic Press.
- Furukawa, K., E. Heinzle, and L. J. Dunn. 1983. Influence of oxygen on the growth of *Saccharomyces cerevisiae* in continous culture. *Biotechnol. Bioeng.* 25: 2293-2317.
- Hensirisak, P. 1997. Scale-up the use of a microbubble dispersion to increase oxygen transfer in aerobic fermentation of Baker' s yeast. M.S. thesis. Virginia Polytechnic Institute and State University.
- Hubbard, D. W. 1987. Scale-up strategies for bioreactors. In *Biotechnology Process Scale-up and Mixing*. ed. C. S. Ho, and J. Y. Oldshue, 168-184. New York: American Institute of Chemical Engineers.
- Humphrey, A. 1998. Shak flask to fermentor: What have we learn?. *Biotechnol. Prog.* 14:3-7.
- Ju, L.-K., and G. G. Chase. 1992. Improved scale-up strategies of bioreactors. *Bioprocess Eng.* 8:49-53.

- Ju, L.-K., and A. Sundararajan. 1994. The effects of cells on oxygen transfer in bioreactors: physical presence of cells as solid particles. *Chem. Eng. J.* 59 (1): B15-B21.
- Ju, L.-K., and A. Sundararajan. 1995. The effects of cells on oxygen transfer in bioreactors. *Bioprocess Eng.* 13 (5):271-278.
- Junker, B. H., T. A. Hatton, and D. I. C. Wang. 1990. Oxygen transfer enhancement in aqueous/perfluorocarbon fermentation systems: I. Experimental observations. *Biotechnol. Bioeng.* 35:578-585.
- Karow, E. O., W. H. Bartholomew, and M. R. Sfat. 1953. Oxygen transfer and agitation in submerged fermentations. *Agric. Food Chem.* 1 (4): 302-306.
- Kaster, J. A. 1988. Increased oxygen transfer in a yeast fermentation using a microbubble dispersion. M.S. thesis. Virginia Polytechnic Institute and State University.
- Kaster, J. A., D. J. Michelsen, and W. H. Velander. 1990. Increased oxygen transfer in a yeast fermentation using a microbubble dispersion. *Appl. Biochem. Biotechnol.* 24/25:469-484.
- Mateles, R. I. 1971. Calculation of the oxygen required for cell production. *Biotechnol. Bioeng.* 13:581-582.
- Mavituna, F. 1996. Strategies for bioreactor scale-up. In *Computer and Information Science Applications in Bioprocess Engineering*, ed. A. R. Moreira, and K. K. Wallace, 125-142. Dordrecht: Kluwer Academic Publishers.
- Maxon, W. D., and M. J. Johnson. 1953. Aeration studies on propagation of baker's yeast. *Ind. Eng. Chem.* 45 (11):2554-2560.

- Miller, G. L. 1959. Use of dinitrosalicylic acid reagent for determination of reducing sugar. *J. Biol. Chem.* 31 (3):426-428.
- Modak, J. M., H. C. Lim, and Y. J. Tayeb. 1986. General characteristics of optimal feed rate profiles for various fed-batch fermentation processes. *Biotechnol. Bioeng.* 28 (9):1396-1407.
- Moser, A. 1996. Oxygen transfer and microbial growth. In *Computer and Information Science Applications in Bioprocess Engineering*, ed. A. R. Moreira, and K. K. Wallace, 377-394. Dordrecht: Kluwer Academic Publishers.
- Motarjemi, M., and G. J. Jameson. 1978. Mass transfer from very small bubbles-the optimum bubble size for aeration. *Chem. Eng. Sci.* 33 (11):1415-1423.
- Onodera, M., H. Nishibori, H. Tanaka, N. Ogasawara, and A. Ohkawa. 1993. Effects of antifoam agents on cultivation of baker's yeast. *Biosci. Biotechnol. Biochem.* 57 (3): 486-487.
- Oolman, T. O., and H. W. Blanch. 1986. Bubble coalescence in stagnant liquids. *Chem. Eng. Commun.* 43:237-261.
- Orlowski, J. H., and J. P. Barford. 1987. The mechanism of uptake of multiple sugars by *Saccharomyces cerevisiae* in batch culture under fully aerobic conditions. *Appl. Microbiol. Biotechnol.* 25:459-463.
- Oyama, Y., and K. Endoh. 1955. Power characteristics of gas-liquid contacting mixers. *Chem. Eng. (Japan)*. 19:2-11.
- Perry, R. H., D. W. Green, and J. O. Maloney, eds. 1984. *Perry's Chemical Engineers Handbook*. 6h ed. New York: McGraw-Hill Book Company.

- Reed, G., and H. J. Pepler. 1973. *Yeast technology*. Westport, C. T. AVI Pub. Co.
- Richard, J. W. 1961. Studies in aeration and agitation. *Progress in Industrial Microbiology*. 3:143-172.
- Rushton, J. H., and J. Y. Oldshue. 1953. Mixing-present theory and practice. *Chem. Eng. Prog.* 49 (5):267-275.
- Rushton, J. H., E. W. Costich, and H. J. Everett. 1950. Power characteristics of mixing impellers. *Chem. Eng. Prog.* 46:395-404.
- Sebba, F. 1971. Microfoams-an unexploited colloid system. *J. Colloid Interface Sci.* 35 (4):643-646.
- Sebba, F. 1985. An improved generator for micron-size bubbles. *Chem. Ind. (London)*. 4:91-92.
- Sebba, F. 1987. *Foams and Biliquid Foams-Aphrons*, New York: John Wiley & Son.
- Sousa, M. L., and J. A. Teixeira. 1996. Characterization of oxygen uptake and mass transfer in flocculent yeast cell cultures with or without a flocculation additive. *Biotechnol. Lett.* 18 (3):229-234.
- Stanbury, P. F., A. Whitaker, and S. J. Hall. 1995. *Principles of Fermentation Technology*. 2d ed. New York: Elsevier Science Ltd.
- Taguchi, H., and A. E. Humphrey. 1966. Dynamic measurement of volumetric oxygen transfer coefficient in fermentation system. *J. Ferment. Tech. (Japan)*. 44:881-889.

Tatterson, G. B. 1991. *Fluid Mixing and Gas Dispersion in Agitation Tanks*. New York: McGraw-Hill, Inc.

Van' t Riet, K. 1983. Mass transfer in fermentation. *Trends Biotechnol.* 1 (4):113-116.

Wang, D. I. C., C. L. Cooney, A. L. Demain, P. Dunnill, A. E. Humphrey, and M. D. Lilly. 1971. *Fermentation and Enzyme Technology*. New York: John Wiley & Son.

APPENDIX

Estimated power consumption.

A1.0 Impeller power consumption.

The power consumption during agitation of non-gassed Newtonian liquids can be represented by a dimensionless group termed the power number (N_p):

$$N_p = \frac{P}{\rho N^3 D_i^5}$$

where N_p = the power number,

P = the external power from the agitator (W),

ρ = the liquid density (g cm^{-3}),

N = the impeller speed (s^{-1}), and

D_i = the impeller diameter (cm).

The power number is the ratio of external applied force (P) to the inertial force ($\rho N^3 D_i^5$) delivered to the liquid. Fluid motion in an agitated vessel can be described by the dimensionless number known as the Reynolds number, which is a ratio of inertial force to viscous force:

$$N_{Re} = \frac{\rho N D_i^2}{\mu}$$

where N_{Re} = the Reynolds number, and

μ = the liquid viscosity ($\text{g cm}^{-1} \text{s}^{-1}$).

The Reynolds number is calculated and the power number is taken from the graph between the log of Reynolds number and the log of power number (Rushton et al, 1950). From the power number, the power is calculated from the correlation between the power number and power.

For a gassed system, the power consumption is less than for a non-gassed system. To estimate the power consumption for agitation fermentation under aeration, the aeration number (N_a) introduced by Oyama and Endoh (1955) is expressed

$$N_a = \frac{Q}{ND_i^3}$$

where N_a = the aeration number, and

Q = the volumetric gas flow rate ($\text{cm}^3 \text{ s}^{-1}$).

The calculated aeration number is correlated to the ratio of gassed power (P_g) to non-gassed power (P_o). The gassed power is calculated from the this ratio times the non-gassed power.

A2.0 Air compressor power consumption.

The power consumption of air compressor is calculated from

$$\text{Hp} = 0.0154 Q p X$$

where Hp = power consumption (hp),

Q = flow rate ($\text{ft}^3 \text{ min}^{-1}$),

p = pressure ($\text{lb}_f \text{ in}^{-2}$), and

X = factor taken from Table 6-1 (Perry et al, 1984 pp 6-17).

A3.0 MBD generator power consumption.

MBD motor, MBD pump, and recycle pump are the devices consumed power.

A3.1 Power consumption of MBD motor.

$$P = I \times V$$

where P = power (W),

I = current of motor at 4000 rpm (amp), and
V = voltage of motor (voltage).

A3.2 Power consumption of MBD and recycle pump.

The power consumption was calculated from the steady-state macroscopic mechanical energy balance (Bird et al, 1960). The steady-state macroscopic mechanical energy balance is

$$\Delta \frac{1}{2} \langle v \rangle^2 + g\Delta h + \frac{p^2}{p^1} \frac{1}{\rho} dp + W + \sum_i \left(\frac{1}{2} \langle v \rangle^2 \frac{L}{D} f \right)_i + \sum_i \left(\frac{1}{2} \langle v \rangle^2 e_v \right)_i = 0$$

where $\langle v \rangle$ = the average velocity in the pipe line (ft min⁻¹),
 Δh = the height difference between 2 points (ft),
 p = the pressure at points 1 and 2 (lb_f in⁻²),
 W = the work of pump (ft² s⁻²),
 L = the pipe length (ft),
 D = the internal diameter of pipe (ft),
 f = the friction factor,
 e_v = the friction loss factor.

The work of pump was calculated then times with the mass flow rate of liquid. The product from the work of pump times the mass flow rate of liquid was the power of pump.

VITA

The author, Pramuk Parakulsuksatid, was born July 18, 1969 in Thailand. He graduated with a Bachelor of Science degree in Biotechnology from Kasetsart University in Bangkok, Thailand in 1993.

After graduation, Pramuk had opportunity to work with the Thai-wa Company as production supervisor for 1 year. He studied the Master program in Chemical Engineering at Chulalongkorn University in 1994. In 1995, he received scholarship from his government in 1996 to study in USA. He began pursuing the Master of Science degree in Biological Systems Engineering at Virginia Polytechnic Institute and State University in the Fall of 1996.